GROWING SEASON CARBON DIOXIDE EXCHANGE OF TWO CONTRASTING PEATLAND ECOSYSTEMS

AARON JAMES GLENN
B.Sc. - Plant Biology (Hons.), University of Alberta, 2003

A Thesis
Submitted to the School of Graduate Studies
of the University of Lethbridge
in Partial Fulfilment of the
Requirements for the Degree

MASTER OF SCIENCE

Department of Biological Sciences
University of Lethbridge
LETHBRIDGE, ALBERTA, CANADA

Abstract

The CO_2 flux of two peatlands in northern Alberta was examined during the 2004 growing season using eddy covariance measurements of net ecosystem exchange (NEE), chamber measurements of total ecosystem respiration, and empirical models driven by meteorological inputs. The two ecosystems, a poor fen and an extreme-rich fen, differed significantly in plant species composition, leaf area index, aboveground biomass and surface water chemistry. The mean diurnal pattern of NEE at the peak of the season was similar between the sites, however, the extreme-rich fen had a higher photosynthetic and respiratory capacity than the poor fen. Over the 6 month study, the poor fen was shown to accumulate between 2 to 3 times more carbon than the extreme-rich fen despite having a lower photosynthetic capacity. The evergreen nature of the poor fen site allowed for a longer season of net CO_2 uptake than the deciduous species that dominated the extreme-rich fen.

Acknowledgements

I wish to thank my thesis supervisor Dr. Larry Flanagan for giving me the opportunity to pursue graduate studies in his research lab at the University of Lethbridge. Thanks to Dr. Flanagan for always challenging me to do my best and for helping me achieve the most significant milestone of my academic career and one of the most meaningful life experiences thus far. I would also like to acknowledge the feedback and support from the other members of my thesis supervisory committee, Dr. Derek Peddle and Dr. Stewart Rood. I really appreciate the excellent scholarly advice and encouragement they gave, as well as, all of the insight I gained from the additional perspectives they provided during our committee meetings.

A big thank you goes out to the other students and staff of the Flanagan lab and the Department of Biological Sciences at the University of Lethbridge. I gratefully acknowledge all the help you provided me over the last couple of years and for greatly enhancing and enriching my experience as a young, aspiring scientist and teacher. I wish you all the best in the years to come, wherever life may take you. Last but not least, I wish to thank all of my family and friends who have given me endless encouragement, inspiration and support, and have always told me that I can accomplish anything.

This research was conducted as part of the Fluxnet-Canada Research Network. Funding was provided in the form of research grants to Dr. L.B. Flanagan from the Natural Sciences and Engineering Research Council of Canada (NSERC), Canadian Foundation for Climate and Atmospheric Studies (CFCAS) and BIOCAP Canada.

Table of Contents

List of Tables

List of Figures

List of Abbreviations and Symbols

α = photochemical efficiency (mol CO_2 mol^{-1} PPFD).

A_{max} = maximum possible GPP at infinite PPFD ($\mu mol\ m^{-2}\ s^{-1}$).

CPECS = closed-path eddy covariance system.

Δc = change in CO_2 concentration ($\mu mol\ mol^{-1}$).

Δt = change in time (s).

DOY = day of year.

EC = eddy covariance.

E_{R1} = random error of EC measurements, calculated by the daily-differencing approach (Eq. 16).

E_{R2} = random error of EC measurements, calculated with measured and modelled NEE (Eq. 17).

E_{SYS} = systematic error of EC measurements as related to the degree of turbulent mixing.

F = instantaneous vertical scalar (CO_2, H_2O, or H) flux measured with the EC technique.

FACE = free-air CO_2 enrichment.

F_c = instantaneous vertical CO_2 flux measured with the EC technique ($\mu mol\ m^{-2}\ s^{-1}$).

FCRN = Fluxnet-Canada Research Network.

F_s = CO_2 flux storage term ($\mu mol\ m^{-2}\ s^{-1}$).

GPP = gross primary production ($\mu mol\ CO_2\ m^{-2}\ s^{-1}$ or g C m^{-2} $time^{-1}$).

H = sensible heat flux ($W\ m^{-2}$).

h = air column height (m).

h_{PBL} = height of the planetary boundary layer (m).

IPCC = Intergovernmental Panel on Climate Change.

IRGA = infra-red gas analyzer.

K_m = the Michaelis-Menten constant for a biochemical reaction.

LAI = leaf area index (m^2 m^{-2}).

L & T - NEE model = non-linear regression describing NEE that uses Lloyd and Taylor's (1994) equation 11 for modelling the TER term (Eq. 15).

L & T - TER model = non-linear regression that uses Lloyd and Taylor's (1994) equation 11 for modelling TER (Eq. 12).

LE = latent heat flux (W m^{-2}).

ME = modelling efficiency statistic (Eq. 14).

NEE = net ecosystem exchange (μmol CO_2 m^{-2} s^{-1} or g C m^{-2} $time^{-1}$).

NEE_{mod} = modelled value of NEE.

NEE_{obs} = observed or measured value of NEE using the EC technique.

NPP = net primary production.

NWWG = National Wetlands Working Group.

OPECS = open-path eddy covariance system.

P = rate of photosynthesis.

PCO cycle = photorespiratory carbon oxidation cycle (or photorespiration).

PCR cycle = photosynthetic carbon reduction cycle.

P_{max} = maximum possible rate of photosynthesis at infinite PPFD.

PPFD = photosynthetically-active photon flux density (μmol m^{-2} s^{-1}).

ppmv = parts per million by volume.

Q_{10} = temperature sensitivity coefficient for TER (dimensionless).

Q_{10} - NEE model = non-linear regression describing NEE that uses the Q_{10} equation for modelling the TER term (Eq. 13).

Q_{10} - TER model = non-linear regression that uses the Q_{10} equation for modelling TER (Eq. 11).

R_{10} = the rate of TER at 10°C or 283.15 K (μmol m^{-2} s^{-1}).

ρ_a = the density of dry air (mol m^{-3}).

Rubisco = ribulose-1,5-bisphosphate carboxylase/oxygenase.

SAT = sonic anemometer-thermometer.

σ_w = standard deviation of vertical velocity fluctuations (m s^{-1}).

$[S]$ = substrate concentration.

T = air temperature (°C or K).

TER = total ecosystem respiration (μmol m^{-2} s^{-1}).

u_* = friction velocity (m s^{-1}).

V = the rate of a biochemical reaction.

V_{max} = the maximum velocity of a biochemical reaction.

w = vertical wind velocity (m s^{-1}).

x = scalar molar mixing ratio (mol mol^{-1} dry air).

X_{max} = horizontal distance (m) from an EC tower with the maximum contribution to measured fluxes.

$X_{90\%}$ = horizontal distance (m) from an EC tower within which 90 % of measured fluxes originate.

Z_m = SAT measurement height (m).

Z_o = aerodynamic roughness length (m).

1. Introduction

In an age of unprecedented anthropogenic alteration of major biogeochemical cycles, climate, and ecosystem functioning, the importance of biometeorological and ecophysiological studies cannot be overstated. The global carbon (C) cycle is an example of a major biogeochemical process that has undergone significant human-induced perturbation and is tightly linked to terrestrial ecosystems and climate (Goulden et al. 1996; Asner and Seastedt, 1997; Aubinet et al. 2000; Grace and Mahli, 2002).

1.1 Earth's changing atmosphere

According to analyses of Antarctic ice cores (Neftel et al. 1994; Barnola et al. 2003) and ongoing monitoring at Mauna Loa Observatory in Hawaii since 1958 (Keeling and Whorf, 2004) the atmospheric concentration of carbon dioxide (CO_2) has been rising in an exponential fashion since the dawn of the Industrial Revolution (~ 250 years before present). The mean concentration of CO_2 has increased from pre-industrial Holocene levels of ~ 280 parts per million by volume (ppmv) of dry air (Friedli et al. 1986; Neftel et al. 1994; Barnola et al. 2003), to 316 ppvm in 1959, and the unprecedented level of approximately 376 ppmv currently (Keeling and Whorf, 2004). Rising combustion of fossil fuels and cement production (Marland et al. 2003), as well as land-use changes, such as deforestation (Fearnside, 2000; Houghton and Hackler, 2002), contribute to a transforming global C cycle in which net emissions of CO_2 into the atmosphere are greater than the sequestering ability of the Earth's sinks (Bazzaz, 1990; Bowes, 1993; Asner and Seastedt, 1997; IPCC, 2001). If current anthropogenic emission trends persist, the planet's atmospheric CO_2 concentration will double from the pre-industrial level this century.

1.1.1 Terrestrial ecosystems and elevated carbon dioxide

There are many possible consequences for global biota as a result of rising CO_2

concentrations. These may be direct, such as the effect that elevated CO_2 can have on photosynthesis for the majority of terrestrial plants. The primary carboxylation enzyme involved in photosynthesis, which catalyzes the first, and major rate-limiting step in the photosynthetic carbon reduction (PCR) cycle, is ribulose-1,5-bisphosphate carboxylase/oxygenase or Rubisco (Farquhar et al. 1980; Bowes, 1993; Drake et al. 1997; Chapin III et al. 2002). As the name suggests, Rubisco is a bicatalytic enzyme that catalyzes both carboxylation and oxygenation reactions in chloroplasts, with oxygen (O_2) and CO_2 competing for the same active site. The carboxylation of CO_2 by Rubisco initiates the PCR cycle, while the oxygenase role of Rubisco initiates the photorespiratory carbon oxidation (PCO) cycle, or photorespiration (Farquhar et al. 1980). Hence, under conditions of elevated atmospheric CO_2, the amount of carbon fixed by the PCR cycle increases relative to the amount oxidized or "lost" due to photorespiration (Bazzaz, 1990; Bowes, 1993; Drake et al. 1997).

It should be noted that the enhancement of photosynthesis and associated photorespiratory decline has only been well documented for plants with C_3 type metabolism, with fewer studies examining the effect on plants with C_4 or Crassulacean acid metabolism (CAM), and no overwhelming trends resulting from the data (Bazzaz, 1990; Bowes, 1993). Perhaps, because C_4 and CAM plants have evolved physiological mechanisms that concentrate cellular CO_2 and exhibit virtually no photorespiration, the direct impact of increasing atmospheric CO_2 on their photosynthetic metabolism is negligible. However, as previously explained, the general short-term effects of elevated CO_2 levels on C_3 photosynthesis are known and C_3 plants constitute approximately 95 % of terrestrial vegetation biomass (Bowes, 1993), so rising atmospheric CO_2 levels may significantly impact Earth's gross primary production (GPP).

In addition to the direct enhancement of C_3 photosynthesis, conditions of elevated CO_2 can also increase water-use efficiency and nutrient-use efficiency of plants (Drake et al. 1997; IPCC, 2001). Increased water-use efficiency results from the partial closure of stomata in response to higher CO_2 levels, leading to less transpirational water loss in plants relative to the amount of carbon gained (Eamus, 1991; Drake et al. 1997; Körner, 2000). Increased nutrient-use efficiency, especially nitrogen (N)-use efficiency, can be the result of plants requiring lower tissue concentrations of photosynthetic enzymes to carry out photosynthesis at given rates under elevated CO_2 (McGuire et al. 1995; Drake et al. 1997; Curtis and Wang, 1998; Peterson et al. 1999; Körner, 2000).

Whether the impact of future CO_2 "fertilization" on terrestrial plant physiology will be biome-specific, species-specific, short-term or long-term, is highly debatable at present because of multiple interacting factors and potential feedbacks regulating hydrology, nutrient-cycling, photosynthesis and respiration in natural ecosystems compared to traditional controlled greenhouse or growth-chamber studies of CO_2 enrichment. Some progress has been made over the past decade in studying the effects of elevated CO_2 on natural ecosystems through the free-air CO_2 enrichment (FACE) studies (FACE, 2004). However, these studies have numerous temporal, spatial and monetary constraints, as it is very difficult to mimic a gradual rise of CO_2 concentrations over multiple years without taking the time to conduct such experiments on Earth's various different ecosystems.

1.1.2 Earth's climate and elevated carbon dioxide

Besides the direct effects elevated CO_2 could have on GPP in ecosystems, the implications of rising atmospheric CO_2 concentrations for the Earth's biosphere are also indirect. Since CO_2 acts as a "greenhouse gas" by absorbing radiant energy in the infra-red spectrum (Oke, 1987; Bonan and Shugart, 1989; Jones, 1992), elevated atmospheric

concentrations are expected to significantly contribute to global climate change by modifying average temperatures and regional precipitation patterns (IPCC, 2001).

There currently is evidence of altered temperature and precipitation patterns associated with the post-industrialization period of increasing anthropogenic CO_2 emissions (Gullet and Skinner, 1992; Environment Canada, 1995; IPCC, 2001; Moore et al. 2002). Globally, the 1990s have been the warmest decade, with 1998 being the warmest year based on reliable instrument records (Environment Canada, 1999; National Oceanic and Atmospheric Administration, 1999). Coincidentally, 1998 is also the year exhibiting the greatest increase in mean atmospheric CO_2 concentration since measurements began at Mauna Loa Observatory (Keeling and Whorf, 2004). The second warmest year on instrumental surface temperature records is 2002, while 2003 is third and 2004 is fourth (World Meteorological Organization, 2004, 2005).

1.2 Terrestrial ecosystems and the global carbon cycle

Large uncertainty exists in determining the fate of up to half the anthropogenically released CO_2 (Aubinet et al. 2000; Grace and Mahli, 2002). The "missing sink" could be in aboveground vegetation, the soil, the ocean, or some combination of the three (Asner and Seastedt, 1997; Aubinet et al. 2000). It is postulated that the missing sink could be partially due to a number of interacting human-induced environmental forcing factors on terrestrial ecosystems, such as CO_2 fertilization, increased nitrogen deposition and fertilization, and increasing surface temperatures, which further confounds the problem (Schimel, 1995; Houghton et al. 1998).

Current knowledge of how terrestrial ecological systems contribute to the dynamic C cycle is limited, and better understanding of the gaseous flux of CO_2 between various ecosystems and the atmosphere is required for gaining better elucidation of the global C

budget (Goulden et al. 1996; Aubinet et al. 2000). Accurately determining the influence that various types of terrestrial vegetation exert on the atmosphere and vice versa is imperative to understanding the coupling of Earth's ecosystems to global climate and biogeochemical cycles (Mahli et al. 1999; Aubinet et al. 2000; Barford et al. 2001; Schimel et al. 2001; Schulze et al. 2002). Furthermore, revealing the underlying ecophysiological factors governing net ecosystem exchange (NEE) of CO_2 is necessary to formulate hypotheses, create models and strengthen future predictions regarding the role of terrestrial vegetation in the global C balance and potential climatic change (Goulden et al. 1996; Aubinet et al. 2000; Barford et al. 2001; Flanagan et al. 2002; Griffis et al. 2003; Gu et al. 2003; Kowalski et al. 2003).

1.2.1 Peatland ecosystems and the global carbon cycle

Peatlands are examples of terrestrial ecosystems that play a major role in the global C cycle and associated climatic feedbacks (Gorham, 1991; Moore et al. 1998; O' Neil, 2000; Turetsky et al. 2000). In Canada, peatlands are defined as wetland ecosystems with a minimum organic soil depth of 40 cm (NWWG, 1988; Johnson et al. 1995). Peatlands form when net primary production (NPP) consistently exceeds rates of decomposition due to cool and anaerobic conditions, leading to long-term C accumulation (Vitt, 1994; Vitt et al. 1995; Silvola et al. 1996; Szumigalski and Bayley, 1996a; Thormann and Bayley, 1997a).

Peatlands can be further classified, based on various hydrological, vegetative and water chemistry criteria, into bogs and fens (Vitt, 1994; Vitt et al. 1995; Szumigalski and Bayley, 1996a; Thormann and Bayley, 1997b). Bogs are ombrogenous ecosystems, influenced by waters solely derived from precipiation, whereas fens are geogenous or minerotrophic ecosystems, influenced by groundwaters that have come in contact with mineral soils (Vitt, 1994; Vitt et al. 1995). Fens can be classified vegetatively as *Sphagnum*

moss-dominated poor fens, and *Carex* spp. / "brown moss"-dominated rich fens (Vitt et al. 1995). Rich fens are further subdivided into moderate-rich and extreme-rich fens, according to a well documented bog-rich fen gradient based on numerous vegetative and water chemistry characteristics (Sjörs, 1952; Vitt et al. 1975; Vitt and Slack, 1984; Vitt, 1994; Vitt et al. 1995; Szumigalski and Bayley, 1996a; Thormann and Bayley, 1997a, 1997b). The water chemistry of bogs and poor fens is characterized by low pH, low electrical conductivity, and low base cation concentrations, and these three chemical components increase along the gradient up to extreme-rich fens, which are more alkaline, base cation rich, and have high electrical conductivities.

Bog and fen ecosystems are very important because they contain approximately 1/3 of the world's soil C pool and represent the largest pool of C in the Canadian terrestrial biosphere (Gorham, 1991). Canada contains between 30 – 40 % of the world's peatlands, covering 10 -14 % of the entire land surface (NWWG, 1988; Gorham, 1991), and ≥ 20 % of the interior boreal region (Szumigalski and Bayley, 1996a; Thormann and Bayley, 1997a; Turetsky et al. 2000).

Peatlands are more tightly coupled to climate and the hydrological cycle than many other terrestrial ecosystems making them susceptible to the effects of future climate change (Silvola et al. 1996; Moore et al. 1998, Hilbert et al. 2000; Bubier et al. 2003). Incidentally, the western interior of Canada, and other high latitude locations, in which peatlands occupy a significant percentage of land area, coincide geographically to where some of the greatest climate change has been detected (Gullet and Skinner, 1992; Environment Canada, 1995; IPCC, 2001; Moore et al. 2002), and is expected to occur over the course of this century (Hogg and Hurdle, 1995; Price and Apps, 1996; Schindler, 1997; Hogg et al. 2002; *and references therein*).

Like all terrestrial ecosystems a number of environmental factors play important roles governing the rate of CO_2 exchange in peatlands and projected climate change can be expected to affect these regulating factors (Bubier et al. 2003). A common example of the climatological dependence of C cyling in peatlands is that lowering of the water table can quickly (within a single growing-season) change an ecosystem from a sink to a large source of CO_2 by exposing a greater volume of peat to aerobic conditions, making it more conducive to decomposition and respiratory processes (Silvola et al. 1996; Moore et al. 1998; Freeman et al. 2001; Bubier et al. 2003). The implications arising from such dynamic ecosystems for global climate and C cycles are enormous, considering that the oxidation of 1 % of the estimated organic C stored in Canadian peatlands (NWWG, 1988; Gorham, 1991) is equivalent to approximately 10 years of Canada's current (2000) anthropogenic CO_2 emissions (Environment Canada, 2002a). However, relatively little information exists regarding the environmental controls on CO_2 exchange within the various different peatland types. Because peatlands are such an important component of the global C cycle and cover a large portion of Canada's land area, any knowledge gained regarding the functional ecology of these poorly understood ecosystems could prove invaluable. Accurately predicting the consequences of global climate change, as well as, potential interactions and feedbacks with the atmosphere requires a broader comprehension of the underlying environmental mechanisms governing the NEE of various types of peatlands.

1.3 Measuring net ecosystem exchange of carbon dioxide

Traditional studies of CO_2 exchange by plant canopies and soils have been conducted with chamber techniques or leaf cuvettes (Baldocchi et al. 1988; Baldocchi, 2003). Such studies have been carried out sucessfully in a variety of ecosystems, including peatlands (Kim and Verma, 1992; Shurpali et al. 1995; Silvola et al. 1996; Suyker et al. 1997; Bubier

et al. 2003). These chamber and cuvette experiments have proved valuable for measuring diurnal variations of CO_2 fluxes and defining environmental response characteristics, like photosynthetic light-response curves and relationships between respiration and temperature. However, due to overwhelming spatial and temporal constraints, these methods can make it difficult to generate enough replicates to give a statistically significant representation of an ecosystem's natural variability (Baldocchi et al. 1988; Baldocchi, 2003).

Measurements of NEE over longer periods of time have traditionally been conducted by quantifying temporal changes of biomass and soil C. These ecosystem "carbon inventories" have been successful for estimating annual NPP in many cases, including peatland ecosystem NPP (Reader and Stewart, 1972; Szumigalski and Bayley 1996a; Thormann and Bayley, 1997a, 1997b), but also contain potential drawbacks. Such drawbacks or limitations stem from the reliance of biomass estimates on allometric relationships that may not adequately encompass biological heterogeneity (Gower et al. 1999), and the difficulty in obtaining reliable ecosystem scale soil C inventories, due to large spatial variability (Baldocchi, 2003).

Tower-based micrometeorological techniques deliver an alternative method for obtaining the net exchange of entities, such as energy, water vapour and CO_2, between ecosystems and the atmosphere (Baldocchi et al. 1988; Wyngaard, 1990; Aubinet et al. 2000; Baldocchi, 2003). Due to advances in micrometeorological instrumentation and data acquisition systems over recent decades, a method known as the eddy covariance technique has emerged as a prominent and useful scientific tool for studying biosphere-atmosphere interactions (Baldocchi et al. 1988; Goulden et al. 1996; Aubinet et al. 2000; Baldocchi, 2003).

Eddy covariance (EC) is a technique that employs micrometeorological theory to

interpret above-canopy measurements of the covariance between vertical wind velocity and scalar concentration fluctuations (Wyngaard, 1990; Moncrieff et al. 1997; Aubinet et al. 2000; Baldocchi, 2003). It has gained popularity in recent years for ecosystem flux measurements due to a number of reasons. Most notably, EC provides researchers with the methodology to measure the net exchange of CO_2 over an entire ecosystem, *in situ* and virtually non-invasively, with minimal disturbance to the surrounding environment. As well, EC provides the means to evaluate NEE across a range of time scales, from hours to years, providing an effective alternative to the temporal constraints of older net CO_2 exchange studies.

EC is especially worthwhile for studies of ecosystem physiology or functioning (Baldocchi, 2003). It can be employed for quantifying how NEE is altered under variable environmental conditions, whether naturally or anthropogenically induced; for diurnal, weekly, seasonal or inter-annual time scales. EC has been employed to explicate the C balance of a number of environments worldwide, from various forest types (Wofsy et al. 1993; Hollinger et al. 1999; Mahli et al. 1999; Barford et al. 2001; Schulze et al. 2002; Griffis et al. 2003; Kowalski et al. 2003), grasslands (Verma et al. 1989; Flanagan et al. 2002), peatlands (Neumann et al. 1994; Shurpali et al. 1995; Suyker et al. 1997; Joiner et al. 1999; Campbell and Smith, 2001; Lafleur et al. 2001; Jacobs et al. 2003; Lafleur et al. 2003) and tundra ecosystems (Eugster et al. 1997; Vourlitis and Oechel, 1999).

EC has proven exceptionally useful for resolving seasonal and inter-annual dynamics of ecosystem CO_2 exchange, and for determining how environmental variables such as species composition (Griffis et al. 2003), water availability (Flanagan et al. 2002), temperature (Goulden et al. 1998; Lafeur et al. *in press*) and solar radiation input (Ruimy et al. 1995; Frolking et al. 1998; Hollinger et al. 1999; Barford et al. 2001; Gu et al. 2003)

govern NEE processes.

Currently the eddy covariance technique is employed to measure NEE by regional networks at over 180 sites worldwide as part of the FLUXNET program (Baldocchi et al. 2001; Baldocchi, 2003; FLUXNET, 2005). The main goal of the FLUXNET project is to gain further understanding of how Earth's numerous terrestrial ecosystems interact with the atmosphere and influence regional and global climate patterns. In the context of global change, the knowledge gained is essential for future models and predictions regarding the reaction and potential feedbacks from ecosystems as they are increasingly faced with widespread changes in environmental forcing effects.

1.4 Modelling net ecosystem exchange of carbon dioxide

The measurement of CO_2 exchange above an ecosystem is the net result between the competing flux processes of gross primary production (GPP) and total ecosystem respiration (TER). When adopting the meteorological sign convention, net fluxes of CO_2 into the atmosphere are considered positive (+), while net uptake by the ecosystem is considered negative (-) in notation, therefore yielding a basic NEE equation (Eq.) of the form:

$$NEE = - GPP + TER \quad (1)$$

Although there are numerous contributing environmental factors governing GPP, TER, and therefore NEE (Eq. 1), it is desirable to derive simple relationships based on one or two of the most important variables regulating the biological processes of photosynthesis and respiration. These ecological relationships generally take the form of non-linear empirical models, such as photosynthetic light-response curves and exponential relationships between respiration and temperature. While oversimplified mechanistically, such empirical relationships have proven accurate predictors of NEE (Griffis et al. 2003) and are extensively used for "gap-filling" C budgets based on EC measurements (Falge et al. 2001) and other

biogeochemical models. Perhaps the most useful aspect of these simple physiological relationships is that once they are derived for a certain ecosystem and phenological stage, the only inputs required for estimating NEE at the site are easily measured meteorological variables such as temperature and light input. Also, if the derivation of the parameters in models is conducted in a standard manner, it allows straightforward comparison of photosynthetic and respiratory processes across a variety of terrestrial ecosystems.

1.4.1 Modelling ecosystem photosynthesis

The common light-response curve used to model photosynthesis originates from the Michaelis-Menten approach to non-allosteric enzyme kinetics, which describes the rate of a biochemical reaction (V) by the following equation (Landsberg, 1977; Campbell, 1999),

$$V = \frac{V_{max}[S]}{K_m + [S]} \tag{2}$$

where V_{max} is the maximum velocity of the reaction, $[S]$ is the substrate concentration and K_m is the "Michaelis-Menten constant" for the reaction (equal to $[S]$ at one half of V_{max}).

In an analogous fashion, the equation for the rate of photosynthesis (P) as dependent on incident light (as photosynthetically-active photon flux density (PPFD)) takes the following form,

$$P = \frac{P_{max}\alpha\text{PPFD}}{P_{max} + \alpha\text{PPFD}} \tag{3}$$

where P_{max} is the maximum possible rate of photosynthesis (at infinite PPFD) and α is the photochemical efficiency or apparent quantum yield (initial slope of the light-response curve) of the biological process.

When plotted graphically, Eq. 2 or Eq. 3, will model the rate of the reaction as a non-linear, rectangular hyperbola (Landsberg, 1977). Initially, the rate increases in a near-linear

fashion as a function of substrate concentration (PPFD in Eq. 3), but with continued increases in [*S*], the reaction velocity slows as some other component of the process becomes limiting or detrimental, the linear relationship begins to curve, and eventually levels off asymtotically at saturation. Equation 3 is written in a way, such that at low light levels CO_2 assimilation is limited by the photochemical efficiency of the process (Smith, 1938; Landsberg, 1977), while at high light levels it is limited by some other mechanism, such as the rate of CO_2 diffusion to the site of photosynthesis (Montieth, 1965; Landsberg, 1977), the electron transport capacity or the amount and activity of Rubisco (Farquhar et al. 1980; Evans, 1989).

Although Eq. 3 is empirical in form, its utility has been demonstrated in numerous biological studies with a wide variety of plant species (Landsberg, 1977). The photosynthetic light-response curve has proven a useful tool in plant physiology for differentiating photochemical efficiencies (α) and maximum capacities (P_{max}) between different leaves, individuals and species, under a variety of environmental conditions and stressors.

The original light-response model for photosynthesis (Eq. 3), was developed and tested at the individual leaf level using cuvette techniques and artificial light sources for controlling illumination density. Despite the potential biological bias and associated experimental error with the traditional methodology, similar light-response curves have proven robust at the ecosystem or "big leaf" level for modelling NEE. Many investigators have successfully applied the light-NEE relationship in the field, by utilizing chambers (Bubier et al. 2003) or micrometeorological techniques (Ruimy et al. 1995; Frolking et al. 1998). The relationship between NEE and PPFD (when using meteorological notation) can be described by the equation,

$$NEE = -\frac{A_{max}\alpha PPFD}{A_{max} + \alpha PPFD} + TER \quad (4)$$

where A_{max} is the maximum possible value of GPP (at infinite PPFD), α is the photochemical efficiency or apparent quantum yield (initial slope of the light-response curve), and TER is the y-intercept of the light-response curve.

It is important to note the inclusion of the TER term in Eq. 4, as it makes the light-response of NEE mechanistically different than the light-response of photosynthesis alone (Eq. 3). The TER parameter corresponds to the y-intercept of the non-linear, rectangular hyperbola (Eq. 4), which is NEE when incident PPFD = 0. This parameter is considered equal to the average TER for the particular period of time from which the light-response curve was derived (Ruimy et al. 1995; Frolking et al. 1998; Hollinger et al. 1999; Kowalski et al. 2003). The inclusion of this term is necessary for modelling NEE light-response, because as previously discussed, NEE is the sum of the competing atmospheric CO_2 flux processes of GPP and TER (Eq. 1), whereas the original photosynthesis model (Eq. 3), describes photosynthesis exclusively. A disadvantage inherent to the common NEE light-response model (Eq. 4) is that TER is strongly dependent on temperature (discussed further in section 1.4.2) and there is commonly a large diurnal temperature variation over the course of a day, lagging slightly behind the incoming PPFD. Therefore, a more robust NEE relationship would include a temperature measurement to model the TER component in Eq. 4.

1.4.2 Modelling ecosystem respiration

The process of respiration, whether microbial, plant, or animal, is essentially cellular based, therefore most models adopt the basic principles of chemical kinetics developed by van't Hoff and Arrhenius in the late 19th century (Lloyd and Taylor, 1994; Stoy and Zhang,

2004). The most important of these principles is the relationship between enzymatic reactions and temperature, that is commonly described by a simple exponential model, which is the inverted form of the original 1898 van't Hoff equation (Lloyd and Taylor, 1994; Stoy and Zhang, 2004). Although this exponential relationship has been employed extensively in biology to model the temperature response of respiration, it has long been criticized for being too empirical and having no rational basis (Lloyd and Taylor, 1994). Many researchers prefer to model respiration based on the more mechanistic chemical reaction relationship derived by Arrhenius in 1889, that is based on earlier work by van't Hoff in 1884, and includes an activation energy (minimum energy required to create a chemical reaction) parameter (Lloyd and Taylor, 1994; Fang and Moncrieff, 2001).

Upon examination of residual error values of recent TER measurements as a function of temperature it is clear that neither the traditional exponential model of van't Hoff nor an exponential Arrhenius equation provide unbiased estimates of respiration, as both systematically underestimate respiration at low temperatures and overestimate at high temperatures (Lloyd and Taylor, 1994; Fang and Moncrieff, 2001; Stoy and Zhang, 2004). Lloyd and Taylor (1994) recognized that the inadequacy of the Arrhenius model may be due to the assumption of a constant activation energy across the myriad of experimental temperatures encountered in respiration studies, despite evidence from kinetic theory that suggests the required activation energy of a chemical reaction will decrease with temperature (Kavanau, 1951). Therefore, Lloyd and Taylor (1994) developed an Arrhenius based respiration model according to a standardized 10°C temperature reference and introduced a temperature-adjusted, activation-energy-like parameter (their Equation 11).

More recently, investigators have proposed another exponential model for the relationship between temperature and respiration, based on the original exponential van't

Hoff equation, which includes the famous 'Q_{10}' parameter (Tjoelker et al. 2001). Q_{10} represents the sensitivity of respiration to temperature, more specifically, the proportional change in the rate of respiration for a 10°C change in temperature (Ryan, 1991; Franz et al. 2004). It has been recognized that plant and enzymatic Q_{10} decline with increasing temperature (Tjoelker et al. 2001), much like the activation energy in Arrhenius models (Lloyd and Taylor, 1994). As well, the calculation of Q_{10} is dependent upon the slope of the fitted model and the temperature range used in its derivation, therefore, Tjoelker et al. (2001) have suggested the use of a "temperature-corrected Q_{10}" exponential model, which has increased in use by researchers. The major scientific benefit of using either the Q_{10} model or Lloyd and Taylor approach is that it allows workers to compare rates of soil and ecosystem respiration at a standardized temperature that is ecologically meaningful (eg. 10°C).

1.5 Growing season carbon dioxide exchange of two contrasting peatlands

The major objective of this study was to improve the understanding of the ecological processes contributing to contemporary net CO_2 exchange in northern peatland ecosystems. Northern Alberta, Canada is a region that has > 20 % peatland cover (Johnson et al. 1995; Vitt et al. 1998), with wetland types spanning the bog to rich fen gradient readily accessible by road, providing a convenient opportunity for conducting comparative ecological studies between contrasting peatland types experiencing a similar climate. Comparison studies of peatland water chemistry (Vitt et al. 1975; Vitt et al. 1995), NPP (Szumigalski and Bayley, 1996a; Thormann and Bayley, 1997a, 1997b) and decomposition (Szumigalski and Bayley, 1996b) have been performed by others in the region and it was the aim of this study to extend the comparative studies to net CO_2 exchange measurements and analysis. Other researchers have employed a comparative approach to studying regional variation in surface mass and energy fluxes from Alaskan arctic tundra ecosystems during a single season using

mobile micrometeorological techniques (Eugster et al. 1997), and the present study applied similar methodology at contrasting peatlands located in the boreal region of northern Alberta.

Two peatland sites were selected for this study, and consisted of a *Sphagnum*-dominated poor fen and a *Carex*-dominated extreme-rich fen. These ecosystems represent the two opposite ends of the poor to extreme-rich fen gradient, and as such, differ significantly in plant species composition (poor fen dominated by non-vascular moss species *vs.* extreme-rich fen dominated by vascular plant species) and water chemistry characteristics (nutrient-limited poor fen *vs.* nutrient-rich extreme-rich fen). It was therefore hypothesized that GPP, TER and possibly NEE may also contrast between the peatland sites because of the differences between the ecosystems in dominant plant functional types and nutrient availability.

Based on intermittent CO_2 flux measurement campaigns and continuous supporting meteorological measurements made at the two contrasting peatland sites in northern Alberta during the 2004 growing season, empirical NEE and TER models were developed to address the following research questions: (1) Do the contrasting peatland types differ in terms of cumulative growing season carbon budgets (based on the magnitude of the CO_2 sink or source strength)? (2) Are the peak season rates of NEE different between the sites? (3) How do the contributing processes of GPP and TER influence questions (1) and (2) at each site? And (4) what environmental and biological factors exert the greatest control over photosynthesis and respiration in these peatland ecosystems?

2. Materials and Methods

2.1 Characteristics of study sites

2.1.1 Location, climate and general site descriptions

The peatland ecosystems studied during the 2004 growing season consisted of a poor fen and an extreme-rich fen and were located in north-central Alberta, Canada, within approximately 150 km and 1° latitude of each other. These two peatland sites act as auxiliary sites to the Western Peatland flux station of the Fluxnet-Canada Research Network (FCRN), one of seven ecosystem research stations located in a longitudinal transect across the southern boreal forest of Canada (FCRN, 2005).

The poor fen (55.54°N, 112.33°W; 730 m a.s.l.) was located approximately 120 km northeast of Athabasca, AB (54.82°N, 113.52°W), in the Central Mixedwood Subregion of the Boreal Natural Region of Alberta (Vitt et al. 1998; Alberta Natural Heritage Information Center, 2005). The extreme-rich fen (54.47°N, 113.32°W; 670 m a.s.l.) was located approximately 30 km south of Athabasca, in the Dry Mixedwood Subregion of the Boreal Natural Region. The climate of the region was classified as subhumid, continental, and was characterized by long, cold winters and short, cool summers, with a frost-free period of 85 to 90 days (Alberta Natural Heritage Information Center, 2005). The mean annual temperature for the region (Athabasca, AB) was 2.1°C (Environment Canada, 2002b). Average annual precipitation was 504 mm, with approximately 382 mm from rainfall and 122 mm from snowfall. Mean growing season (May to October) temperature was approximately 12°C with 370 mm of precipitation, the majority of which occurs in June and July (Environment Canada, 2002b).

The poor fen site (Figure 20, Appendix B) was a "patterned fen". Patterned fens are

characterized by open, wet pools or "flarks", alternating with drier, elevated ribs in the surface, orientated perpendicular to the direction of water flow in the peatland, known as "strings" (Vitt et al. 1998). The poor fen had a distinct microtopography, consisting of alternating hummocks (elevations in the peat surface), and hollows (depressions in the peat surface). The plant species composition (following Moss (1983) for vascular species and Anderson (1990) for *Sphagnum* spp.) of the poor fen was dominated by a continuous ground layer of *Sphagnum* spp., consisting of a mixture of *S. angustifolium* ([C. Jens. *ex* Russ.] C. Jens. *in* Tolf), *S. magellanicum* (Brid.), and *S. fuscum* ([Schimp.] Klinggr.). The evergreen shrub *Andromeda polifolia* (L.), the herb *Smilacina trifolia* ([L.] Desf.), and the sedge *Carex limosa* (L.) were present, as were dwarf (average height < 0.75 m) *Picea mariana* ([Mill.] BSP.) and *Larix laricina* ([Du Roi] K.Koch) trees along strings in the fen.

The extreme-rich fen site (Figure 21, Appendix B) was a sedge-dominated peatland that was part of a larger wetland complex, in a former north-south drainage channel (Vitt et al. 1995), and was located west of a 60 ha. lake (Thormann and Bayley, 1997a). The microtopography of this peatland was mainly flat, with occasional small hummocks. The depth of peat at the site ranged from 2 to 2.5 m (Thormann and Bayley, 1997a). The plant species composition (following Moss (1983) for vascular species and Anderson et al. (1990) for brown moss species) of the extreme-rich fen mainly consisted of *Carex lasiocarpa* (Ehrh.) and a discontinuous mat of the brown moss species *Drepanocladus aduncus* ([Hedw.] Warnst.) and *Aulacomnium palustre* ([Hedw.] Schwaegr.) occurring at the base of the sedge plants. Shrubs (average height < 0.5 m) covered approximately 5 % of the fen and consisted primarily of *Salix pedicellaris* (Pursh) and the occasional *Betula pumila* (L.) *var. glandulifera* (Regel). This site was studied by Vitt et al. (1995) and known as their "extreme-rich fen", as well as by Szumigalski and Bayley (1996a, 1996b) and Thormann and Bayley

(1997a, 1997b), and known as their "lacustrine sedge fen".

2.1.2 Surface water chemistry

To further characterize and verify classification of the peatland types under study, surface water was collected from both sites at mid-season (July 30, 2004) and analysed for a number of indicator chemical parameters of trophic status (Table 1). Ambient surface water was collected in 500 mL polystyrene bottles from standing hollow water at the poor fen and from a slight depression (< 10 cm) dug in the peat at the extreme-rich fen. The sample bottles were kept in a cooler until analysis began. The analysis of peatland surface water was performed by the Limnology Laboratory at the University of Alberta (Limnology Service Unit, 2005) in Edmonton, Alberta, beginning the morning of July 30, 2004.

Results from the chemical analyses verified the classification of peatlands studied, with all elemental and nutrient parameters being of lower concentration at the poor fen than at the extreme-rich fen (Table 1). In particular, the differences in the pH, electrical conductivity and base cation (Ca^{2+}, Mg^{2+}, and K^{+}) content between the sites illustrates the chemical gradient present from the acidic (pH = 4.0), nutrient-limited poor fen, and the close to neutral pH (6.5), nutrient-enriched surface waters of the extreme-rich fen. The values of the surface water chemical parameters (Table 1) fall within the range of Vitt (1994) for Canadian peatland classification of the poor to rich fen gradient, and those measured in other water chemistry studies by Vitt et al. (1995) and Thormann and Bayley (1997a) at the extreme-rich fen site.

2.2 Vegetation sampling and analysis

On July 1, July 29 and September 1, 2004 at the poor fen, and June 1, July 5, July 30 and September 26, 2004 at the extreme-rich fen, aboveground vascular and non-vascular plant biomass was harvested for analysis. Replicate samples (n = 6) were obtained by

randomly placing a 20 x 50 cm (0.1 m^2) Daubenmire frame within a 10 x 20 m (200 m^2) sampling plot that consisted of five 1.5 x 20 m (30 m^2) subplots, each separated by a row for walking. Vegetation was sampled in this manner to minimize disturbance to the peatland sites and any potential future samples of aboveground vascular and non-vascular plants.

At the poor fen, all aboveground vascular plant biomass in the randomly placed frame was clipped at ground level and a 10 x 10 cm subsample of *Sphagnum* moss was harvested. At the extreme-rich fen all aboveground vascular and non-vascular plant biomass was harvested from within the frame. Aboveground vegetation was separated by species into live (green tissue) and necrotic (standing dead) biomass. Live biomass was kept for further analysis while the standing dead was discarded. All live *Sphagnum* spp. (*S. angustifolium*, *S. magellanicum*, and *S. fuscum*) at the poor fen was combined as one vegetation type, as were all brown moss species (*D. aduncus* and *A. palustre*) present at the extreme-rich fen.

The total leaf area of vascular plants at the two sites was determined for all live tissue using a leaf area meter (model LI-3100 Area Meter, LI-COR, Lincoln, Nebraska, USA). Measurements were scaled up and ecosystem leaf area was expressed as a leaf area index (LAI, $m^2\ m^{-2}$). At the poor fen, a constant leaf area of 1 $m^2\ m^{-2}$ was assumed for the continuous *Sphagnum* moss ground cover and was added to the leaf area meter measurements of the vascular plant species, to give a total (vascular + non-vascular) LAI for the peatland. At the extreme-rich fen, brown moss area from each sample was determined with the leaf area meter and added to the vascular plant leaf area to determine total LAI for the ecosystem. Sorted vascular and non-vascular plant samples from each clip-plot were dried in an oven at 60°C for at least 48 h and then weighed with an electronic balance (model PJ400, Mettler, Greifensee, Switzerland). Weights were scaled up and aboveground biomass was expressed as g m^{-2}.

At the poor fen site, the contribution of the small *P. mariana* and *L. laricina* trees to the total aboveground biomass and LAI of the peatland was determined in November, 2004. Randomly selected, replicate 10 x 10 m quadrats (n = 12) within the poor fen were located with a GPS unit (model GPS12, Garmin International Inc., Olathe, Kansas, USA) and sampled. The height and basal diameter (diameter at peat surface) of every *P. mariana* and *L. laricina* tree within each quadrat was measured. Seven *P. mariana* trees that encompassed the range of individual heights encountered during the quadrat samping were harvested, and site-specific allometric models (following Szumigalski and Bayley, 1996a; Chen et al. 1997; Gower et al. 1999) were developed to correlate non-destructive measurements made (basal diameter and height) with total biomass and needle biomass. The allometric equation used was of the form,

$$\log_{10}(\text{biomass}) = A + B\,(\log_{10}(\text{basal diameter}^2 \times \text{height})), \qquad (5)$$

where A is the y-intercept, and B is the slope of the linear regression. The coefficient of determination (r^2) values of the regressions performed for the harvested *P. mariana* were 0.99 for total biomass and 0.97 for needle biomass. A correction factor was applied to all allometric equations to account for logarithmic bias (Sprugel, 1983; Gower et al. 1999). The *P. mariana* needle biomass (g m^{-2}) estimated from the quadrat measurements and allometric relationships was added to the vascular and non-vascular plant biomass from the frame harvests, to yield the total aboveground biomass at the poor fen. Total biomass of *L. laricina* at the poor fen was calculated with an allometric regression equation (from Szumigalski and Bayley, 1996a) derived for small *L. laricina* at a wooded, moderate-rich fen (54.47°N, 113.28°W) in the Athabasca region. Because *L. laricina* was estimated to be a negligible component of the aboveground biomass at the poor fen in the present study (total aboveground biomass ≈ 0.5 g m^{-2}), no *L. laricina* trees were destructively sampled to

determine site-specific allometric relationships, and *L. laricina* needles were not included in the total aboveground biomass or LAI. A subsample of small branches (n = 25) was used to determine the hemi-surface area of *P. mariana* needles at the poor fen using the volume displacement method (Appendix in Chen et al. 1997) and to develop a log-transformed allometric equation between needle biomass and hemi-surface area ($r^2 = 0.97$). This relationship was used to determine the LAI ($m^2\ m^{-2}$) of *P. mariana*, which was added to the leaf area of the moss and other vascular plants present, to give the total LAI at the poor fen for each of the periods that aboveground biomass was sampled.

The total N and C content of the *Sphagnum* spp., *C. limosa*, *A. polifolia*, *S. trifolia*, *P. mariana* and *L. laricina* from mid-season (July 29, 2004) at the poor fen, and *C. lasiocarpa* and the brown moss species (*D. aduncus* and *A. palustre*) from mid-season (July 30, 2004) at the extreme-rich fen was determined with an elemental analyser (model NC2500, CE Instruments, ThermoQuest Italia, Milan, Italy). Samples were homogenized with a coffee bean grinder or mortar and pestle, and mean N and C content as percent of weight were calculated for each species based on the replicate biomass samples (n = 6) from mid-season. As well, aboveground N content of each peatland ($g\ m^{-2}$) was estimated by accumulating the N content of all the species analysed, accounting for the proportion of aboveground biomass each constituted within the respective ecosystem.

2.3 Site micrometeorological infrastructure

Two triangular, lattice-type, aluminum instrumentation towers were installed at each of the peatland sites prior to the 2004 field season. The masts were mounted on separate wooden pallets and secured by 3 lengths of guy wire anchored to posts driven into the peat. Towers were regularly checked for level, and had to be adjusted slightly as was needed over the course of the season.

One tower at each site was equipped with a package of meteorological instruments that continuously monitored environmental conditions over the 6 months. Only the meteorological sensors with measurements relevant to this study are discussed henceforth. An air temperature and relative humidity probe (model HMP45C (Vaisala Inc.), Campbell Scientific, Inc., Logan, Utah, USA) inserted within a naturally ventilated radiation shield (model 41002, Gill Multi-Plate Radiation Shield, R.M. Young Company, Traverse City, Michigan, USA) was mounted on the meteorological tower at a height of 2 m. Net radiation was measured at a height of 3 m by a net radiometer (model NR Lite, Kipp & Zonen, Delft, The Netherlands). Incoming PPFD was measured at 3 m with a quantum sensor (model LI-190SA, LI-COR Inc., Lincoln, Nebraska, USA). A tipping-bucket rain gauge was used to measure event and cumulative precipitation (model CS700, Campbell Scientific, Inc., Edmonton, Alberta, Canada). Water table depth (WTD) relative to average hummock height was measured at each site in a well using a float and counterweight system attached to a potentiometer. All meteorological measurements, with the exception of the rain gauge, were recorded as half-hourly means by a datalogger (model CR23X Micrologger, Campbell Scientific Inc., Edmonton, Alberta, Canada). Data were downloaded from the datalogger to a laptop or palmtop computer system during site visits. Any missing meteorological data due to power failure or system maintanence (< 1 % of possible half-hour periods at the poor fen and 1.9 % of possible half-hour periods at the extreme-rich fen) were filled by linear interpolation.

A second instrumentation tower at each of the sites was used to support a mobile eddy covariance system (discussed in section 2.4.1) during intermittent flux measurement campaigns conducted over the growing season. Power was supplied to the instrumentation towers at each site by an array of six 12 V deep-cycle batteries that were charged by three 70

W solar panels (the two instrumentation towers and power supply at each site are shown in Figure 22, Appendix B).

2.4 Measuring net ecosystem exchange of CO_2, H_2O, and sensible heat

2.4.1 Eddy covariance measurements

The eddy covariance (EC) technique (Baldocchi et al. 1988; Moncrieff et al. 1997; Aubinet et al. 2000; Baldocchi, 2003) was used to measure net ecosystem fluxes of CO_2, water vapour (or latent heat (*LE*)) and sensible heat (*H*) at the two peatland sites. The mobile EC system consisted of a three-dimensional sonic anemometer-thermometer (SAT; model CSAT3, Campbell Scientific, Inc.), used to measure wind velocity and direction, as well as temperature fluctuations, and a fast response open-path infra-red gas analyser (IRGA; model LI7500, LI-COR Inc.), used to simultaneously measure changes in scalar (CO_2 and H_2O) molar densities (Figure 23, Appendix B). During each EC flux measurement campaign, the SAT and IRGA were installed side by side on separate horizontal booms mounted at a height of 3 m on the second instrumentation tower at the peatland sites. The instruments were orientated away from the tower towards the direction of prevailing winds (west), with a distance of 30 cm between the center of the transducers on the SAT and the midpoint of the IRGA's optical path. The IRGA was mounted at a 45° angle to the horizontal. Output signals from the SAT and IRGA were sampled at a frequency of 10 Hz by a programmed datalogger (model CR5000, Campbell Scientific Inc.) and recorded to a flash memory storage card.

Prior to the beginning of the 6 month field study, the open-path IRGA was calibrated for CO_2 using a certified gas standard referenced to the Canadian Greenhouse Gases Measurement Laboratory of the Meteorological Service of Canada (Downsview, Ontario) and for water vapour using a portable dew point generator (model LI-610, LI-COR Inc.). The single, mobile EC system was initially installed at the poor fen site on April 30, 2004, and

then moved back and forth between the two peatland sites every 12 to 18 days throughout the 2004 growing season (Table 2). As well, a comparison of CO_2, *LE* and *H* fluxes with a closed-path EC system was conducted at the main FCRN Western Peatland flux station (a treed, moderate-rich fen) from September 1 to September 7, 2004 (Appendix A). Each measurement campaign consisted of (1) setting up the portable EC system at a peatland site, (2) measuring and recording data for 12 to 18 days (a 1 GB data card would be full in ~ 18 days), (3) taking the equipment down, (4) swapping the full data card from the CR5000 for one that was empty, (5) calibrating the IRGA for CO_2 with certified standard gas in a temperature-controlled hut, and (6) moving and installing the equipment at the other peatland site for a new campaign. In most cases, steps 3 through 6 were completed in less than 24 hours (Table 2) with minimal downtime for the EC system.

Processing of high-frequency EC data was performed with a MATLAB (The Mathworks Inc., 2002) program. Peatland fluxes (*F*) of CO_2, H_2O, and *H* were calculated as the mean covariance of vertical wind velocity (*w*) and scalar concentration (*x*) fluctuations,

$$F = -\rho_a \overline{w'x'} \tag{6}$$

where *F* is the instantaneous vertical flux of CO_2 (μmol m^{-2} s^{-1}), H_2O (mmol m^{-2} s^{-1}), *LE* or *H* (W m^{-2}), ρ_a is the density of dry air (mol m^{-3}), *w* is the vertical wind velocity (m s^{-1}), and *x* is the scalar molar mixing ratio (mol mol^{-1} dry air) with over bars indicating time averaging. Primes denote instantaneous fluctuations from the 30 minute mean, for example:

$$w' = w - \overline{w} \tag{7}$$

$$x' = x - \overline{x} \tag{8}$$

Coordinate rotations (Baldocchi et al. 1988; Aubinet et al. 2000) were performed with the MATLAB program to align the mean vertical velocity measurements normal to the mean

wind streamlines prior to scalar flux calculations. A positive value for F represents net scalar flux into the atmosphere, while a negative value indicates net scalar flux into the ecosystem.

An air column CO_2 storage term (F_s) was added to the calculated CO_2 fluxes (F_c) for the determination of net ecosystem exchange (NEE),

$$NEE = F_c + F_s \quad (9)$$

and was estimated using the single level measurements of CO_2 concentration with the open-path IRGA and the following equation,

$$F_s = \frac{\rho_a h \Delta c}{\Delta t} \quad (10)$$

where F_s is the CO_2 flux storage term (μmol m^{-2} s^{-1}), ρ_a is the density of dry air (mol m^{-3}), h is the air column height beneath the EC sensors (m), Δc is the change in CO_2 mixing ratio (μmol mol^{-1}), and Δt is the change in time (s).

A filtering algorithm was applied in a series of two passes to remove significant outliers from the EC flux data sets at both peatland sites. During each pass, the data were filtered such that all half-hourly NEE values that were greater than 3 standard deviations from the mean were rejected and excluded from all further analysis and calculations.

A flux footprint analysis was conducted at both sites using the simple parameterisation of Kljun et al. (2004a, b). Using this model, a number of footprint estimations were calculated based on the input of σ_w, the standard deviation of vertical velocity fluctuations (m s^{-1}); $u*$, the friction velocity (m s^{-1}); Z_m, the SAT measurement height (m); h_{PBL}, the height of the planetary boundary layer (m); and estimates of Z_o, the roughness length (m) for each peatland ecosystem. The output from the footprint predictions gave X_{max}, the horizontal distance (m) from the EC tower with the maximum contribution to the measured fluxes, and $X_{90\%}$, the horizontal distance (m) from the EC tower within which 90 %

of measured fluxes originate, under the particular set of conditions input into the model.

At the poor fen, X_{max} varied between 30 and 50 m, while $X_{90\%}$ was estimated to be between 90 and 125 m from the EC tower, depending on the atmospheric conditions during the time that the footprint prediction was calculated. There was approximately 250 m of fetch to the west, 100 m to the north, 80 m to the east and 300 m to the south from the EC tower at the poor fen, indicating that the maximum surface contribution to measured fluxes always originated from within the peatland site, while fetch was slightly limited in the north, northeast and east directions. At the extreme-rich fen, X_{max} varied between 35 and 45 m, while $X_{90\%}$ was estimated to be between 110 and 120 m from the EC tower, depending on the atmospheric conditions during the time that the footprint prediction was calculated. There was approximately 120 m of fetch to the west, over 600 m to the north, 80 m to the east, and 220 m to the south of the EC tower at the extreme-rich fen. Therefore, the estimated maximum surface contribution to measured fluxes always originated from within the peatland, while fetch was slightly limited to the east of the EC tower.

2.4.2 Chamber respiration measurements

Total ecosystem respiration (TER) was measured at the two peatland sites in early and late July, 2004 with a portable gas exchange system (model LI-6200, LI-COR Inc., Lincoln, Nebraska, USA) and a dynamic, closed chamber (model LI-6000-09, Soil Respiration Chamber, LI-COR Inc.; see Figure 24, Appendix B). Black, ABS-plastic collars (15 cm long, 10 cm inside diameter) were inserted into the peat at each site in early June to a depth of either 6 or 10 cm, giving a total volume of the chamber and collar of 1680 cm^3 or 1366 cm^3. The chamber was vented to the atmosphere to maintain pressure equilibrium. Aboveground vegetation in the collars was left intact so that chamber measurements would reflect TER (plant + peat respiration).

A set of measurements was made at multiple collars (n = 12 at the poor fen, n = 9 at the extreme-rich fen) during intervals throughout the day in early July (July 1 and 4 at the poor fen; July 2 and 5 at the extreme-rich fen) and late July (July 29 at the poor fen; July 28 and July 30 at the extreme-rich fen). The rate of TER was calculated as the mean of all collars during a single set of measurements, which took 30 to 45 minutes to complete.

Mean rates of TER from each set of measurements in early and late July at both sites were fit to non-linear regressions as a function of the mean half-hourly air temperature (from the meteorological tower) for the respective period. Two regression models were utilized to investigate the relationship between TER and air temperature, to facilitate comparison between the peatland sites. The first model (Q_{10} - TER model) was based on the Q_{10} equation (Tjoelker et al. 2001),

$$\text{TER} = R_{10} Q_{10}^{\left(\frac{T-10}{10}\right)} \tag{11}$$

where R_{10} is the rate of TER (μmol m^{-2} s^{-1}) at 10°C, Q_{10} is the temperature sensitivity coefficient for TER (dimensionless), and T is air temperature (°C). The second model (L & T - TER model) used was Equation 11 from Lloyd and Taylor (1994),

$$\text{TER} = R_{10} e^{308.56\left(\frac{1}{56.02} - \frac{1}{T-227.13}\right)} \tag{12}$$

where R_{10} is the rate of TER (μmol m^{-2} s^{-1}) at 283.15 K (10°C) and T is air temperature (K).

Non-linear, least squares regressions were used to calculate the R_{10} and Q_{10} parameters for the TER models, as fit to the chamber respiration and T measurements. The regressions were performed with Systat10 (SPSS Inc., 2000) using the Gauss-Newton method, with the R_{10} parameter bound between 0.1 and 6.0 (μmol m^{-2} s^{-1}) for both TER models and Q_{10} between 1.8 and 2.2 for the Q_{10} - TER model (Eq. 11).

2.5 Growing season carbon budget calculations

Based on the continuous meteorological measurements and five EC flux campaigns conducted (Table 2) at each of the peatlands, carbon (CO_2-C) budgets for the 2004 growing season were calculated for the poor and extreme-rich fen sites. Data from each of the five flux campaigns were split into two time periods (Table 3) and mean diurnal patterns (bin-averages by time of day) of NEE, PPFD and air temperature were calculated for a total of ten time periods from each peatland. These mean diurnal trends were used to parameterize ten non-linear regression models, one for each of the distinct EC measurement periods at the peatland sites (Table 3). The initial non-linear regression equation (Q_{10} - NEE model) employed to investigate the relationship between NEE and the measured meteorological variables, PPFD and air temperature, was a combination of the common NEE light-response curve (Eq. 4) and the Q_{10}-TER model (Eq. 11),

$$\mathrm{NEE} = -\frac{A_{max}\,\alpha\mathrm{PPFD}}{A_{max}+\alpha\mathrm{PPFD}} + R_{10}Q_{10}^{\left(\frac{T-10}{10}\right)} \qquad (13)$$

where A_{max} is the ecosystem's maximum possible GPP (μmol m^{-2} s^{-1}) at infinite PPFD (μmol m^{-2} s^{-1}), α is the initial slope of the light-response curve or the photochemical efficiency (mol CO_2 mol^{-1} PPFD), R_{10} is the rate of TER (μmol m^{-2} s^{-1}) at 10°C, Q_{10} is the temperature sensitivity coefficient for TER (dimensionless), and T is air temperature (°C).

Non-linear, least squares regressions were used to calculate estimates of the A_{max}, α, R_{10} and Q_{10} parameters from the Q_{10} - NEE model (Eq. 13), as fit to the mean diurnal patterns of NEE, PPFD and T for each of the ten time periods at the two sites (Table 3). The regressions were performed with Systat10 (SPSS Inc., 2000) using the Gauss-Newton method, with the A_{max} parameter bound between 0.1 and 40 (μmol m^{-2} s^{-1}), α between 0.01 and 0.08 (mol CO_2 mol^{-1} PPFD), R_{10} between 0.1 and 6.0 (μmol m^{-2} s^{-1}) and Q_{10} between 1.8

and 2.2.

Each of the parameters (A_{max}, α, R_{10}, Q_{10}) derived from the modelled periods over the course of the growing season was plotted separately as a function of time (the day of year (DOY) that fell in the center of each modelled time period (Table 3)). Only the model parameters derived from time periods when the coefficient of determination (r^2) of the non-linear regression model was greater than 0.20 were plotted. Polynomial relationships were fit to each of the model parameters as a function of the DOY. The polynomial equations were then used to estimate the NEE model parameters (A_{max}, α, R_{10}, and Q_{10}) as dependent on time (DOY), over the course of the 2004 growing season between Period 1.1 and Period 5.2 (Table 3). For the beginning of the season at the extreme-rich fen site, May 1 to May 13, 2004 (DOY: 122-134), the parameters derived from the Period 1.1 (Table 3) non-linear regression model for that site were used. For the end of the season at the poor fen site, October 13 to October 31 (DOY: 287-305), the NEE model parameters from the Period 5.2 non-linear regression were used.

All half-hourly values of NEE over the 6 months were simulated for both of the peatland sites using the Q_{10} - NEE model (Eq. 13) as parameterized by DOY (daily values for each of the model parameters were calculated by the four respective polynomial relationships), and half-hourly measurements of the driving meteorological variables (PPFD and T). Modelled half-hourly NEE values were compared to available EC measurements of NEE over the 6 months at each of the sites using Model II (geometric mean) regressions (Sokal and Rohlf, 1995) and the modelling efficiency (ME) statistic (Janssen and Heuberger, 1995; Reichstein et al. 2002),

$$ME = 1 - \frac{\sum_{i=1}^{n}(NEE_{obs} - NEE_{mod})^2}{\sum_{i=1}^{n}(NEE_{obs} - \overline{NEE}_{obs})^2} \quad (14)$$

where NEE_{obs} are the available measurements of NEE by the EC system and NEE_{mod} are the corresponding modelled values of NEE for each half hour period.

The cumulative 2004 growing season C budgets for each peatland site were estimated in two ways. First, the CO_2-C balances were calculated solely as the sum of the modelled values of half-hourly NEE over the 6 months. Secondly, net CO_2 exchange over the 6 months was calculated by the integration of available EC measurements of NEE and gap-filling data with the NEE model when EC measurements were not available.

The u_* (friction velocity) threshold for acceptable CO_2 flux measurements by the EC system was varied by increments of 0.05 m s^{-1} (from $u_* > 0.0$ to $u_* \geq 0.25$ m s^{-1}) prior to the calculation of mean diel trends of NEE for each of the ten modelled periods and the subsequent derivation of seasonally-dependent non-linear regression model (Eq. 13) parameters. The six u_* thresholds applied to the EC measurements were separately used to model half-hourly NEE at the two peatland sites, and modelled estimations of NEE were compared to available EC measurements which satisfied the criteria (Table 4). From this u_* threshold analysis, it was determined from the slopes and r^2 values of the regressions between modelled and measured NEE (Table 4) that a threshold u_* of 0.15 m s^{-1} would be applied to EC measurements before the comparison of growing season C budgets or peak-season rates of NEE between the sites. The slope and r^2 values increased substantially with the u_* threshold from 0.10 to 0.15 m s^{-1} at both sites, but did not differ significantly at more stringent levels (0.20 and 0.25 m s^{-1}, Table 4). It was also important to retain the highest number of EC observations (n) as possible for the development of NEE models, which made

applying the u_* threshold of 0.15 m s^{-1} the most appropriate at both peatland sites. As well, visual inspection of nocturnal NEE measurements at the two sites provided further confidence in applying the 0.15 m s^{-1} threshold, as there was much greater variability in nighttime fluxes at lower u_* values (Figure 1).

As an additional methodological evaluation of the peatland CO_2 exchange models developed from EC measurements, a second non-linear regression model was used to study the relationship between the mean diurnal patterns of NEE ($u_* \geq 0.15$ m s^{-1}) and the measured meteorological variables, PPFD and T, from each of the ten periods listed in Table 3. The second NEE model (L & T - NEE model) was a combination of common NEE light-response curve (Eq. 4) and the L & T - TER model (Eq. 12),

$$\mathrm{NEE} = -\frac{A_{max}\alpha\mathrm{PPFD}}{A_{max}+\alpha\mathrm{PPFD}} + R_{10}e^{308.56\left(\frac{1}{56.02}-\frac{1}{T-227.13}\right)} \qquad (15)$$

where all parameters and variables are as defined in Eq. 13, with the exception of T being measured in K.

Non-linear, least squares regressions were used to estimate the A_{max}, α, and R_{10} parameters of the L & T - NEE model (Eq. 15), as fit to the mean diurnal trends of NEE, PPFD and T for each of the ten time periods with available EC measurements at the two sites (Table 3). The regressions were performed with Systat10 (SPSS Inc., 2000) using the Gauss-Newton method, with A_{max} bound between 0.1 and 40 (μmol m^{-2} s^{-1}), α between 0.01 and 0.08 (mol CO_2 mol^{-1} PPFD), and R_{10} between 0.1 and 6.0 (μmol m^{-2} s^{-1}).

Half-hourly rates of NEE and the 2004 growing season CO_2 - C balances at the two peatland sites were calculated using DOY-dependent L & T - NEE model (Eq. 15) parameters in the same manner as previously discussed for the parameters derived from the Q_{10} - NEE model (Eq. 13) regressions. Modelled half-hourly NEE values using the L & T -

NEE model were compared to available EC measurements over the 6 months at each of the sites using Model II (geometric mean) regressions (Sokal and Rohlf, 1995) and the modelling efficiency statistic (Janssen and Heuberger, 1995; Reichstein et al. 2002; Eq. 14).

2.6 Estimation of uncertainty in net ecosystem exchange measurements

To evaluate the relative error of the growing season C budgets calculated for the two peatland sites based on the measurement of NEE by the EC system, uncertainty analyses were performed. The uncertainty associated with EC measurements consists of random and systematic errors (Goulden et al. 1996; Baldocchi, 2003). The major random errors in NEE measurements are related to the EC system instrumentation, as well as, statistical uncertainties associated with variation in the turbulent transport of scalars and flux footprint heterogeneity (Aurela et al. 2002; Flanagan and Johnson, 2005; Hollinger and Richardson, 2005). The prevalent systematic error associated with EC flux measurements is related to the degree of turbulent mixing and any corresponding screening procedures applied, such as the use of a u_* threshold for acceptable values (Aurela et al. 2002; Flanagan and Johnson, 2005). Generally, the higher the limit is for u_*, the greater the TER and lower the NEE (Aurela et al. 2002), due to the underestimation of ecosystem respiration under atmospheric conditions of inadequate turbulent mixing, especially during nocturnal hours (Goulden et al. 1996).

The composite random error of the EC measurements in the present study was estimated using two different methods. First, the random error was calculated using the repeated sampling method or daily differencing approach (Hollinger and Richardson, 2005),

$$E_{RI} = \frac{1}{\sqrt{2}}\sigma(x_1 - x_2) \qquad (16)$$

where E_{RI} is the random error associated with the EC measurements, as calculated based on the standard deviation (σ) of differences between measurements of NEE made at the same

site on different days (x_1 and x_2), at the same time of the day and under similar environmental conditions (differences in PPFD < 75 μmol m^{-2} s^{-1}, T < 3°C, and wind speed < 1 m s^{-1}).

The second approach utilized to estimate the random error of NEE calculations at the peatland sites consisted of evaluating the differences between available EC measurements and modelled values (Aurela et al. 2002),

$$E_{R2} = \sqrt{\frac{\sum_{i=1}^{n}(NEE_{obs} - NEE_{mod})^2}{(n-1)n}} \qquad (17)$$

where E_{R2} is the random error associated with the statistical uncertainties of EC measurements and the scatter in the model results. NEE_{obs} refers to available half-hourly measurements of NEE by the EC system ($u^* \geq 0.15$ m s^{-1}), NEE_{mod} are the corresponding modelled values of NEE obtained using either the Q_{10} - NEE model or the L & T - NEE model approaches, and n is the number of half-hourly NEE measurements ($u^* \geq 0.15$ m s^{-1}) over the 2004 growing season.

To estimate the systematic error (E_{SYS}) of NEE measurements by the EC system as related to the degree of turbulent mixing, a u^* sensitivity test was performed. This was accomplished by varying the u^* threshold for acceptable NEE values prior to the calculation of cumulative growing season CO_2 balances at each peatland site. Separate 6 month CO_2-C budgets were calculated using u^* thresholds of 0.10, 0.15, 0.20 and 0.25 m s^{-1}, and the derived Q_{10} - NEE model (Eq. 13) parameters for each. The differences between the CO_2-C budgets calculated with the four u^* thresholds were used to estimate the relative systematic uncertainty of NEE measurements at each site.

The total uncertainty of the 6 month carbon balances for each of the peatland sites was calculated using two separate approaches, according to the method employed to estimate the random error (E_{R1} (Eq. 16) or E_{R2} (Eq. 17)). The estimates of random and systematic

uncertainty associated with the EC measurements of NEE were combined in quadrature, according to the error accumulation principle, to obtain separate total estimations of error using the two different methods ($E_{R1} + E_{SYS}$ and $E_{R2} + E_{SYS}$).

Table 1. Comparison of surface water chemistry parameters between the two contrasting peatlands in northern Alberta during the 2004 growing season. Surface water was collected for analysis from each peatland site in late July 2004.

	Poor Fen	Extreme-rich Fen
pH	4.0	6.5
Conductivity ($\mu S\ cm^{-1}$)	42.5	180.3
NH_4^+ ($\mu g\ L^{-1}$)	47.4	423.1
NO_3^- ($\mu g\ L^{-1}$)	5.2	29.6
Total P ($\mu g\ L^{-1}$)	19.3	488.1
K^+ ($mg\ L^{-1}$)	0.53	14.8
Ca^{2-} ($mg\ L^{-1}$)	0.86	18.2
Mg^{2+} ($mg\ L^{-1}$)	0.33	6.90

Table 2. Eddy covariance (EC) measurement campaigns at the two peatland sites in northern Alberta during the 2004 growing season. Time periods according to the day of year are shown in brackets below calendar dates (2004 was a leap year). A comparison between the open-path EC system used in this study and a closed-path EC system was conducted from September 1 to September 7, 2004 at the main FCRN Western Peatland flux station (Appendix A).

	Poor Fen	Extreme-rich Fen
Period 1	May 1 - May 13 (122 - 134)	May 14 - May 31 (135 - 152)
Period 2	June 1 - June 17 (153 - 169)	June 17 - July 5 (169 – 187)
Period 3	July 7 - July 25 (189 - 207)	July 27 - August 13 (209 – 226)
Period 4	August 13 - August 31 (226 - 244)	September 13 - September 26 (257 – 270)
Period 5	September 27 - October 12 (271 - 286)	October 12 - October 30 (286 – 304)

Table 3. Eddy covariance measurement periods used to parameterize seasonally-dependent non-linear regression models at the two peatland sites during the 2004 growing season. The day of year in the middle of each time period is given in parentheses below the calendar dates.

	Poor Fen	Extreme-rich Fen
Period 1.1	May 1 - May 6 (124)	May 14 - May 22 (139)
Period 1.2	May 7 - May 13 (131)	May 23 - May 31 (148)
Period 2.1	June 1 - June 8 (156)	June 17 - June 25 (173)
Period 2.2	June 9 - June 17 (165)	June 26 - July 5 (183)
Period 3.1	July 7 - July 15 (193)	July 27 - August 4 (213)
Period 3.2	July 16 - July 25 (202)	August 5 - August 13 (222)
Period 4.1	August 13 - August 22 (230)	September 13 - September 19 (260)
Period 4.2	August 23 - August 31 (239)	September 20 - September 26 (267)
Period 5.1	September 27 - October 4 (274)	October 12 - October 20 (290)
Period 5.2	October 5 - October 12 (282)	October 21 - October 30 (299)

Table 4. The effect of applying various friction velocity (u_*) thresholds to eddy covariance (EC) measurements on peatland CO_2 exchange models. Column headers (in *italics*) are u_* thresholds (m s^{-1}), for which the EC values used in the derivation of Q_{10} - NEE model (Eq. 13) parameters must satisfy $u_* \geq x$. The slope of the regression between modelled and measured NEE is given for each u_* threshold, with the 95 % confidence intervals in parentheses. r^2 is the coefficient of determination for the regression, and n is the number of half-hourly EC observations over the 6 month study which satisfy the u_* threshold criteria.

		0.0	*0.05*	*0.10*	*0.15*	*0.20*	*0.25*
Poor Fen	slope	0.50 (0.49-0.52)	0.61 (0.58-0.63)	0.83 (0.81-0.86)	0.93 (0.90-0.96)	0.95 (0.92-0.97)	0.93 (0.90-0.96)
	r^2	0.26	0.26	0.60	0.74	0.76	0.73
	n	2971	2565	2047	1708	1399	1065
Extreme-rich Fen	slope	0.77 (0.75-0.80)	0.77 (0.75-0.80)	0.80 (0.78-0.82)	0.98 (0.96-1.00)	0.98 (0.96-1.00)	1.07 (1.04-1.10)
	r^2	0.36	0.50	0.59	0.79	0.82	0.80
	n	2965	2585	2172	1760	1405	1029

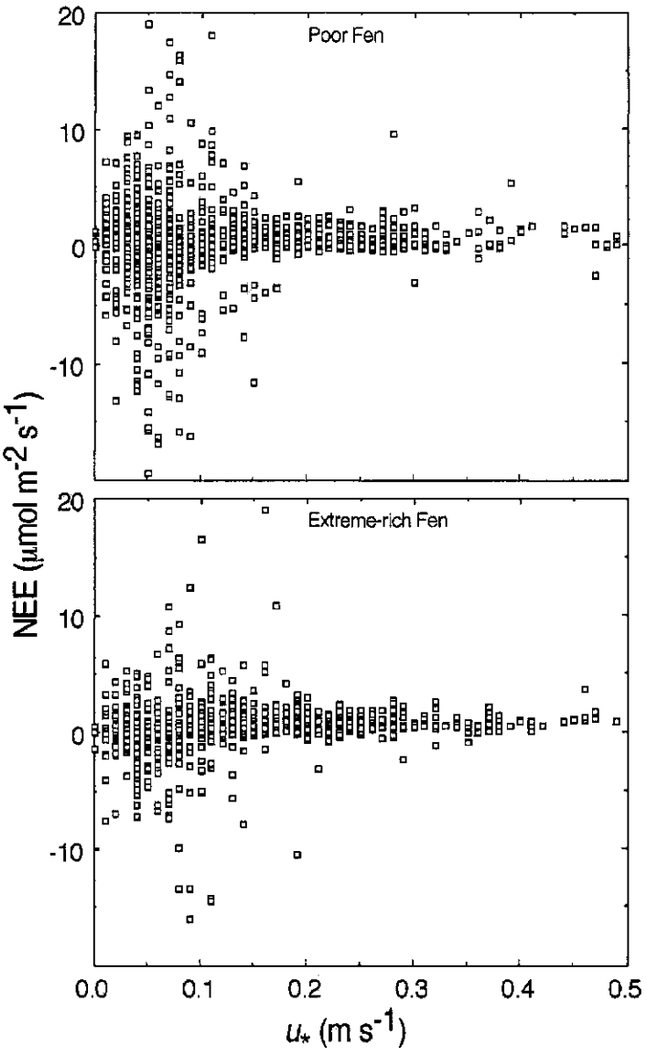

Figure 1. Relationship between nocturnal (PPFD < 1 μmol m^{-2} s^{-1}) net ecosystem exchange (NEE) and friction velocity (u_*) at the two peatland sites in northern Alberta during the 2004 growing season.

3. Results

3.1 Meteorological and environmental conditions

With the exception of July, the 2004 growing season (May – October) in northern Alberta was characterized by cooler than normal average daily temperatures at both peatland sites, and the poor fen consistently had lower average temperatures than the extreme-rich fen (Table 5). However, the 6 month mean daily temperatures at both sites were not significantly different from the average conditions at Athabasca (54.82°N, 113.52°W), the location of the nearest W.M.O standardized meteorological station, according to the standard deviation of the 30-year (1971 - 2000) normal (Table 5). Interestingly, the poor fen experienced minimum temperatures below 0°C every month of this 6 month study, while sub-zero temperatures only occurred during May, June, September, and October at the extreme-rich fen. Maximum mean half-hourly temperatures at the sites over the 6 month period were 27.8°C and 28.9°C, occurring in August at the poor fen, and July at the extreme-rich fen, respectively.

Over the course of the 6 months (May - October, 2004), the poor fen received slightly above-average precipitation (449.6 mm) while the extreme-rich fen had near-normal accumulation (394.0 mm) compared to the 30-year mean (± SD) of 370.4 ± 80.7 mm (Table 6). The monthly precipitation totals exhibited variability between the sites in May, July, August, and September, as well as deviation from the 30-year normals at Athabasca during many months of this study (Table 6). For example, in May, July, and September, near-normal precipitation amounts were recorded at the extreme-rich fen, while the poor fen received significantly more moisture compared to the 30-year means during these months. The opposite situation occurred in August, in which precipitation inputs were above-average at the extreme-rich fen, and closer to normal at the poor fen. In June, both sites were drier than the regional mean, while in October both received average precipitation amounts.

The poor fen received more incident photosynthetically-active radiation every month of the 2004 growing season study than the extreme-rich fen (Table 7). The cumulative incident photosynthetically-active photon flux density over the entire 6 month study was approximately 1000 mol m^{-2} greater at the poor fen site than the extreme-rich fen site (Table 7).

During the 2004 growing season, the water table was always < 40 cm below the average hummock height at the poor fen, and < 30 cm beneath the average hummock height at the extreme-rich fen (Figure 2). Decreases and increases in water table depth were related to the intensity and frequency of precipitation at the sites, as indicated by the rapid response of the water table to dry and wet periods over the summer. During the first half of summer, both sites displayed a similar pattern of changes in water table depth, as the water table decreased at the poor fen throughout June (DOY: 153-182) and at the extreme-rich fen during late June (DOY: 170-182), and increased at both sites significantly during a number of wet days in July (DOY: 183-213, Figure 2). At the poor fen site during the second half of summer, the water table dropped over most of August (DOY: 214-240), then rose after a number of precipitation events in late August (DOY: 241-244) and the first half of September (DOY: 245-260), then receded slightly by the end of the study. In contrast, at the extreme-rich fen during the second half of the season, the water table continued to rise throughout August and into early September (DOY: 214-250), eventually stabilizing within 10 cm below the average hummock height by the end of the study, and about 10 cm higher than it was in early June (DOY: 153, Figure 2).

3.2 Aboveground biomass production and plant community characteristics

The poor fen had a greater amount of live aboveground biomass and a higher leaf area index (LAI) than the extreme-rich fen throughout the 2004 growing season (Figure 3).

Live aboveground biomass and LAI (mean ± SE, n = 6) at the poor fen peaked in late July (DOY: 211) at 230.9 ± 15.3 g m^{-2} and 1.52 ± 0.03 m^2 m^{-2}, respectively. At the extreme-rich fen these values were 157.1 ± 16.6 g m^{-2} for peak live aboveground biomass and 1.09 ± 0.06 m^2 m^{-2} for peak LAI (DOY: 212, Figure 3). The total nitrogen (N) content (mean ± SE, n = 6) of the live aboveground biomass in late July 2004 at the extreme-rich fen was calculated to be 3.0 ± 0.1 g m^{-2}, which was about 1.3 times greater than that of the poor fen at 2.3 ± 0.2 g m^{-2}.

The plant community of the poor fen site was dominated by non-vascular *Sphagnum* spp., as indicated by the live aboveground biomass of each plant species at the peak of the 2004 growing season (Table 8). *A. polifolia*, *C. limosa*, *S. trifolia* and *P. mariana* also significantly contributed to the total aboveground biomass of the poor fen, while *Oxycoccus microcarpus* (Turcz.), a *Salix* sp., *Menyanthes trifoliata* (L.) and *Drosera rotundifolia* (L.) were present at the site in much smaller quantities than the dominant species. At the extreme-rich fen, the live aboveground biomass at the peak of the growing season was dominated by *C. lasiocarpa* and brown moss species (Table 8). *Rumex* sp., *Galium trifidum* (L.), *Rubus acaulis* ([Michx.] Focke.) and *S. pedicellaris* were also present at the extreme-rich fen site, with much lower values of live aboveground biomass than the dominant plant species.

The *Sphagnum* spp. at the poor fen comprised approximately 66 % of the total LAI at the site and had a total N content of 7.8 mg g^{-1} at the peak of the 2004 growing season (Table 9). In contrast, the dominant plant species at the extreme-rich fen site, the vascular perennial sedge, *C. lasiocarpa,* accounted for approximately 60 % of the total LAI, and had a total N content of 19.3 mg g^{-1} in late July (Table 9). The ratio of C:N at the peak of the 2004 growing season was approximately 57.4 for the *Sphagnum* spp. capitula at the poor fen, and 23.6 for

the *C. lasiocarpa* leaves at the extreme-rich fen (Table 9), the species that are the most significant litter and peat producers in each respective ecosystem.

3.3 Eddy covariance measurements

3.3.1 Sensible and latent heat exchange

There was a significant difference between the peatland sites in the mean diurnal trends of sensible (*H*) and latent (*LE*) heat fluxes during the first three EC measurement campaigns of the 2004 growing season (Figure 4). At the poor fen, the mean diurnal patterns of *LE* values were always greater than *H* values during the first three measurement periods, resulting in mean Bowen ratios (*H*:*LE*) that were less than 1. The partitioning of turbulent heat fluxes exhibited a different trend during the early season at the extreme-rich fen site, where mean diurnal *H* values exceeded *LE* during much of first two EC measurement periods, with mid-day Bowen ratios greater than unity (Figure 4). However, as the growing season progressed, mean diurnal values of *LE* surpassed those of *H* at the extreme-rich fen (Period 3, Figure 4), and the mean Bowen ratios dropped below unity for all times of the day. Mean diurnal values of *LE* continued to be greater than *H* for all times of the day at both peatland sites for the remainder of the 2004 growing season (Period 4 and Period 5, data not shown).

The relationships between net radiation and the sum of turbulent heat fluxes ($H + LE$) from Period 3 (peak season) and for all EC measurement periods combined (Period 1 - Period 5), were highly significant for both sites (Figure 5). Unfortunately, the ground (storage) heat flux was not measured or calculated at either peatland site, therefore these relationships do not provide a test for energy balance closure. However, the slope of the regressions between net radiation and the resultant heat fluxes were slightly lower at the poor fen than the extreme-rich fen site (Figure 5), perhaps indicative of a larger energy storage

term at the poor fen site.

3.3.2 Seasonal trends in net ecosystem exchange

The first (Period 1) and last (Period 5) EC measurement campaigns at the two sites (Table 2) represent the beginning and end of the growing season and do not exhibit significant diurnal trends of NEE (Figure 6). The three EC campaigns conducted at the sites between the beginning and end of the season (Period 2 - Period 4, Table 2) show distinct diurnal patterns of NEE, with net CO_2 uptake reaching a maximum at approximately local noon and significant loss of CO_2 to the atmosphere occurring during night hours at both sites (Figure 6). As well, the mean nocturnal and early morning NEE values exhibit a lot more variability (greater SE) than daytime measurements, mainly due to less replication because of inadequate turbulent mixing, and other limitations inherent to open-path EC measurements, such as possible dew formation and frost accretion on the IRGA during these times.

At the poor fen, the mean daily minimum of NEE was approximately -2 μmol m^{-2} s^{-1} during Period 2 (June 1 - June 17), -5 μmol m^{-2} s^{-1} during Period 3 (July 7 - July 25), and -4 μmol m^{-2} s^{-1} for Period 4 (August 13 - August 31) of the 2004 growing season (Figure 6). The typical average nighttime NEE values measured at the poor fen, which correspond to total ecosystem respiration, ranged from approximately 1 μmol m^{-2} s^{-1} during Period 2, to 2 μmol m^{-2} s^{-1} during Period 3 and Period 4. At the extreme-rich fen, the mean daily minimum of NEE was approximately -3 μmol m^{-2} s^{-1} during Period 2 (June 17 - July 5), -5 μmol m^{-2} s^{-1} for Period 3 (July 27 - August 13), and -2 μmol m^{-2} s^{-1} for Period 4 (September 13 - September 26). The mean rates of nighttime NEE during these same periods at the extreme-rich fen were approximately 1 μmol m^{-2} s^{-1} for Period 2 and Period 4, and 2 μmol m^{-2} s^{-1} during Period 3 (Figure 6).

There was a significant correlation between NEE, light input (PPFD) and air temperature (T) for Period 2, Period 3, and Period 4 at both peatland sites during the 2004 growing season (Table 10; Table 11). Seasonal variation was observed from Period 2 to Period 4 in the photosynthetic (A_{max} and α) and respiratory (R_{10}) capacities at each of the peatland sites based on the Q_{10} - NEE model (Eq. 13, Table 10) and the L & T - NEE model (Eq. 15, Table 11). The A_{max} parameter varied from 3.9 to 9.8 μmol m^{-2} s^{-1} at the poor fen and between 5.6 and 12.8 μmol m^{-2} s^{-1} at the extreme-rich fen for these EC measurement periods (Table 10; Table 11). The photochemical efficiency (α) was similar at both sites for each of the time periods, and varied from 0.016 to 0.034 mol mol^{-1}, while the normalized rate of TER, R_{10}, was between 1 and 2 μmol m^{-2} s^{-1} for both of the fitted NEE models (Table 10, Table 11). The Q_{10} parameter (from the Q_{10} - NEE model, Eq. 13) was consistently 1.8 during these periods at the poor fen, and declined from 2.0 to 1.8 at the extreme-rich fen (Table 10). However, Q_{10} did not differ significantly from 2 for either site or time period, as it was bound between 1.8 and 2.2 for the non-linear regressions.

3.3.3 Peak growing season net ecosystem exchange

At the peak of the 2004 growing season, the diurnal trends of NEE at the two contrasting peatland ecosystems were similar (Figure 7). Both sites exhibited a mean peak rate of net CO_2 uptake of approximately 5 μmol m^{-2} s^{-1}, and nighttime rates of CO_2 loss of approximately 2 μmol m^{-2} s^{-1} during the mid-season periods.

Peak 2004 growing season light-response curves of gross primary production (GPP) at the two sites were derived using the Q_{10} - NEE model (Eq. 13) as fit to Period 3 (Table 2) mean diel patterns of NEE, PPFD and T (Figure 8). The peatlands had very similar photochemical efficiencies (initial slope of light-response curve, α) but differed in their

maximum photosynthetic capacities (A_{max}) at this time. The extreme-rich fen had a significantly greater photosynthetic capacity (A_{max}) than the poor fen at the peak of the growing season, according to the 95 % C.I. of the parameter estimate, with a value of 12.1 compared to 9.2 μmol m^{-2} s^{-1} according to the Q_{10} - NEE model (Table 10) and 12.8 compared to 9.8 μmol m^{-2} s^{-1} according to the L & T - NEE model (Table 11).

3.4 Chamber respiration measurements

There was a significant correlation between air temperature and measurements of TER using the chamber method at both peatland sites in early and late July 2004 (Figure 9). Two different non-linear regression models for TER were fit to the chamber measurement campaigns (Table 12). Both models fit the data well with coefficients of determination (r^2) ranging from 0.77 to 0.91. The L & T - NEE model consistently gave lower R_{10} values than the Q_{10} - TER model, however these values were not significantly different (Table 12). The poor fen had significantly lower R_{10} values than the extreme-rich fen in both early and late July, according to both TER models. The R_{10} parameter decreased at both sites between early and late July, however, this was only significant according to the L & T - TER model (Table 12). The Q_{10} parameter, used only in the Q_{10} - TER model (Eq. 11), did not differ significantly from 2 for either site or time, because it was bound between 1.8 and 2.2 for the non-linear regressions.

3.5 Growing season carbon budget calculations

The two non-linear regression models (the Q_{10} - NEE model (Eq. 13) and the L & T - NEE model (Eq. 15)) fit the relationship between NEE and the driving meteorological variables (T and PPFD) much better for EC measurement campaigns conducted during periods of significant biological activity (Period 2.1 to Period 4.1) than those at the beginning and end of the 2004 growing season, according to the r^2 values of the non-linear

regressions (Table 13; Table 14). At the poor fen site, the r^2 values for the Period 1.2 non-linear regressions were < 0.20 according to both NEE models (Table 13), so the photosynthetic and respiration parameters derived from this time were not included in the DOY-dependent polynomial fits (Figure 10). At the extreme-rich fen site, the r^2 values for the Period 4.2 and Period 5.2 non-linear regressions were < 0.20, according to both NEE models (Table 14), so the photosynthetic and respiration parameters derived from these two times were discarded from the DOY-dependent polynomial fits (Figure 10).

There was close correspondence in the seasonal trends of estimated non-linear regression parameters (A_{max}, α, R_{10}) describing NEE using either the Q_{10} - NEE model (Eq. 13) or the L & T - NEE model (Eq. 15) over the course of the 6 month study (Figure 10). At the poor fen, there was excellent agreement between the two NEE models for estimates of α (slope = 1.03, r^2 = 0.99) and R_{10} (slope = 0.97, r^2 = 0.97), while the parameter estimates for A_{max} were slightly higher using the L & T - NEE model than using the Q_{10} - NEE model (slope = 1.05, r^2 = 1.00). At the extreme-rich fen, there was close agreement between the two NEE models for estimates of A_{max} (slope = 1.03, r^2 = 1.00) and α (slope = 1.01, r^2 = 0.99), while there was more variability in the estimates of R_{10} (slope = 0.94; r^2 = 0.51).

A_{max} ranged from approximately 1 to 11 μmol m^{-2} s^{-1} at the poor fen and from 0.5 to 15 μmol m^{-2} s^{-1} at the extreme-rich fen over the course of the season, while α ranged from approximately 0.010 to 0.040 mol mol^{-1} at the poor fen and 0.010 to 0.030 mol mol^{-1} at the extreme-rich fen (Table 10; Table 11; Figure 10). The estimated seasonally-dependent values for R_{10} ranged from approximately 0.1 to 2.4 μmol m^{-2} s^{-1} at the poor fen and from 0.8 to 2.0 μmol m^{-2} s^{-1} at the extreme-rich fen. As was the case with modelling the chamber respiration measurements with the Q_{10} - TER model (Eq. 11), Q_{10} was bound between 1.8 and 2.2 at

both sites when fitting the Q_{10} - NEE model (Eq. 13), and as such, did not show a distinct seasonal pattern (Figure 10). The r^2 values of the polynomial relationships between NEE model parameter estimates and time (day of year) were always ≥ 0.57 for A_{max}, α, R_{10}, and < 0.50 for Q_{10} for the two peatland sites (Table 15).

According to the Model II regressions performed, there was good agreement between modelled half-hourly NEE, using either non-linear regression model (Eq. 13 or Eq. 15), and available EC measurements ($u_* \geq 0.15$ m s^{-1}) over the 6 month study (Figure 11; Figure 12). The models fit the measured fluxes better at the extreme-rich fen than the poor fen, as indicated by the higher slope and r^2 values. At the poor fen, the Q_{10} - NEE model fit the measured fluxes slightly better than the L & T - NEE model, according to higher slope and r^2 values (Figure 11; Figure 12). For the extreme-rich fen site, there was little difference between the relationships of modelled and measured NEE using the two different models. Calculation of the modelling efficiency (*ME*) statistic (Eq. 14) gave similar patterns of correspondence between modelled and measured NEE at the two sites as did the r^2 values of the Model II regression results. At the poor fen, *ME* was 0.73 for the Q_{10} - NEE model and a lower value of 0.66 for the L & T - NEE model. The calculated *ME* for NEE at the extreme-rich fen site was 0.78 for the Q_{10} - NEE model and 0.75 for the L & T - NEE model.

The monthly CO_2-C budgets calculated from the models illustrate a distinct seasonal difference between the two peatland sites (Figure 13). According to the Q_{10} - NEE model, the poor fen was a net CO_2 sink for four of the six months (peaking at 44 g C m^{-2} in July) and a slight CO_2 source of 3 g C m^{-2} in May and September of 2004. In contrast, the Q_{10} - NEE model calculated that the extreme-rich fen was a significant net CO_2 sink for only two of the months over the growing season (peaking at 30 g C m^{-2} in August), a CO_2 source of 8 g C m^{-2} in May, a source of 13 g C m^{-2} in October, and essentially CO_2 neutral in June and September

(Figure 13). The L & T - NEE model indicated a similar seasonal pattern of monthly CO_2 exchange for the poor fen, with the exception of May and September being modelled slight CO_2 sinks rather than sources as calculated from the Q_{10} - NEE model (Figure 13). For the extreme-rich fen, the monthly CO_2 exchange pattern according to the L & T - NEE model was slightly different than that modelled with the Q_{10} - NEE model, with June calculated to be a slight CO_2 sink rather than source, and September a significant CO_2 sink of -8 g C m^{-2}. However, a distinct seasonal difference in the magnitudes of monthly CO_2 exchange was evident between the sites using either approach to modelling NEE, and this was especially pronounced in June (Figure 13).

When integrated over the entire 6 month study period, the poor fen was modelled to be a net C sink that was two to three times greater than the extreme-rich fen, depending on the respiration model employed to determine NEE (Table 16). The integration of available EC measurements and gap-filling periods with either non-linear regression model consistently gave slightly more negative values for the growing season sums of NEE (greater CO_2-C sink) at the two peatland sites. The Q_{10} - NEE model gave slightly lower values of total GPP, TER and NEE than the L & T - NEE model at both sites (Table 16) but the values of the three components of the 6 month C budgets were similar. The poor fen had lower totals of GPP and TER than the extreme-rich fen, but the balance between competing CO_2 fluxes was much closer at the extreme-rich fen resulting in a lower net C gain (NEE) over the 2004 growing season (Table 16). Both approaches to estimating the 6 month C budgets for the peatland sites gave similar ratios of total carbon loss through respiration (TER) to total carbon gain via photosynthesis (GPP). The ratio of cumulative TER:GPP was approximately 0.7 at the poor fen and 0.9 at the extreme-rich fen for the 2004 growing season, according to both models.

3.6 Estimation of uncertainty in net ecosystem exchange measurements

Using the daily differencing approach (Eq. 16), a composite random uncertainty of 33.3 % (based on an absolute E_{R1} value of 0.7 μmol m^{-2} s^{-1} and an average 6 month NEE (absolute) value of 2.1 μmol m^{-2} s^{-1}) was calculated for the EC measurements conducted at the poor fen over the entire 2004 growing season. A composite random error of 43.7 % (based on an absolute E_{R1} value of 0.7 μmol m^{-2} s^{-1} and an average 6 month NEE (absolute) value of 1.6 μmol m^{-2} s^{-1}) was obtained for the extreme-rich fen site according to the daily differencing approach.

The random error, associated with the EC measurements of NEE, estimated using the second approach (E_{R2}, Eq. 17) was much lower than the random uncertainty calculated using the daily differencing approach (E_{R1}, Eq. 16). At the poor fen site, the calculation of E_{R2} resulted in composite random error estimations of 1.7 % and 1.9 % using the Q_{10} - NEE model (Eq. 13) and L & T - NEE model (Eq. 15) respectively, when modelling half-hourly rates of NEE. For the extreme-rich fen site the calculation of E_{R2} gave random error estimates of 2.3 % and 2.5 %, applying the Q_{10} - NEE model (Eq. 13) and L & T - NEE model (Eq. 15) approaches respectively.

The systematic error (E_{SYS}) of EC measurements associated with the degree of turbulent mixing was estimated by performing a u_* threshold sensitivity analysis on the cumulative growing season CO_2-C budgets at each site. The u_* sensitivity analysis for the poor fen site gave 6 month CO_2 exchange balances of -83, -90, -84 and -76 g C m^{-2} (as calculated with the Q_{10} - NEE model) for u_* thresholds of 0.10, 0.15, 0.20 and 0.25 m s^{-1}, respectively. This results in an estimation of E_{SYS} at the poor fen of ± 7 g C m^{-2} or 7.8 % on the $u_* \geq 0.15$ m s^{-1} net CO_2 balance of -90 g C m^{-2} 6 $months^{-1}$. At the extreme-rich fen site,

cumulative growing season CO_2 budgets of -60, -31, -39, and -24 g C m^{-2} were obtained using $u*$ thresholds of 0.10, 0.15, 0.20 and 0.25 m s^{-1}, respectively. This results in an estimation of E_{SYS} at the extreme-rich fen site of ± 18 g C m^{-2} or 58.1 % on the $u* \geq 0.15$ m s^{-1} net CO_2 balance of -31 g C m^{-2} 6 $months^{-1}$.

The total relative error for the EC measurements of NEE at the poor fen site was 34.2 % using the first approach to calculating total uncertainty ($E_{R1} + E_{SYS}$) and 8.0 % using the second method ($E_{R2} + E_{SYS}$), according to the error accumulation principle. For the extreme-rich fen, total relative uncertainties of 72.7 % and 58.1 % were obtained using the first and second approaches to estimating the total error associated with the EC measurements.

Table 5. Comparison of mean daily temperatures (°C) at the two northern Alberta peatland sites for six months during the 2004 growing season. 30-year normals (1971-2000) are from Athabasca, Alberta (54.82°N, 113.52°W) and represent the mean ± SD. Mean daily temperatures were considered significantly different from the average conditions at Athabasca if they were outside of the monthly 30-year normal ± SD, and are indicated with **bold** text.

	Poor Fen	Extreme-rich Fen	30-year normal
May	**4.5**	**7.2**	10.6 ± 1.5
June	**11.8**	13.6	14.2 ± 0.9
July	15.3	16.4	16.2 ± 1.0
August	**11.3**	**13.1**	15.2 ± 1.8
September	**5.8**	**7.6**	9.8 ± 1.8
October	**-0.8**	**1.4**	4.1 ± 1.7
May 1 - October 31	8.0	9.9	11.7 ± 4.5

Table 6. Comparison of total precipitation (mm) at the two northern Alberta peatland sites for six months during the 2004 growing season. 30-year normals (1971-2000) are from Athabasca, Alberta (54.82°N, 113.52°W) and represent the mean ± SD. Precipitation totals were considered significantly different from the average conditions at Athabasca if they were outside of the monthly 30-year normal ± SD, and are indicated with **bold** text.

	Poor Fen	Extreme-rich Fen	30-year normal
May	**95.0**	53.8	47.3 ± 27.0
June	**22.8**	**27.6**	91.7 ± 36.8
July	**170.6**	130.4	104.5 ± 47.6
August	35.8	**99.0**	62.6 ± 28.9
September	**101.6**	60.4	42.8 ± 30.0
October	23.8	22.8	21.5 ± 15.2
May 1 - October 31	449.6	394.0	370.4 ± 80.7

Table 7. Comparison of cumulative incident photosynthetically-active photon flux densities (mol m^{-2}) at the two northern Alberta peatland sites for six months during the 2004 growing season.

	Poor Fen	Extreme-rich Fen
May	1092	879
June	1395	1039
July	1252	923
August	929	710
September	558	412
October	380	298
May 1 - October 31	5606	4261

Table 8. Live aboveground biomass (green leaves of vascular plants, needles of *Picea mariana*, and *Sphagnum* capitula) of species at the contrasting northern Alberta peatland sites during the peak of the 2004 growing season. Vegetation was sampled on July 29, 2004 at the poor fen, and July 30, 2004 at the extreme-rich fen. Values represent the mean ± SE, n = 6.

Site	Species	Biomass ($g\ m^{-2}$)
Poor Fen	*Carex limosa*	16.5 ± 3.5
	Smilacina trifolia	14.8 ± 2.0
	Andromeda polifolia	22.4 ± 5.2
	Salix sp.	3.0 ± 1.4
	Oxycoccus microcarpus	5.2 ± 1.4
	Menyanthes trifoliata	1.0 ± 1.0
	Drosera rotundifolia	0.8 ± 0.8
	Picea mariana	11.1 ± 4.6
	Sphagnum spp.	156.1 ± 18.2
Extreme-rich Fen	*Carex lasiocarpa*	74.6 ± 4.0
	Galium trifidum	1.2 ± 0.6
	Rumex sp.	4.7 ± 4.7
	Salix pedicellaris	0.3 ± 0.3
	Rubus acaulis	0.6 ± 0.6
	Brown moss	75.7 ± 18.1

Table 9. Comparison of the dominant plant species at the two contrasting peatland sites, according to % of total leaf area index (LAI), total nitrogen (N) content (mg g^{-1}) and C:N ratios. Vegetation was sampled on July 29, 2004 at the poor fen and July 30, 2004 at the extreme-rich fen. Total N content values and C:N ratios represent the mean ± SE, n = 6, for *Sphagnum* spp. capitula at the poor fen, and green *Carex lasiocarpa* leaves at the extreme-rich fen.

	Poor Fen	Extreme-rich Fen
	Sphagnum spp.	*Carex lasiocarpa*
% total site LAI	66	60
Total N content (mg g^{-1})	7.8 ± 0.9	19.3± 0.4
C:N ratio	57.4 ± 2.6	23.6± 0.2

Table 10. Comparison of non-linear regression parameters estimated using the Q_{10} - NEE model (Eq. 13) for three biologically active periods at each peatland site during the 2004 growing season. Models were parameterized using mean diurnal patterns of net ecosystem exchange (NEE), photosynthetically-active photon flux density (PPFD) and air temperature (T) from eddy covariance measurement Period 2, Period 3, and Period 4 (Table 2) at each of the sites. Values in parentheses represent the 95 % confidence intervals of parameter estimates, while r^2 is the coefficient of determination for each regression model.

Site	Parameter	Time Period		
		2	3	4
Poor Fen	A_{max}	3.9 (3.4 - 4.4)	9.2 (8.0 - 10.4)	9.0 (6.8 – 11.2)
	α	0.017 (0.013 - 0.021)	0.034 (0.025 - 0.043)	0.023 (0.012 – 0.034)
	R_{10}	1.4 (1.3 - 1.5)	1.6 (1.4 - 1.8)	1.9 (1.4 – 2.4)
	Q_{10}	1.8 (1.5 - 2.1)	1.8 (1.4 - 2.2)	1.8 (1.0 – 2.6)
	r^2	0.95	0.96	0.90
Extreme-rich Fen	A_{max}	7.9 (6.9 - 8.9)	12.1 (10.6 - 13.6)	5.6 (2.2 – 9.0)
	α	0.025 (0.018 - 0.032)	0.032 (0.025 - 0.039)	0.016 (0.003 – 0.029)
	R_{10}	1.7 (1.4 - 2.0)	1.9 (1.6 - 2.2)	1.3 (0.8 – 1.8)
	Q_{10}	2.0 (1.7 - 2.3)	1.8 (1.5 - 2.1)	1.8 (0.6 – 3.0)
	r^2	0.95	0.97	0.70

Table 11. Comparison of non-linear regression parameters estimated using the L & T - NEE model (Eq. 15) for three biologically active periods at each peatland site during the 2004 growing season. Models were parameterized using mean diurnal trends of net ecosystem exchange (NEE), photosynthetically-active photon flux density (PPFD) and air temperature (T) from eddy covariance measurement Period 2, Period 3, and Period 4 (Table 2) at each of the sites. Values in parentheses represent the 95 % confidence intervals of parameter estimates, while r^2 is the coefficient of determination for each regression model.

Site	Parameter	Time Period		
		2	3	4
Poor Fen	A_{max}	4.4 (3.9 - 4.0)	9.8 (8.9 - 10.7)	9.8 (7.4 – 12.2)
	α	0.017 (0.013 - 0.021)	0.034 (0.026 - 0.042)	0.023 (0.012 – 0.034)
	R_{10}	1.5 (1.3 - 1.7)	1.4 (1.2 - 1.6)	1.9 (1.4 – 2.4)
	r^2	0.93	0.96	0.88
Extreme-rich Fen	A_{max}	8.4 (7.4 - 9.4)	12.8 (11.4 - 14.2)	6.4 (2.6 – 10.2)
	α	0.025 (0.018 - 0.032)	0.033 (0.026 - 0.040)	0.016 (0.004 – 0.028)
	R_{10}	1.6 (1.4 - 1.8)	1.7 (1.5 - 1.9)	1.4 (0.9 – 1.9)
	r^2	0.94	0.97	0.67

Table 12. Comparison of estimated parameters from two non-linear regression models of total ecosystem respiration (TER) as a function of air temperature at the two contrasting peatland sites. The Q_{10} - TER model (Eq. 11) and L & T - TER model (Eq.12) were parameterized with respiration chamber measurements made during early and late July 2004 at the two sites. Data in parentheses represent the 95 % confidence intervals of parameter estimates, while r^2 is the coefficient of determination for each regression model.

			Poor Fen	Extreme-rich Fen
July 1 - July 5	Q_{10} - TER model	R_{10}	0.73 (0.59 - 0.87)	1.50 (1.18 – 1.82)
		Q_{10}	1.92 (1.56 - 2.28)	2.20 (1.73 – 2.67)
		r^2	0.84	0.86
	L & T - TER model	R_{10}	0.61 (0.58 - 0.64)	1.44 (1.35 – 1.53)
		r^2	0.84	0.85
July 29 - July 30	Q_{10} - TER model	R_{10}	0.59 (0.51 - 0.67)	1.09 (0.83 – 1.35)
		Q_{10}	1.80 (1.54 - 2.06)	1.98 (1.48 – 2.48)
		r^2	0.91	0.81
	L & T - TER model	R_{10}	0.48 (0.44 -0.52)	0.95 (0.88 – 1.02)
		r^2	0.81	0.77

Table 13. Non-linear regression coefficients of determination (r^2) from the Q_{10} - NEE model (Eq. 13) and the L & T - NEE model (Eq. 15) for 10 eddy covariance measurement periods (Table 3) at the poor fen site during the 2004 growing season.

Period	1.1	1.2	2.1	2.2	3.1	3.2	4.1	4.2	5.1	5.2
Day of Year	124	131	156	165	193	202	230	239	274	282
Q_{10} model: r^2	0.54	0.17	0.90	0.94	0.91	0.81	0.94	0.69	0.28	0.49
L & T model: r^2	0.54	0.18	0.83	0.94	0.91	0.80	0.90	0.69	0.28	0.49

Table 14. Non-linear regression coefficients of determination (r^2) from the Q_{10} - NEE model (Eq. 13) and the L & T - NEE model (Eq. 15) for 10 eddy covariance measurement periods (Table 3) at the extreme-rich fen site during the 2004 growing season. NF indicates that there was no fit obtained between the data set and the non-linear regression model.

Period	1.1	1.2	2.1	2.2	3.1	3.2	4.1	4.2	5.1	5.2
Day of Year	139	148	173	183	213	222	260	267	290	299
Q_{10} model: r^2	0.59	0.64	0.88	0.96	0.95	0.97	0.94	0.14	0.29	0.10
L & T model: r^2	0.59	0.64	0.86	0.96	0.94	0.97	0.91	0.13	0.30	NF

Table 15. Coefficients of determination (r^2) for polynomial relationships between NEE model parameter estimates and time (day of year) for the two peatland sites during the 2004 growing season. Lines representing the polynomial equations are shown in Figure 10.

Site	Model	Parameter	r^2
Poor Fen	Q_{10} - NEE (Eq. 13)	A_{max}	0.96
		α	0.57
		R_{10}	0.73
		Q_{10}	0.44
	L & T - NEE (Eq. 15)	A_{max}	0.95
		α	0.57
		R_{10}	0.68
Extreme-rich Fen	Q_{10} - NEE (Eq. 13)	A_{max}	0.95
		α	0.98
		R_{10}	0.74
		Q_{10}	0.24
	L & T - NEE (Eq. 15)	A_{max}	0.94
		α	0.95
		R_{10}	0.76

Table 16. Comparison of cumulative 2004 growing season carbon (CO_2-C) budgets for the two contrasting peatland ecosystem sites. Seasonal CO_2 exchange was calculated using the Q_{10} - NEE model (Eq. 13) parameters and the L & T - NEE model (Eq. 15) parameters (Figure 10). NEE is net ecosystem exchange (g C m^{-2} 6 $months^{-1}$), GPP is gross primary production (g C m^{-2} 6 $months^{-1}$), and TER is total ecosystem respiration (g C m^{-2} 6 $months^{-1}$). NEE values in parentheses represent net growing season C budgets calculated by the integration of available half-hourly eddy covariance measurements ($u_* \geq 0.15$ m s^{-1}) and gap-filling periods lacking measurements using each respective NEE model.

		Poor Fen	Extreme-rich Fen
Q_{10} - NEE model	NEE	-90 (-95)	-31 (-37)
	GPP	-340	-358
	TER	250	327
	TER:GPP	0.7	0.9
L & T - NEE model	NEE	-106 (-108)	-46 (-50)
	GPP	-359	-380
	TER	253	336
	TER:GPP	0.7	0.9

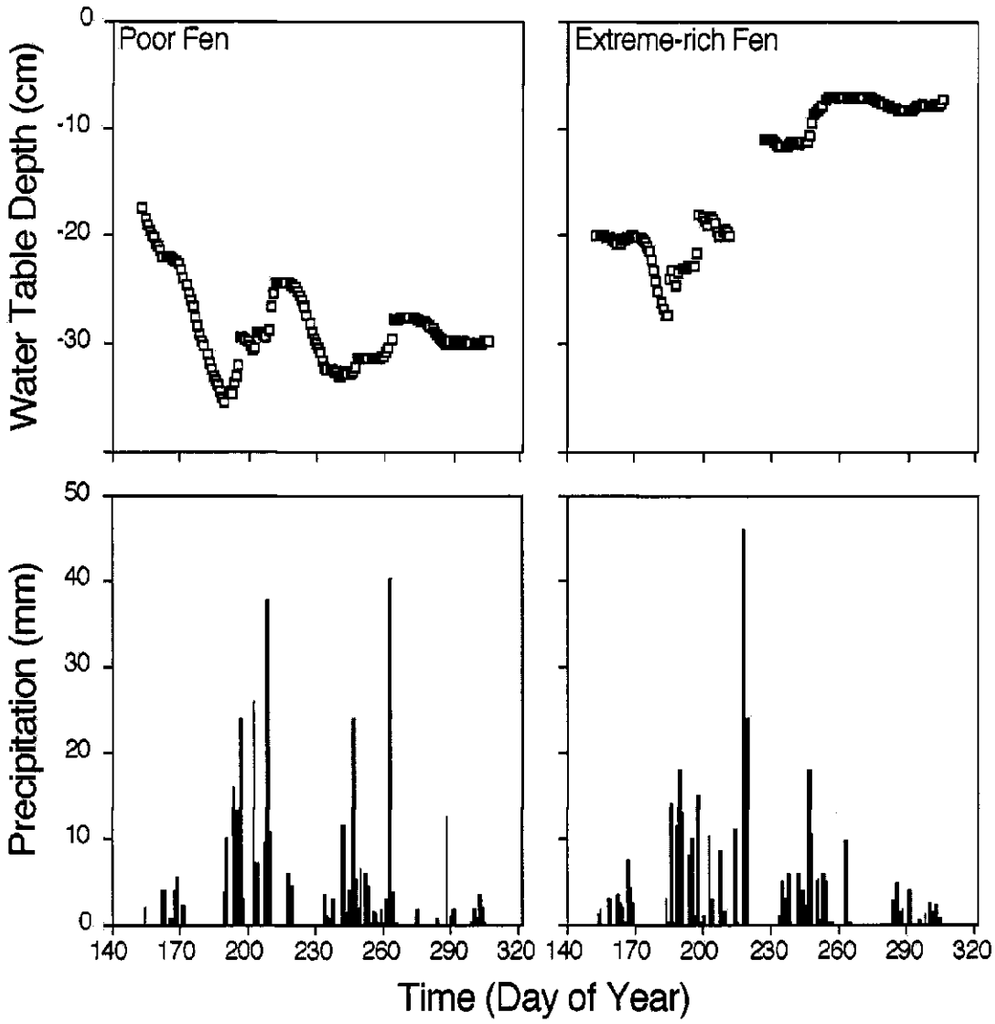

Figure 2. Seasonal pattern of daily precipitation totals (bottom graphs) and average daily water table depths (top graphs) at the contrasting northern Alberta peatland sites during the 2004 growing season. Data from the poor fen site is shown on the graphs on the left, data from the extreme-rich fen site is shown on the graphs on the right. Missing water table depth data at the extreme-rich fen (Day of Year: 212 - 226) was due to mechanical failure of the recording system.

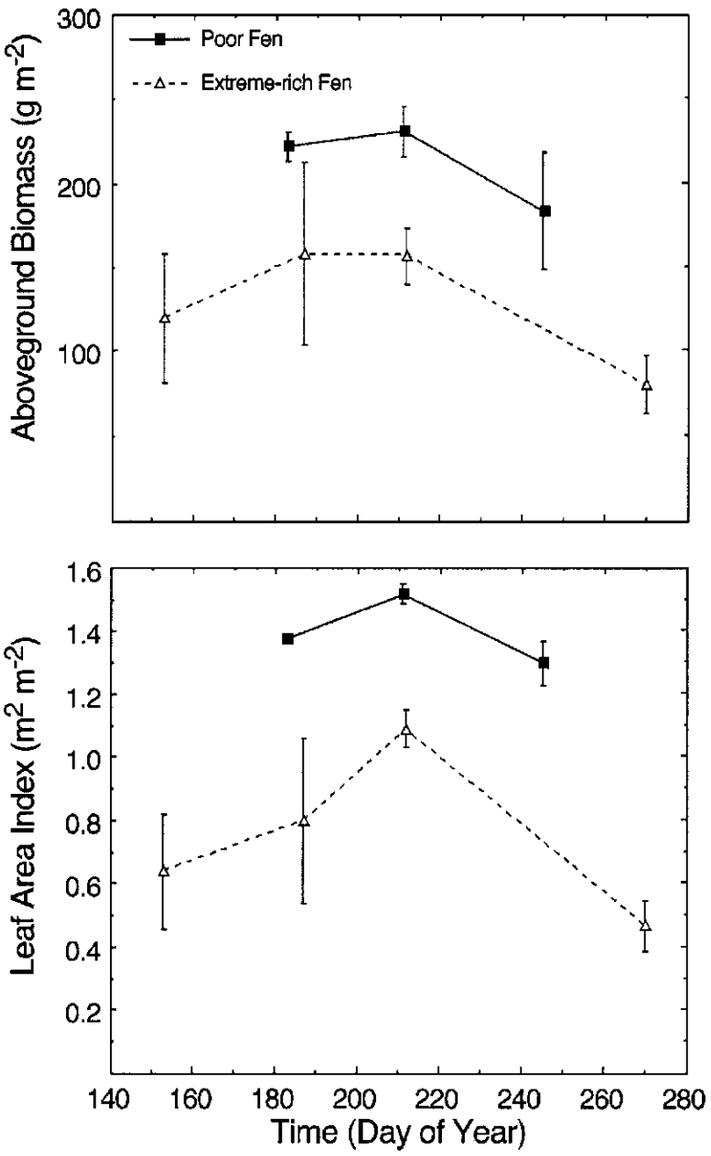

Figure 3. Seasonal pattern of aboveground biomass and leaf area index at the two contrasting northern Alberta peatlands during the 2004 growing season. Values represent the mean ± SE, n = 6.

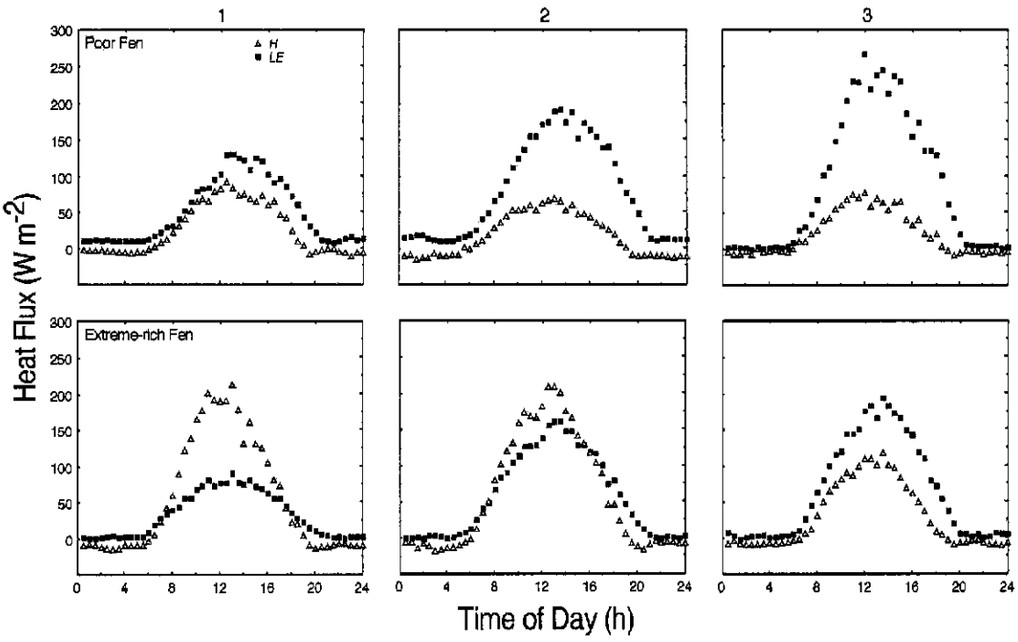

Figure 4. Mean diurnal trends of sensible (*H*; open triangles) and latent (*LE*; closed squares) heat fluxes at the contrasting northern Alberta peatlands for the first three eddy covariance measurement periods (Table 2) at each site during the 2004 growing season. Top graphs are diurnal heat flux patterns for the poor fen, bottom graphs are for the extreme-rich fen. Numbers at top of figure refer to the first three eddy covariance measurement periods at each site (Table 2).

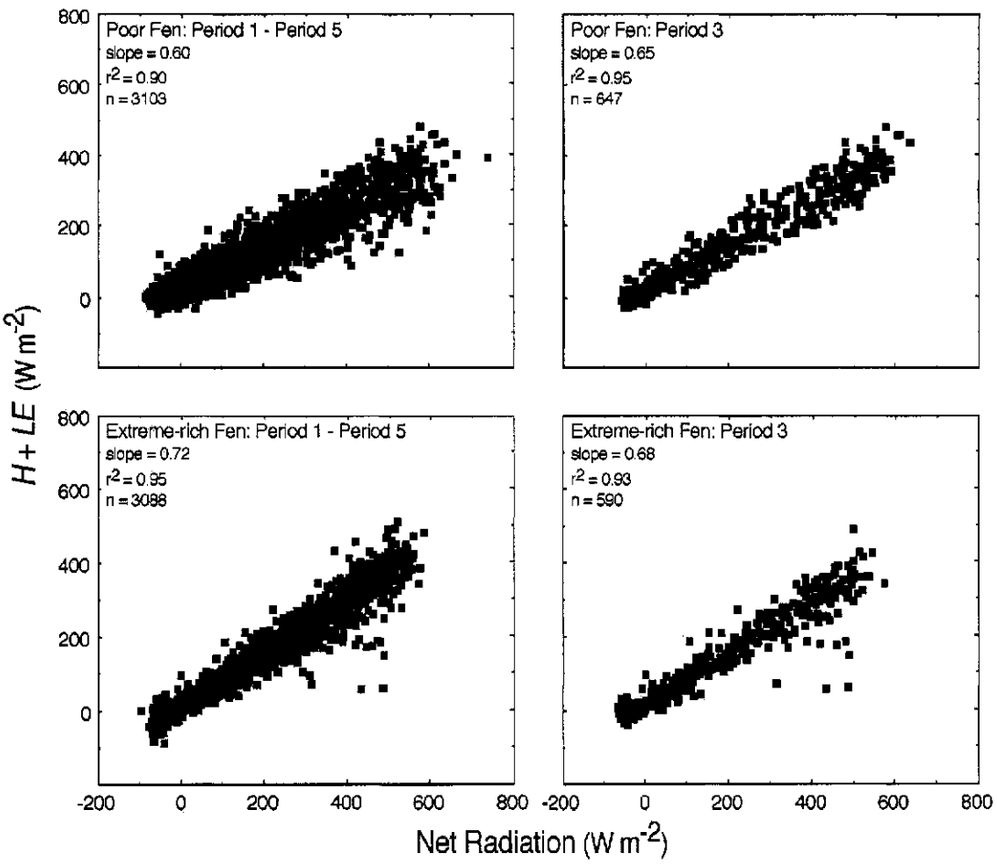

Figure 5. Relationship between net radiation and the sum of sensible (*H*) and latent (*LE*) heat fluxes from Period 1 - Period 5 (graphs on left side) and Period 3 (graphs on right side) eddy covariance measurements made at the poor fen (graphs on top) and extreme-rich fen (graphs on bottom) sites during the 2004 growing season.

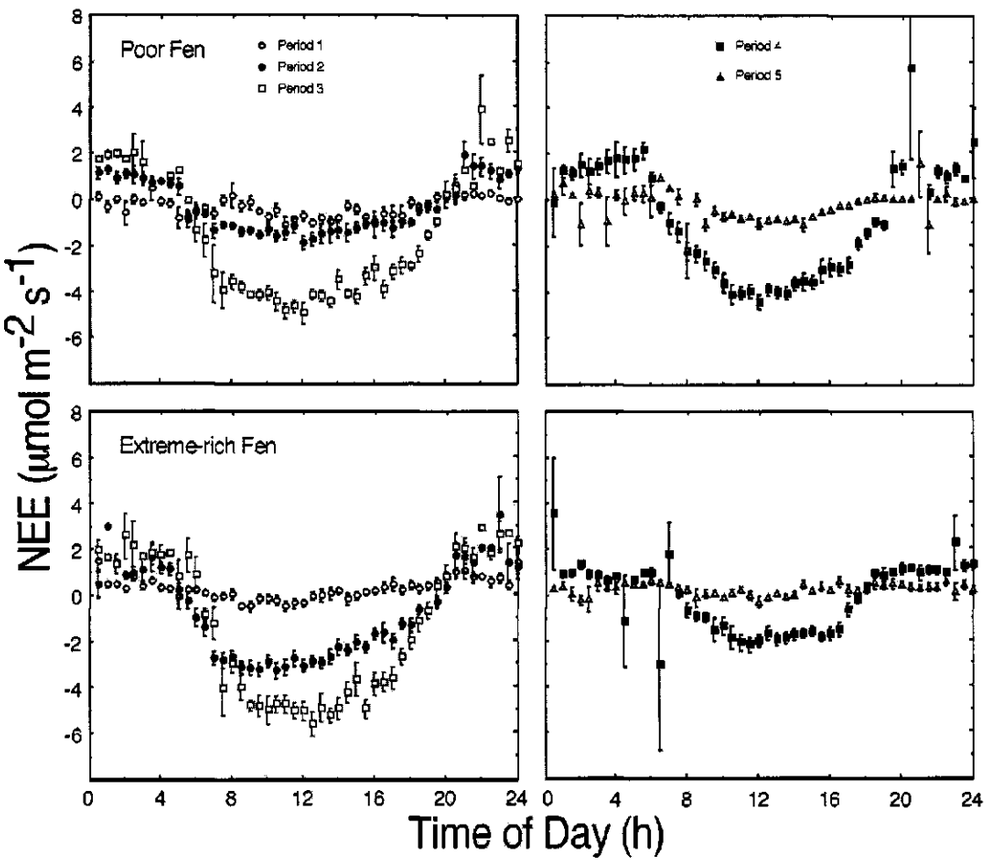

Figure 6. Mean diurnal trends of net ecosystem exchange (NEE, $u_* \geq 0.15$ m s^{-1}) at the contrasting northern Alberta peatlands for five distinct measurement periods (Table 2) at each site during the 2004 growing season. Top graphs are diurnal NEE patterns for the poor fen, bottom graphs are for the extreme-rich fen site. Symbols represent the mean ± SE.

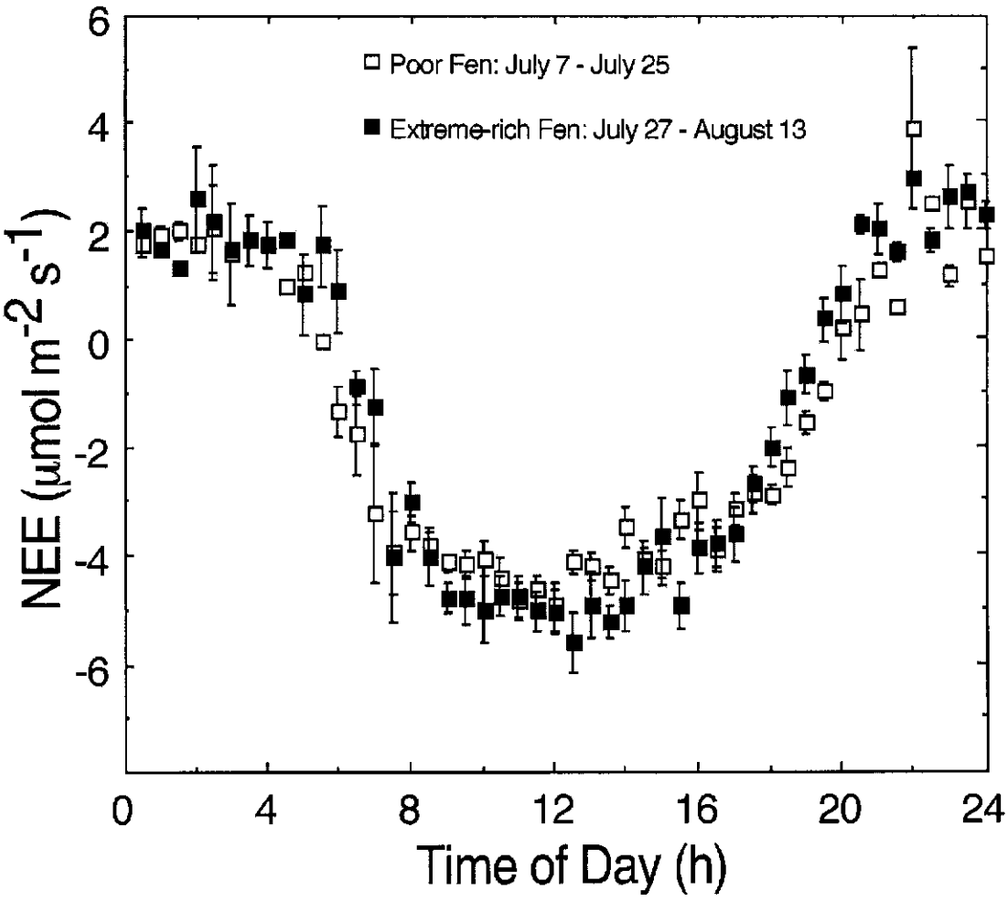

Figure 7. Comparison of the peak season (Period 3, Table 2) diurnal patterns of net ecosystem exchange (NEE, $u_* \geq 0.15$ m s^{-1}) at the two contrasting northern Alberta peatland sites during 2004. Values represent the mean ± SE, n = 1 - 14 for the poor fen, n = 1 - 12 for the extreme-rich fen site.

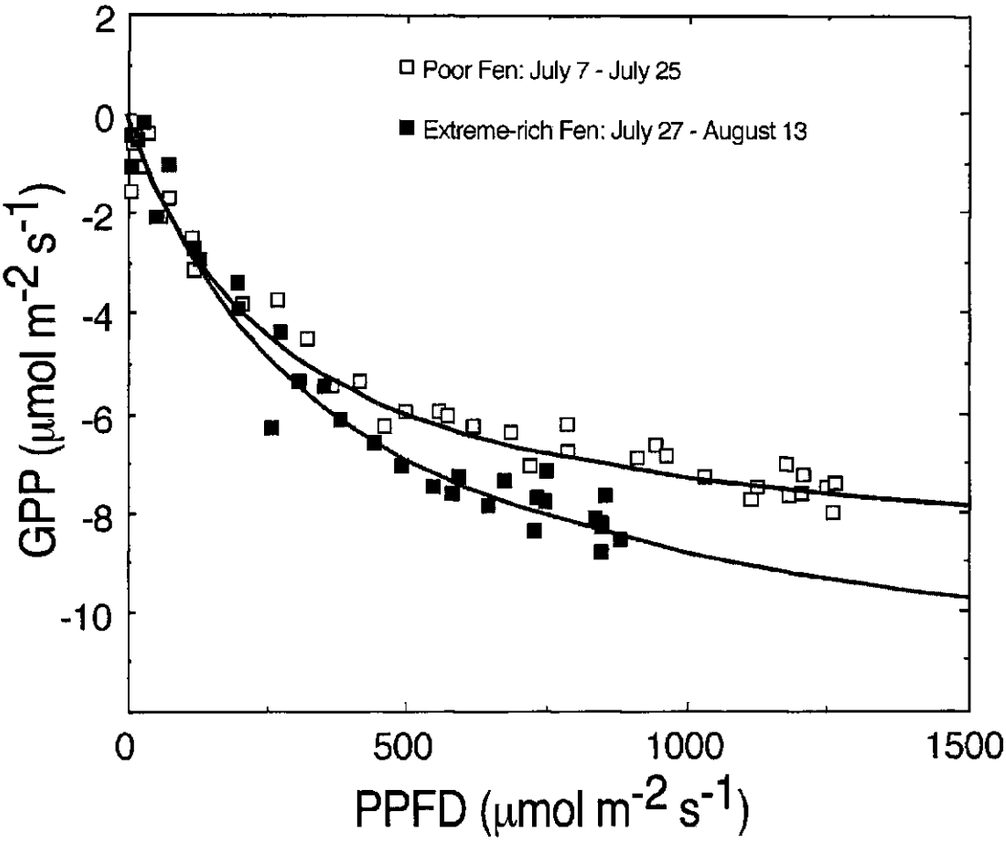

Figure 8. Comparison of peak season light-response curves for gross primary production (GPP) between the two contrasting northern Alberta peatland sites. Relationships were derived from Period 3 (Table 2) diurnal means of net ecosystem exchange (NEE), photosynthetically-active photon flux density (PPFD), and air temperature (T) using the Q_{10} - NEE model (Eq. 13, parameters given in Table 10). Mean diurnal rates of GPP (open and closed squares) were calculated by subtracting modelled total ecosystem respiration (TER, right-hand side of Eq. 13) rates based on T measurements from the mean diurnal rates of NEE when mean PPFD > 1 μmol m^{-2} s^{-1}. Lines on figure represent rectangular hyperbolae (non-linear regressions) fit to the data.

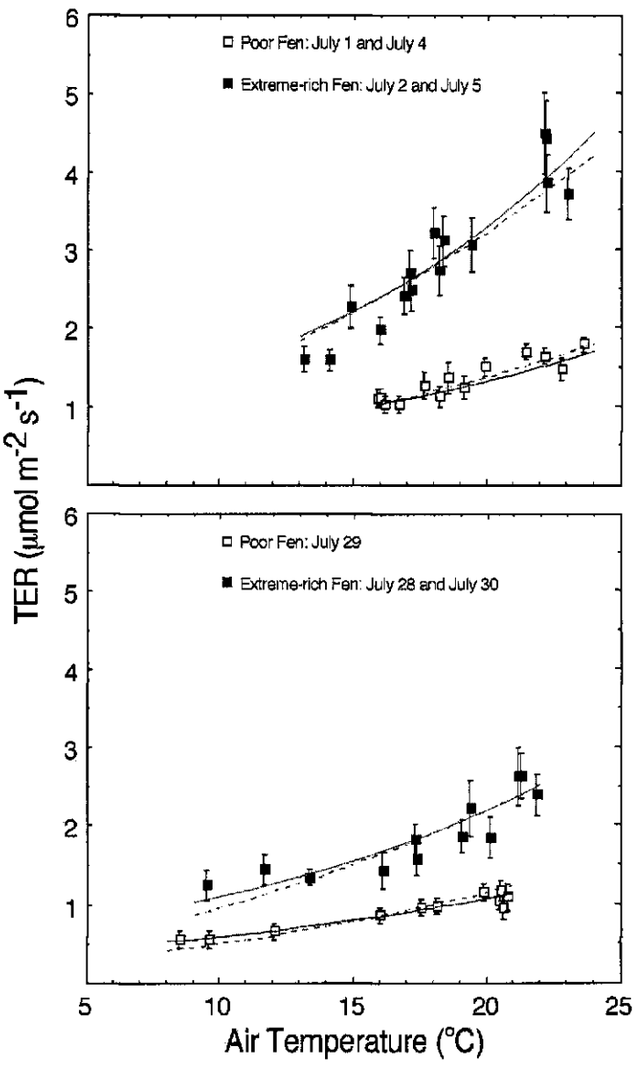

Figure 9. Comparison of chamber measurements of total ecosystem respiration (TER) for early (top figure) and late (bottom figure) July 2004, between the two contrasting northern Alberta peatland sites. Symbols represent the mean ± SE, n = 12 for the poor fen, n = 9 for the extreme-rich fen site. Lines represent the Q_{10} - TER model (Eq. 11, solid lines) and L & T -TER model (Eq. 12, dashed lines) as fit to the respiration chamber and air temperature data (parameters given in Table 12).

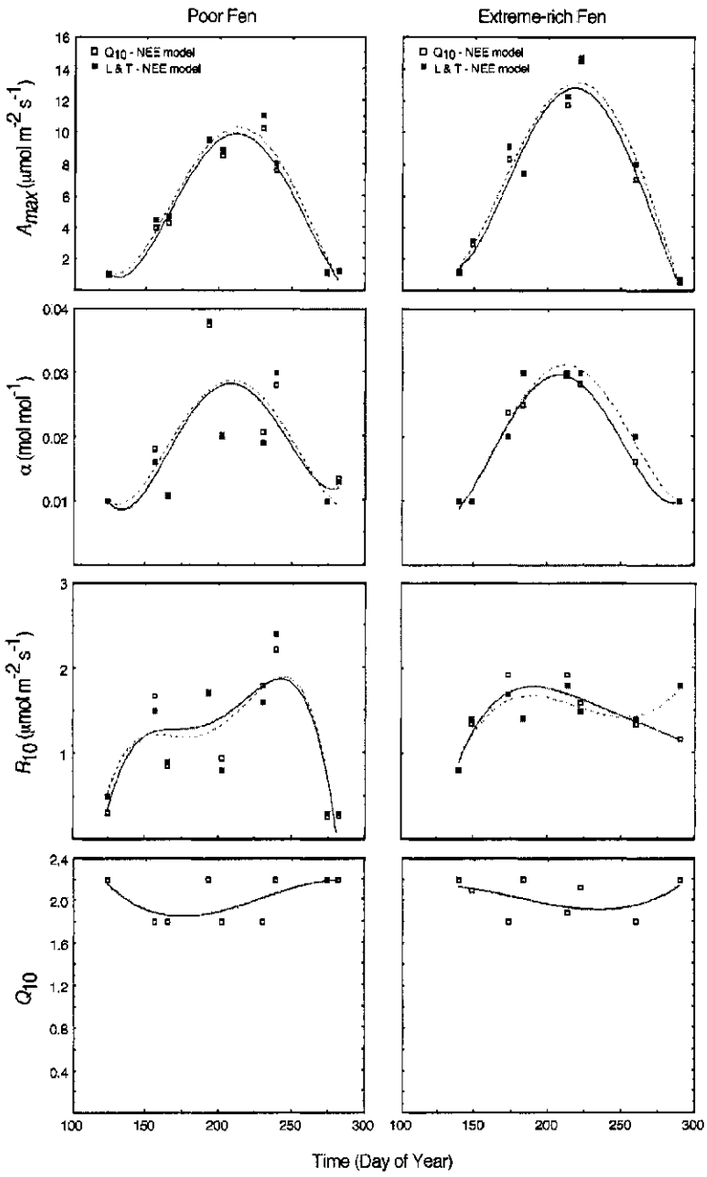

Figure 10. Seasonal trends of non-linear regression parameters at the two contrasting peatland sites over the 2004 growing season. Symbols represent parameter estimates derived from either the Q_{10} - NEE model (Eq. 13; open squares) or the L & T - NEE model (Eq. 14; closed squares) for each particular period modelled (when $r^2 \geq 0.20$). Lines represent the polynomial regressions fit to both the Q_{10} - NEE model parameters (solid lines) and the L & T - NEE model parameters (dashed lines) as a function of the day of year (r^2 values given in Table 15).

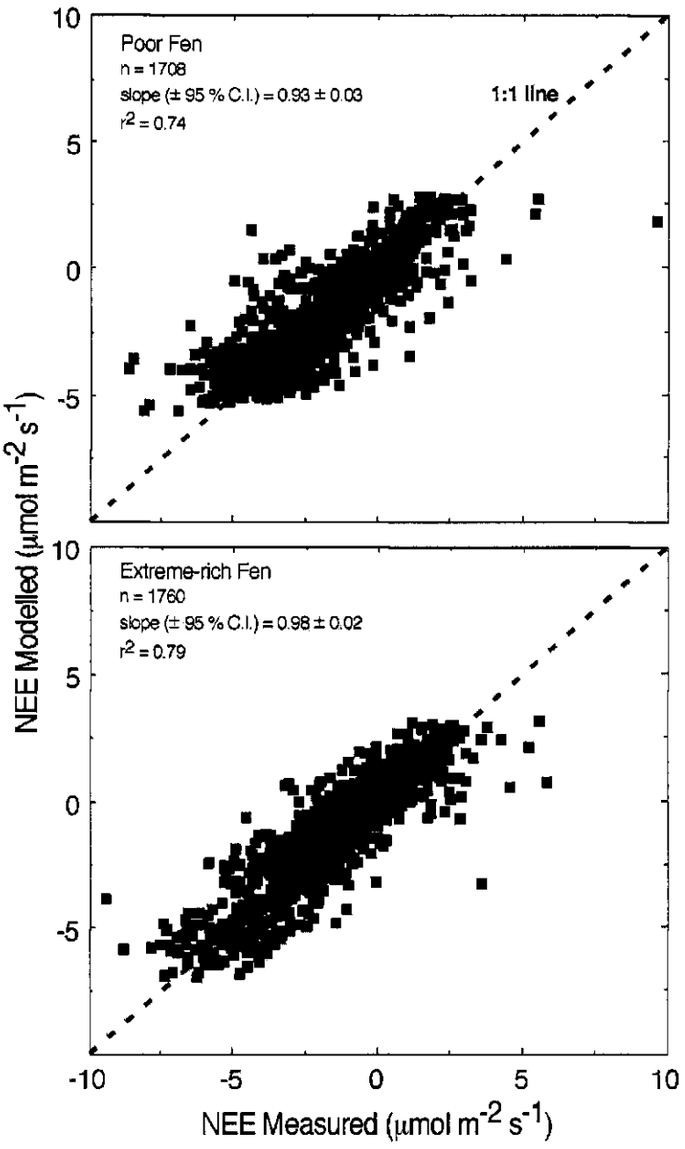

Figure 11. Comparisons of modelled and measured half-hourly net ecosystem exchange (NEE) at the two peatland sites using the Q_{10} - NEE model (Eq. 13). Half-hourly NEE was modelled from measurements of PPFD and T, and the polynomial relationships fit to seasonal parameter estimates as a function of the day of year (Figure 10).

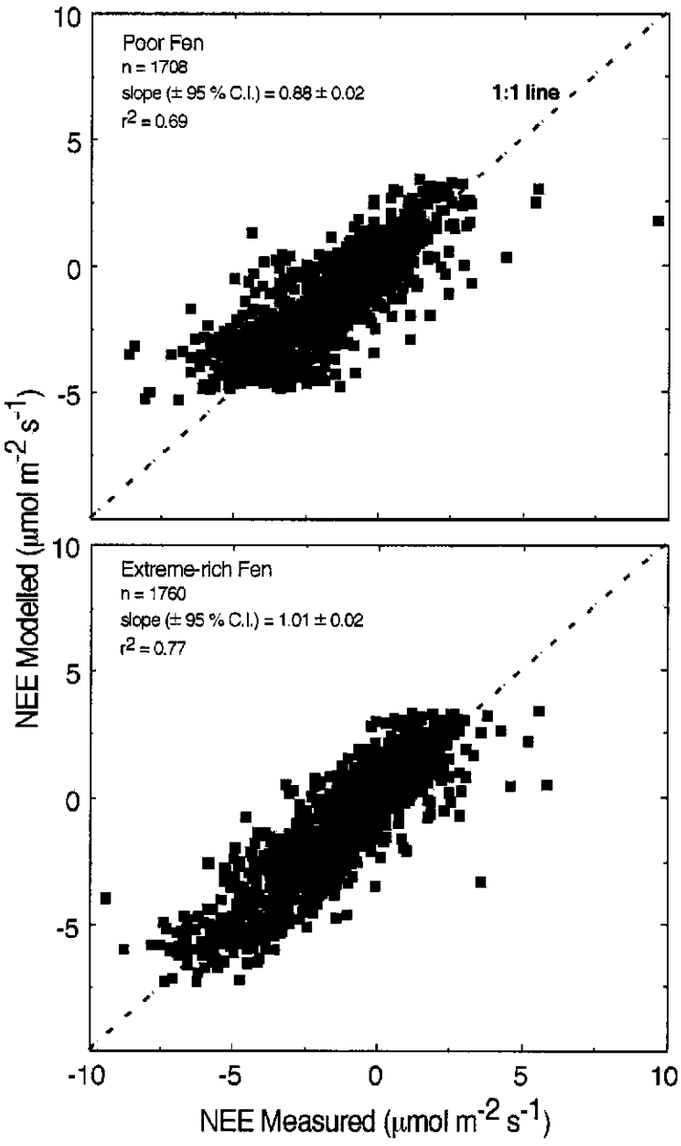

Figure 12. Comparisons of modelled and measured half-hourly net ecosystem exchange (NEE) at the two peatland sites using the L & T - NEE model (Eq. 15). Half-hourly NEE was modelled from measurements of PPFD and T, and the polynomial relationships fit to seasonal parameter estimates as a function of the day of year (Figure 10).

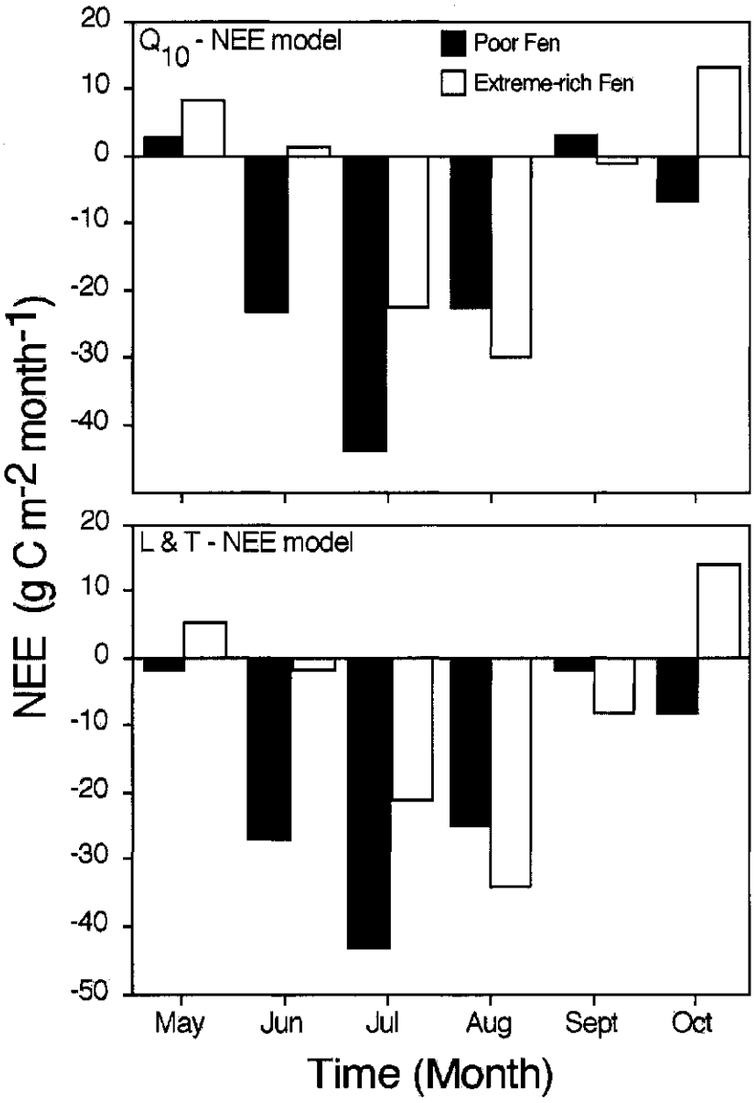

Figure 13. Comparison of monthly carbon (CO_2-C) budgets between the two contrasting northern Alberta peatland sites during the 2004 growing season. Solid bars are the monthly sums of CO_2 exchange for the poor fen, open bars are those for the extreme-rich fen. Two methods of modelling net ecosystem exchange (NEE) were employed: the Q_{10} - NEE model (Eq. 13) parameters and the L & T - NEE model (Eq. 15) parameters (Figure 10).

4. Discussion

4.1 Seasonal trends in net ecosystem exchange

The mean diurnal patterns of NEE (Figure 6) from the five EC measurement campaigns conducted at the two peatland sites during the 2004 growing season (Table 2) illustrate the seasonal trend of biological activity in these northern ecosystems. Period 1 and Period 5 at each site represent the beginning and end of the growing season respectively, and therefore, do not exhibit a significant diurnal trend of net CO_2 uptake during the day and loss at night. The peatland ecosystems have not become biologically active yet during the first campaign, and are entering dormancy during the final campaign of the season, resulting in a lack of significant CO_2 fluxes at both sites during these periods (Figure 6).

The three EC campaigns conducted at the sites between the beginning (Period 1) and end (Period 5) of the season (Period 2 - Period 4, Table 2) correspond to periods of active plant growth and maintenance, and show distinct diurnal trends of NEE, with net CO_2 uptake driven by photosynthesis reaching a maximum around local noon, and a significant net loss of CO_2 from TER occurring during nocturnal hours at both sites (Figure 6). The mean diurnal patterns of NEE from Period 2, Period 3 and Period 4 at each of the peatland sites exhibit the seasonality of biological activity, with peak rates of net daytime CO_2 gain, as well as, net nocturnal loss increasing towards mid-season (Period 3) and decreasing as the growing season came to a close (Figure 6). Differences in NEE correspond to biological activity at the two peatland sites, with the magnitude of CO_2 fluxes associated with variation in the total aboveground biomass and LAI (Figure 3). The greater the photosynthetically-active plant biomass was at each site, the greater the amplitude of mean diurnal trends of NEE. As well, PPFD and temperature increase rapidly towards mid-season at these northern sites and decrease as the season progresses (Table 5; Table 7). Photosynthetically-active

radiation and temperature are the primary abiotic variables driving GPP and TER respectively, therefore they play a significant role in governing rates of NEE.

The seasonal variation in climate and biological activity also corresponds to variation in the photosynthetic (A_{max} and α) and respiratory (R_{10}) parameter estimates from the Q_{10} - NEE model (Table 10) and the L & T - NEE model (Table 11). A general trend was evident in which the A_{max}, α, and R_{10} model parameters increased towards mid-season (along with the driving biotic and abiotic variables) at the sites and began to decrease as the growing season came to a close, with the exception of R_{10} at the poor fen, which increased into August. Similar seasonally-dependent patterns of photosynthetic and respiration parameter estimates due to variation in driving climatic variables and biological phenology have been commonly observed in other ecosystems (Carrol and Crill, 1997; Hollinger et al. 1999; Griffis et al. 2003; Kowalski et al. 2003) and were expected to occur at the two boreal peatland sites examined during the present study.

Estimates of the maximum photosynthetic capacity (A_{max}) and photochemical efficiency (α) obtained for the three biologically active periods at each site during the 2004 growing season (Table 10; Table 11) were generally less than those derived for upland forest and grassland ecosystems (Ruimy et al. 1995; Flanagan et al. 2002; Griffis et al. 2003) but consistent with parameter estimates from other northern peatland ecosystems (Frolking et al. 1998; Bubier et al. 2003). The relationship between PPFD and photosynthesis for peatland ecosystems is different than that for forest and grassland ecosystems because of lower rates of plant productivity due to cool temperatures, saturated soil conditions and lower concentrations of essential nutrients (Frolking et al. 1998).

Unfortunately, there are few NEE studies for which a temperature standardized rate

of respiration has been calculated from daytime or nighttime EC measurements, making it difficult to compare the R_{10} values derived in the current study with other published values for peatland ecosystems. The R_{10} rates for the poor and extreme-rich fen sites in northern Alberta (Table 10; Table 11) are slightly higher than TER values reported for the ombrotrophic Mer Bleue bog near Ottawa, Ontario (Lafleur et al. *in press*). The magnitude of TER at 10°C for the Mer Bleue bog, as calculated using the best exponential fit between air temperature and nighttime EC measurements at the site, is approximately 1 μmol m^{-2} s^{-1}. The R_{10} estimates for the poor fen and extreme-rich fen site are within the range of ecosystem respiration rates (0.5 to 5 μmol m^{-2} s^{-1}) standardized to 12°C for bogs and fens in Finland (Silvola et al. 1996) and the R_{10} value (1.6 μmol m^{-2} s^{-1}) determined for a raised peat bog in New Zealand (Smith et al. *submitted for publication*). Compared to temperature normalized respiration estimates from other terrestrial ecosystems (Reichstein et al. 2002; Kowalski et al. 2003; Flanagan and Johnson, 2005; Wohlfahrt et al. 2005), the R_{10} values derived from the current study are lower (Table 10; Table 11). This is mostly due to lower live biomass and metabolic rates of the peatland plant communities compared to grassland and forest ecosystems (Frolking et al. 1998), and the inhibition of decomposition and TER under the cool and saturated conditions of the peat substrate (Bubier et al. 1998).

4.2 Peak growing season net ecosystem exchange

Both peatland sites in northern Alberta exhibited mean daily maximum rates of net CO_2 uptake of approximately 5 μmol m^{-2} s^{-1} and typical nighttime rates of CO_2 loss of approximately 2 μmol m^{-2} s^{-1} during the peak of the 2004 growing season (Figure 7). These NEE values are similar to those reported for the Mer Bleue bog near Ottawa, which has typical daily peaks of net CO_2 uptake between 4 and 6 μmol m^{-2} s^{-1} and average rates of

nocturnal CO_2 loss via TER between 1 and 3 μmol m^{-2} s^{-1} during July and August (Lafleur et al. 2001; Lafleur et al. 2003). The magnitude of the mean diurnal patterns of NEE during peak season at the two peatland sites in the present study are also similar to those observed in summer over a raised open bog in the Hudson Bay lowlands (Neumann et al. 1994), a boreal fen in northern Manitoba (Lafleur et al. 1997) and to those reported for a subarctic flark fen in northern Finland (Aurela et al. 2002).

Mean diurnal patterns of NEE during Period 3 were similar at the two northern Alberta peatland sites (Figure 7) and occurred when the maximum aboveground biomass and LAI (Figure 3) were maximum at the peak of the 2004 growing season. However, the light-response curves of GPP derived for the same time of the growing season (Period 3, Table 2) were different between the contrasting peatland sites (Figure 8). The extreme-rich fen had a significantly higher maximum photosynthetic capacity (A_{max}) than the poor fen at this time (Table 10; Table 11). Plant tissue N content is positively correlated with photosynthetic capacity because Rubisco, the primary enzyme of the PCR cycle, and the light-harvesting thylakoid membranes of the chloroplast represent the majority of leaf protein (Farquhar et al. 1980; Evans, 1989; Woodward and Smith, 1994; Dang et al. 1997; Jacobs et al. 2003). Therefore, the higher total N content of the aboveground biomass at the extreme-rich fen (3.0 g m^{-2}) compared to the poor fen (2.3 g m^{-2}) and the total N content of the dominant plant species at each of the sites (Table 9) helps explain the differences in the light-response curves for GPP (Figure 8) and the A_{max} parameter (Table 10; Table 11) for the peatland ecosystems observed at the peak of the growing season.

Despite having contrasting physiological capacities for GPP, the mean diurnal trend of NEE did not differ significantly between the two peatland sites at the peak of the growing season (Figure 7). This indicates that the competing ecosystem CO_2 flux process of TER was

different between the two peatland sites. Because the extreme-rich fen had a higher maximum photosynthetic capacity and rate of GPP than the poor fen, then daytime rates of TER must have also been greater at the site during the Period 3 EC measurement campaign.

The R_{10} parameter, which represents the rate of TER at 10°C or the respiratory capacity of an ecosystem, was estimated to be higher at the extreme-rich fen (1.9 μmol m^{-2} s^{-1}) than the poor fen (1.6 μmol m^{-2} s^{-1}) during EC measurement Period 3. Although this difference was not significant according to the 95 % confidence intervals (C.I.) of the R_{10} estimates (Table 10; Table 11), it still resulted in a higher R_{10} used to model TER (and subsequently model GPP) at the extreme-rich fen than the poor fen during the peak season. However, this difference in respiratory capacity (R_{10}) between the peatland sites was not reflected by the mean nocturnal NEE observations, which are equal to TER, and were very similar between the sites (Figure 7). This is most likely the result of sparse replication of nighttime NEE measurements due to inadequate turbulent mixing ($u_* < 0.15$ m s^{-1}) and limitations of the open-path EC system during nocturnal and early morning hours. However, the similarity of the mean diurnal trends of NEE (Figure 7) and the significant difference in the maximum photosynthetic capacity (A_{max}) estimates between the sites during Period 3 (Table 10; Table 11) is indicative of higher peak season rates of TER at the extreme-rich fen compared to the poor fen site. This conclusion is further supported by the mean diurnal patterns of air temperature at the two sites for Period 3, which indicate that average half-hourly T values were almost always lower at the extreme-rich fen than the poor fen during this time period (data not shown). Had the two peatland ecosystems experienced equal air temperatures during the respective Period 3 EC measurement campaigns, it is expected that mean maximum daily rates of net CO_2 uptake would be less at the extreme-rich fen than the poor fen site, due to the overwhelming influence of temperature on TER and therefore, rates

of NEE.

4.3 Chamber respiration measurements

According to chamber measurements conducted in early and late July 2004, the extreme-rich fen had significantly higher rates of ecosystem respiration than the poor fen (Figure 9). The temperature standardized rate of TER, as represented by the R_{10} parameter, was approximately twice as high at the extreme-rich fen site than the poor fen according to both TER models during the time periods over which diurnal chamber measurements of TER were made (Table 12). This indicates that the peak season or maximum respiratory capacity of the poor fen site was half of the extreme-rich fen. The significantly greater R_{10} estimates from the chamber measurements at the extreme-rich fen site compared to the poor fen help explain the similarity of the mean diurnal patterns of NEE during EC measurement Period 3 at the two sites (Figure 7) despite contrasting A_{max} values (Table 10; Table 11) and GPP light response relationships (Figure 8). Due to the bidirectional nature of the CO_2 fluxes contributing to NEE (Eq. 1), higher rates of TER at the extreme-rich fen site compared to the poor fen (Table 12; Figure 9) would have offset any greater CO_2 sequestration at the extreme-rich fen due to higher rates of GPP, resulting in similar mean diurnal trends of NEE at the sites.

The R_{10} parameter, can be considered an index of the respiratory capacity of an ecosystem, when Q_{10} is kept relatively constant (2 ± 10 %), as was the case with models employed in the present study. It allows the direct comparison of the normalized rate of TER between sites, independent of the confounding effect of temperature (Reichstein et al. 2002; Flanagan and Johnson, 2005). Because temperature is the dominant environmental control regulating respiration, the use of the R_{10} parameter allows further exploration of potential environmental and biological controls of TER (Flanagan and Johnson, 2005). In addition to

temperature, another environmental control known to influence TER within peatlands is the water table depth (WTD), with lower water tables enhancing CO_2 production, and higher water tables inhibiting emissions due to the effects of oxygen limitation (Silvola et al. 1996; Bubier et al. 1998; Moore et al. 1998; Freeman et al. 2001; Bubier et al. 2003). The WTD was not a significant factor influencing the difference in R_{10} estimates between the poor and extreme-rich fen during the peak of the 2004 growing season because the WTD was similar, and relatively high at both peatland sites when chamber measurements were made in early (DOY: 183-187) and late July (DOY: 210-212, Figure 2). In fact, despite having greater R_{10} values, the level of the water table was slightly higher at the extreme-rich fen during these time periods (Figure 2). This indicates that the difference in the respiratory capacity between the two peatland sites was primarily biological in nature.

There are three major contributing biotic factors which would result in higher TER in early and late July at the extreme-rich fen than the poor fen. First, there is a strong relationship between photosynthesis, plant metabolism and respiration (Bubier et al. 1998; Amthor, 2000). Because the extreme-rich fen had a higher maximum photosynthetic capacity than the poor fen, as indicated by the A_{max} value derived from the Period 3 EC measurements (Table 10; Table 11) and the N content of the dominant sedge species at the site (Table 8), it follows that TER should be greater as well. Secondly, it has been estimated that 30 - 70 % of total peatland respiration is due to plant roots or root-derived microbial respiration (Silvola et al. 1996; Bubier et al. 1998; Frolking et al. 1998) and that up to 90 % of *Carex* spp. biomass production is belowground (Sjörs, 1991; Thormann and Bayley, 1997b). The belowground biomass of the *C. lasiocarpa* rhizomes at the extreme-rich fen would be expected to be much greater than the belowground biomass of the non-vascular *Sphagnum*-dominated poor fen, resulting in higher rates of chamber measured TER. Thirdly, there is a

positive correlation between the rate of litter decay and N content, and a negative correlation with C:N ratios (Updegraff et al. 1995; Szumigalski and Bayley, 1996). The *Sphagnum* spp. at the poor fen site had a total N content that was less than half of the *C. lasiocarpa* at the extreme-rich fen, and a C:N ratio that was more than two times greater (Table 9). Therefore the expected rate of decomposition would be much less for the poor fen ecosystem, further contributing to a lower respiratory capacity or R_{10} value.

The R_{10} values estimated from the chamber respiration measurements decreased at both sites from early to late July 2004 with both TER models, although this trend was only significant according to the 95 % C.I. from the L & T - TER model (Table 12). Because plant biomass and productivity was equal or even greater in late July compared to early July at both sites (Figure 3), it is possible that the increase in the water table level at both peatland ecosystems, associated with a number of significant precipitation events in July (DOY: 183 - 213, Figure 2), was responsible for the slight reduction of the R_{10} values estimated by chamber measurements at the end of the month compared to the beginning. Such a relationship is consistent with previous studies that have shown water table depth to be an important abiotic factor governing CO_2 emissions from peatlands by inhibiting rates TER and decomposition due to anaerobia (Silvola et al. 1996; Moore et al. 1998; Freeman et al. 2001; Bubier et al. 2003).

Unfortunately, there was a lack of agreement between the R_{10} values estimated from the chamber measurements (Table 12) compared to those derived from corresponding periods of daytime EC measurements (Table 10; Table 11). An exception occurred during early July at the extreme-rich fen site, when the R_{10} estimate from the chamber measurements (Table 12) was close to that obtained by Period 2 (June 17 - July 5) daytime EC measurements (Table 10). The R_{10} parameter estimates determined from chamber

measurements in early and late July at the poor fen, and from late July at the extreme-rich fen (Table 12) were significantly lower than those derived from the Period 3 daytime EC measurements at the sites (Table 10; Table 11). Reasons for the discrepancy in the derived R_{10} values between the two methods are currently unclear, but there are a few possible explanations that may account for the apparent differences. Although an effort was made to place collars for the chamber system in areas of the peatland sites that were similar to the ground surface detected by the EC system, the limited replication of the chamber respiration measurements (n = 12 collars at the poor fen; n = 9 collars at the extreme-rich fen) may not have been entirely representative of the EC flux footprint. As well, the assumption that chamber respiration measurements were completely equal to TER may have been violated. Although vegetation was left intact within the collars so that chamber measurements would represent the sum of aboveground and belowground ecosystem respiration, and both the peatland sites were dominated by low-stature vegetation, it was not possible to enclose all plant types present at the sites during measurements, such as the *P. mariana* at the poor fen and the *Salix* shrubs at the extreme-rich fen. However, because these larger aboveground species constituted a relatively minor component of the aboveground biomass at the two sites (Table 8) this would not solely account for the significant difference in the R_{10} values estimated with the different flux measurement methodologies. Inconsistency between the two methods may have been due, at least in part, to the potentially intrusive and artefactual nature of the chamber measurements compared to measurements by the EC system. Collars were installed at the peatland sites over one month before the chamber measurement campaigns began, but this may not have been adequate time for the vegetation and roots left intact within the collars to acclimate and rejuvenate from the unavoidable disturbance caused by collar placement. As well, effort was exerted to minimize mechanical disruption to the

collars and surrounding vegetation, but due to the experimental nature of the chamber measurements and the logistical difficulty of working on the fragile surface of the peatland ecosystems, some disruption to the sites was inevitable. Additionally, the possibility exists that ecosystem respiration was underestimated by chamber measurements due to dilution effects of concurrent water vapour fluxes from within the collars. The largest errors from water vapour dilution effects are known to occur under low CO_2 flux rates on wet soils on dry, sunny days (LI-COR Inc., 1998). Since the peat was essentially saturated at both sites due to high water tables (Figure 2) when chamber measurements were conducted in July, and no dilution corrections were applied to the measured fluxes, this may also partially account for lower estimations of R_{10} compared to the EC method.

The possible effects of water vapour on the chamber measurements of TER were estimated for a number of sets of measurements for each campaign at the two sites using a dilution correction similar to that recommended by LI-COR (LI-COR Inc., 1998). Because the chamber system employed does not measure concurrent H_2O fluxes, evapotranspiration was estimated based on eddy covariance measurements of water vapour flux. This was accomplished by using the respective half-hourly value of evapotranspiration from the EC system when it was present or by using the bin averaged value of the H_2O flux for the time of day, based on the 5 closest days with available EC measurements to the chamber campaigns for each particular site. The results of this exercise indicated that the CO_2 flux from chamber measurements may have been underestimated by as much as 18 % at the poor fen and 5 % at the extreme-rich fen. Therefore the dilution effect of water vapour on chamber measurements may have been significant, however, it does not appear to be large enough during the campaigns to account for the discrepancy in R_{10} values.

Another factor that may have contributed to the apparent underestimation of TER

using the chamber method compared to EC measurements could have been the influence of aboveground plant biomass on the effective volume of the chamber and collar system. Because a constant geometric volume was assumed when calculating net CO_2 exchange with the chamber system, vegetation inside the collar could have reduced the effective volume during measurements, which would have also lead to an underestimation of TER using the method. It is possible that all of the previously discussed factors influenced the chamber measurements, collectively contributing to a slight underestimation of TER compared to that obtained with EC measurements.

4.4 Growing season carbon budget calculations

The 2004 growing season (May - October) carbon budgets for the poor fen (net CO_2 sink of 90 to 108 g C m^{-2}) and extreme-rich fen site (net CO_2 sink of 31 to 50 g C m^{-2}) in northern Alberta (Table 16) are within the range of estimates obtained for other peatlands in North America. From mid-May to early October in 1994, Suyker et al. (1997) estimated that a boreal minerotrophic patterned fen in central Saskatchewan was a sink for atmospheric CO_2 of approximately 88 g C m^{-2}. At a fen wetland in northern Manitoba, Lafleur et al. (1997) calculated that the site was a net CO_2 source in 1994 of approximately 30 g C m^{-2} between the months of April and September, while in 1996 during the same time period, the ecosystem was a net CO_2-C sink of approximately 92 g m^{-2} (Joiner et al. 1999). From May to October in 1991, an open peatland in north-central Minnesota was estimated to be a net source of CO_2 losing approximately 71 g C m^{-2}, while in 1992 the same ecosystem was net C sink, sequestering about 32 g C m^{-2} over the course of the growing season (Shurpali et al. 1995). During a warm and dry growing season in 1994, a temperate poor fen in New Hampshire was modelled to be a significant source of atmospheric CO_2, losing approximately 145 g C m^{-2} between the months of April and December (Carrol and Crill,

1997). For the same time period as the present study (May to October 2004) a treed, moderate-rich fen (Western Peatland flux station, FCRN, 2005) located in the same region (54.95°N, 113.32°W) as the poor and extreme-rich fen in the present study was estimated to be a significant net sink for CO_2 of approximately 149 g C m^{-2} (Flanagan et al. *unpublished*). The aboveground biomass of the treed, moderate rich fen is dominated by coniferous trees (*P. mariana* and *L. laricina*) and had a peak LAI of approximately 2.7 m^2 m^{-2} in 2004, about twice that of either the poor or extreme-rich fen (Figure 3).

Over the 2004 growing season, the poor fen was calculated to be a net C sink that was two to three times greater than the extreme-rich fen site (Table 16). This was mainly due to the seasonal differences in net CO_2 exchange between the sites, as illustrated by the monthly CO_2-C budgets (Figure 13). The poor fen was modelled to be a significant CO_2 sink for four of the six months (June, July, August and October), peaking at over 40 g C m^{-2} $month^{-1}$ in July, while the extreme-rich fen only had significant net CO_2 gain for two (July and August, Q_{10} - NEE model) or three (July, August, and September, L & T - NEE model) months of the growing season, with a peak uptake between 30 and 35 g C m^{-2} $month^{-1}$ estimated for August (Figure 13). Both sites were modelled to be slight CO_2 sources in May 2004 according to the Q_{10} - NEE model, while in October 2004, the poor fen was a net CO_2 sink compared to the extreme-rich fen, which was estimated to be a significant CO_2 source, according to both NEE models.

A likely explanation for the apparent variation between the sites in the monthly rates of net CO_2 exchange was the difference in the dominant plant functional types found at the contrasting peatlands. The poor fen was a site dominated by *Sphagnum* spp. and other 'evergreen' plant species such as *A. polifolia* and *P. mariana*, while the extreme-rich fen was dominated by the deciduous perennial sedge, *C. lasiocarpa* (Table 8, Table 9). The

evergreen species present at the poor fen site had lower photosynthetic capacities than the sedge at the extreme-rich fen, as indicated by the total N content of the dominant species at the two sites (Table 9), the total N content of the aboveground biomass (2.3 g m^{-2} at the poor fen compared to 3.0 g m^{-2} at the extreme-rich fen) and the light-response curves of GPP derived from peak season measurements of NEE at each of the peatlands (Figure 8). However, the evergreen species at the poor fen were active earlier and later in the season, while it took time for the *C. lasiocarpa* at the extreme-rich fen site to build tissue or leaf out at the start of the season and senescence occurred earlier in the fall.

This contrasting seasonality between the two peatland sites in net CO_2 exchange was especially pronounced in June when the poor fen was a significant sink (> 20 g C m^{-2} $month^{-1}$ according to both models) and the extreme-rich fen was essentially C neutral (Figure 13), indicating that the *C. lasiocarpa* canopy was not fully developed and biologically active yet. Further evidence for the delay in the seasonal *C. lasiocarpa* growth and development at the extreme-rich fen site was provided by measurements of *H* and *LE* from the first three EC campaigns (Figure 4). During the first two EC measurement periods at the extreme-rich fen site, mean values of *H* exceeded *LE* for most times during the day, while later in the season, during Period 3 (July 27 - August 13), mean diurnal values of *LE* surpassed *H*, indicating that transpiration from the active *Carex* canopy was dominating turbulent heat exchange. At the end of the 2004 growing season (October), the poor fen was calculated to be a net CO_2 sink, implying that the *Sphagnum* spp. ground cover was still physiologically active, with rates of GPP exceeding TER, perhaps due to cooler temperatures inhibiting respiration rates more than photosynthesis by this point in the season. The extreme-rich fen site was modelled to be a significant C source in October 2004, indicating the senescence of the *C. lasiocarpa* canopy and the cessation of the growing season. Therefore, the primary variable governing

the contrasting 2004 growing season CO_2-C budgets between the northern Alberta peatland sites was the plant community composition of each ecosystem, and the resulting differences in the seasonal pattern of biological activity.

Another contributing factor influencing the difference between the two peatland sites in their net CO_2-C balances over the course of the six month study were the ratios of C loss through TER compared to C gain through GPP. The ratio of cumulative 2004 growing season TER:GPP was approximately 0.7 for the poor fen and 0.9 for the extreme-rich fen site (Table 16). As well, chamber measurements indicated that peak season rates of TER were significantly greater at the extreme-rich fen than the poor fen in early and late July 2004 (Table 12; Figure 9).

There are a number of possible contributing factors which could result in larger rates of CO_2 loss at the extreme-rich fen compared to the poor fen site, as previously discussed regarding the chamber respiration measurements made at the two sites in July (Section 4.3). First, there is an established correlation between plant productivity and respiration (Amthor, 2000) due to growth and maintanence requirements, and ecosystem level studies have shown similar relationships between GPP and TER (Griffis et al. 2003). Therefore, because the extreme-rich fen had a higher photosynthetic capacity (A_{max}) at peak season (Table 10, Table 11; Figure 8) and greater cumulative GPP over the 6 month study (Table 16), it is intuitive that TER would be greater than at the poor fen as well. Secondly, although belowground (root) biomass was not measured in this study, it is expected that the belowground biomass of the *C. lasiocarpa* rhizomes at the extreme-rich fen would be much greater than the belowground biomass of the non-vascular *Sphagnum*-dominated poor fen. Up to 90 % of *Carex* spp. biomass production is estimated to be belowground (Sjörs, 1991; Thormann and Bayley, 1997b) while *Sphagnum* spp. lack roots, therefore it follows that belowground

respiration would be much greater at the extreme-rich fen than the poor fen, which would directly influence the ratio of TER:GPP. Thirdly, because of the greater lability of *Carex* spp. tissue and derived peat compared to that of *Sphagnum* spp. (Verhoeven and Toth, 1995; Szumigalski and Bayley, 1996; Frolking et al. 1998) rates of decomposition and decay would also be greater at the extreme-rich fen than the poor fen, further contributing to higher ratios of TER:GPP. Previous studies have noted a negative correlation between the rate of decay and C:N ratios, and a positive correlation between decomposition and N content (Updegraff et al. 1995; Szumigalski and Bayley, 1996b). The *Sphagnum* spp. at the poor fen site had a total N content that was less than half of the *C. lasiocarpa* at the extreme-rich fen, and a C:N ratio that was more than two times greater (Table 8), therefore the expected rate of decomposition would be much less at the poor fen. Furthermore, the lower pH of the surface water at the poor fen compared to the extreme-rich fen site (Table 1), and presence of phenolic *Sphagnum* spp. secondary metabolites (Verhoeven and Toth, 1995) may have also further inhibited the rate of peat and litter decay.

As well as the dominant biological controls influencing the contrasting net growing season CO_2-C budgets between the sites, the environmental variables used to model NEE (*T* and PPFD) were slightly different between the two peatland ecosystems during 2004, according to the monthly means of air temperature and sums of PPFD (Table 5, Table 7). For instance, the ratio of cumulative TER:GPP may have been greater at the extreme-rich fen due to warmer mean daily temperatures experienced at the site for all 6 months of the 2004 growing season compared to the poor fen (Table 5), resulting in higher cumulative TER. Furthermore, the extreme-rich fen received less incident PPFD than the poor fen every month of the study (Table 7), which could have reduced the potential GPP at the site and further increased the TER:GPP ratio.

4.5 Estimation of uncertainty in net ecosystem exchange measurements

The total relative uncertainty of the EC measurement based CO_2-C budgets calculated for the two peatland sites during the 2004 growing season depended on the method of estimating the random error component. The daily differencing approach (E_{R1}, Eq. 16) gave a much higher estimation of the composite random uncertainty for EC measurements than did the second method of evaluating the relationship between modelled and measured NEE (E_{R2}, Eq. 17), for both peatland sites (approximately 31 % greater for the poor fen and 42 % greater for the extreme-rich fen).

A logical explanation for the discrepancy between the random uncertainties determined with the two methods (E_{R1} and E_{R2}) is the fundamental difference in the statistical analyses applied. The daily differencing approach (E_{R1}, Eq. 16) is a calculation of the *standard deviation* of differences between independent measurements made under similar environmental conditions whereas E_{R2} (Eq. 17) is a calculation of the *standard error* of differences between measured and modelled NEE values. This difference in the statistical measure of variability calculated utilizing each approach (SD vs. SE) is one reason for the inconsistency in the magnitude of the random uncertainty estimates obtained with the two methods. As well, the daily differencing approach is known to be conservative, as estimations of random error using this method were 20-25 % higher than when uncertainty calculations were performed using two towers sampling at the same site and time (Hollinger and Richardson, 2005). A reason why this method may result in inflated estimations of random error could be due to environmental events such as nocturnal frost or rainfall which may change the state of the ecosystem between measurement periods, and is therefore uncertainty not associated with the actual flux measurements.

While the E_{R1} (Eq. 16) approach gave estimations of random uncertainty for the EC

measurements at the two sites that seem excessive, the estimations obtained utilizing the E_{R2} (Eq. 17) method seem low for current EC instrumentation and data acquisition systems, and the statistical complexity of turbulent transport. It is unlikely that all the random uncertainty in the EC measurements of NEE is accounted for by the relationship with empirically modelled fluxes (Eq. 17) as assumed by applying the approach. The true composite random error of the EC measurements of NEE in the present study was likely somewhere in between that obtained with the two separate approaches of uncertainty evaluation, as supported by the results from a comparison between the EC system employed in the present study and an independent system (Appendix A). The evaluation of the random error associated with flux measurements is currently an area of active research (Hollinger and Richardson, 2005) where more work is required to obtain defensible estimations when applying the EC method and for developing a standardized approach to uncertainty calculation (Goulden et al. 1996; Baldocchi, 2003). As of this writing, the optimal approach to estimating the random uncertainty associated with EC measurements of NEE remains unresolved.

The discrepancy in the random error estimations obtained via the two methods had the largest impact on the total relative uncertainty calculated for the poor fen CO_2-C budget (34.2 % vs. 8.0 %) compared to that determined for the extreme-rich fen (72.7 % vs. 58.1%) during the 2004 growing season (Figure 14). The reason why the method applied to estimating the random error had less of an impact at the extreme-rich fen, and why the total uncertainty was higher than that determined for the poor fen site, is because the systematic error (E_{SYS}) calculated from the u_* threshold sensitivity analysis was so much greater. E_{SYS} was calculated to be 7.8 % for the poor fen and 58.1% for the extreme-rich fen. This is the result of applying the $u_* \geq 0.10$ m s^{-1} threshold to the CO_2-C balance in the sensitivity analysis at the extreme-rich fen site, as it was significantly lower (-60 g C m^{-2}) than that calculated with

the 0.15, 0.20, and 0.25 m s^{-1} thresholds (-31, -39, and -24 g C m^{-2} respectively). Clearly a u_* threshold of 0.10 m s^{-1} was inadequate for the extreme-rich fen site, and TER was underestimated due to NEE measurements under conditions of low turbulent transport, resulting in a much lower value of cumulative growing season NEE (greater CO_2 sink). Support for the use of a higher u_* threshold (ie. $u_* \geq 0.15$ m s^{-1}) was obtained by the comparison of modelled to measured NEE using various friction velocity thresholds (Table 4) and through the visual inspection of nocturnal NEE measurements by the EC system at both sites during the growing season (Figure 1). Further confidence in the NEE measurements and subsequent analysis performed in the present study is provided by the correspondence in the cumulative CO_2-C budgets (NEE, TER and GPP terms) calculated with the two different NEE model approaches, either exclusively or by the gap-filling of available EC measurements (Table 16). The differences in the estimated CO_2-C budgets between the two different NEE model methods or between strictly modelling vs. gap-filling were generally much less than the total uncertainty associated with the NEE measurements calculated for each of the peatland sites

When the estimations of the total relative uncertainty associated with the NEE measurements by the EC system are used to assign error bars to the cumulative growing season CO_2-C budgets, a difference in the magnitude of the C sink strength between the sites is evident (Figure 14), but this difference is much less defined using the first approach to estimating uncertainty ($E_{RI} + E_{SYS}$) for reasons previously discussed. Although the precise scale of the total error associated with the flux measurements conducted during the 2004 growing season remains unclear, the results from the uncertainty analyses performed still indicate that the 6 month CO_2-C budgets at the two contrasting peatland sites are significantly different.

4.6 Implications of study findings and potential future research

The results from the present study suggest that contrasting peatland types along the bog to extreme-rich fen gradient may also vary in their magnitude of cumulative net CO_2 exchange over the course of a growing season, even if peak season rates of NEE appear to be quite similar. The amount and physiological characteristics of the aboveground vegetation at a peatland site seem to be good proxy for estimating net CO_2 exchange in the short and long term. The implications of these findings for future studies support the notion to not only consider peatland ecosystems as one ecological class, but perhaps as two or more distinct landscape types in global analysis research (Frolking et al. 1998). This highlights the need for further ground based studies of NEE spanning the bog to rich fen gradient, and the finer resolution of landscape cover so that it includes the variety and proportion of peatland types encountered, to enhance the accuracy of global C cycling and climate change predictions. The combined use of mobile EC techniques, supporting chamber measurements and empirical models driven by simple meteorological inputs appears to be a cost-effective and worthwhile approach for quantifying how net CO_2 exchange may vary between different peatland types in the same climatic region. Future studies examining NEE between similar peatland types located in different geographical regions could prove useful for predicting the possible effects of climate change on these important ecosystems, if standardized empirical models that allow direct comparison between relevant photosynthetic and respiratory parameters are employed.

During the 2004 growing season both peatland ecosystems in northern Alberta were estimated to be net CO_2-C sinks. However, other studies have shown significant inter-annual variability in net CO_2 exchange at the same peatland ecosystem site (Shurpali et al. 1995; Joiner et al. 1999; Lafleur et al. 2003), which emphasizes the need for multi-year NEE

studies. Although both peatland sites from the present study were calculated to be significant CO_2 sinks during the 2004 growing season, this may not be case during other years, and it would be interesting to see how peak season and cumulative net CO_2 fluxes differ at the sites during years of climatic variation. For example, during years of higher temperatures and less precipitation (resulting in a lower water table depth) it is expected that both ecosystems would be lower CO_2 sinks, due to the greater enhancement of TER relative to GPP. This could be especially important for the extreme-rich fen, which was estimated to be small net CO_2 sink during the 2004 growing season, but may actually be CO_2 neutral or a net source during years with different climatic forcing, such as under higher temperatures and lower water tables.

Potential future climate change causing warmer spring and fall temperatures and an increase in the length of the growing season at the two peatland sites could also result in different net CO_2 balances compared to the current study. At the poor fen site, it is likely that a warmer spring and fall would enhance net seasonal CO_2 sequestration, due to the effect of a longer growing season allowing the dominant evergreen species at the site to actively photosynthesize for a longer duration than in the present study. This would in turn lead to the poor fen becoming a larger net CO_2 sink during the growing season, provided that there is adequate precipitation to maintain the high water table and anaerobic belowground conditions at the site under such a hypothetical climate. However, the findings of the present study indicate that for the extreme-rich fen, it is possible that the effect of a longer growing season could have an opposite effect on the net growing season CO_2-C budget. Earlier snowmelts and warmer spring temperatures may lead to advanced leaf emergence, photosynthetic uptake of CO_2 and greater cumulative biomass production over the growing season by the dominant sedge species at the site compared to the present study. However,

there would likely be a greater net loss of CO_2 at the end of the season compared to the present study, through the occurrence of more respiration and decomposition with the advent of a warmer and prolonged autumn, which could diminish the small net CO_2 sink status of the ecosystem, and possibly even lead to significant net CO_2-C loss from the site under these climatic conditions.

In addition to the implications of future climate change, elevated atmospheric CO_2 concentrations could also impact net CO_2 exchange at the two peatlands in northern Alberta by directly affecting photosynthesis. Although species-specific responses have been observed, *Sphagnum* spp. generally show increased rates of productivity under conditions of elevated CO_2 (Van der Heijden et al. 2000; Mitchell et al. 2002). Therefore, at the poor fen site, it is expected that GPP would increase under higher atmospheric concentrations of CO_2 based on the contemporary dominant species at the site alone. The GPP of vascular plants at the poor fen site would also be expected to increase through enhanced nutrient-use efficiency, although this effect may only be short term, as essential nutrients would diminish further eventually, in the absence of significant inputs. How greater rates of GPP would effect the net CO_2 exchange at the site depends on the dynamics of how elevated CO_2 and other potential global change events (for example, warming and N deposition) would impact the proportion of vascular and non-vascular plants within the ecosystem, and the competitive relationships within and among species. If the poor fen was to continue being an ecosystem dominated by *Sphagnum* spp., conditions of elevated CO_2 could lead to the site becoming a larger net sink for CO_2-C. However, there is evidence that elevated CO_2 may increase the proportion of vascular plants to moss species in peatland ecosystems (Berendse et al. 2001; Freeman et al. 2004). If vascular plants in the ecosystem were to be become a more active component of the poor fen site biomass, one would expect increased aboveground and

belowground (root) autotrophic respiration, as well as, increased belowground heterotrophic respiration, stimulated by increased root exudates into the rhizosphere. This would result in a larger TER term at the poor fen, and lower cumulative net CO_2 gain over the course of a growing season. The extreme-rich fen site is dominated by the vascular species, *C. lasiocarpa*, and according to the July surface water chemisty analysis conducted, does not appear to be limiting for essential nutrients (Table 1). Therefore, under conditions of heightened atmospheric CO_2, the rate of GPP would be enhanced in the ecosystem. As well, the *C. lasiocarpa* plants growing under elevated CO_2 may develop altered leaf biochemistry compared to the present study, with a larger C:N ratio of leaf tissue, as has been observed in other studies (Rogers et al. 1999). A higher C:N ratio of the sedge leaf tissue at the extreme-rich fen would lead to increased C sequestration at the ecosystem by lowering rates of litter and peat decomposition. However, any enhanced CO_2-C gain by the extreme-rich fen through increased GPP and suppressed decomposition would likely be offset through greater rates of TER because of the increased growth rates, litter production and maintenance requirements of the *C. lasiocarpa*, as well as increased belowground heterotrophic respiration caused by larger inputs of plant exudates into the rhizosphere. Other studies indicate that the primary response of wetland plants to elevated CO_2 is increased root exudation, rather than an increase in aboveground plant production, as supported by larger methane emissions (Hutchin et al. 1995) and rising dissolved organic carbon concentrations in rivers draining peatland ecosystems in Wales (Freeman et al. 2004). This suggests that the net CO_2 balance of the extreme-rich fen ecosystem may not be significantly different from that observed during the current study when considering the effects of elevated CO_2 alone, and that resulting climatic conditions will be more important in regulating future rates of growing season NEE at the site.

In addition to contemporary and potential future inter-annual variability in net CO_2 exchange, it is important to realize that the present study only included NEE measurements and calculations during the 6 months which encompassed the growing season. Although this time of the year exerts the greatest influence on NEE due to the overwhelming influence of the seasonal activity of plants in these northern ecosytems, other studies have highlighted the importance of wintertime effluxes of CO_2 on annual C budgets for peatland ecosytems (Lafleur et al. 2001; Aurela et al. 2002). Slow but steady rates of CO_2 loss from peatland ecosytems during winter months can have a significant effect on cumulative net CO_2 balances. For example, it was calculated that the annual CO_2 balance of a subarctic fen in northern Finland would be overestimated by 150 % if the winter emissions from the site were not included (Aurela et al. 2002). The annual importance of wintertime fluxes and the lack of year-round NEE studies in northern peatlands exhibits the necessity for more measurements during non-growing season periods to further elucidate the complete C balance of these ecosystems, especially with the onset of warmer winter temperatures.

Finally, it must be noted that although net CO_2 fluxes dominate the overall C balance of peatlands, exports of C from these ecosystems also occur through methane (CH_4) emissions under anaerobic conditions (Wieder and Yavitt, 1994; Bubier et al. 1995) and the leaching of dissolved organic carbon (DOC), which may have a significant influence on annual C budgets (Moore et al. 1998; Aurela et al. 2002). Further measurements of these additional components contributing to net C cycling in peatlands are required and must be incorporated in future studies in order to estimate complete C budgets. In the context of the present study, CH_4 emissions in particular may have had a pronounced effect on the net C budget of the extreme-rich fen site. This could be due to a combination of the high water table during the growing season causing anaerobic conditions conducive to CH_4 production

(Moore et al. 1998) and the enhancement of fluxes through plant transport and root exudate production of the active sedge-dominated plant community (Bubier et al. 1995). The impact of CH_4 emissions on the net C budget at the extreme-rich fen may have negated the net CO_2-C gain during the 6 months, which would result in the site being either C neutral or a net C source during the 2004 growing season.

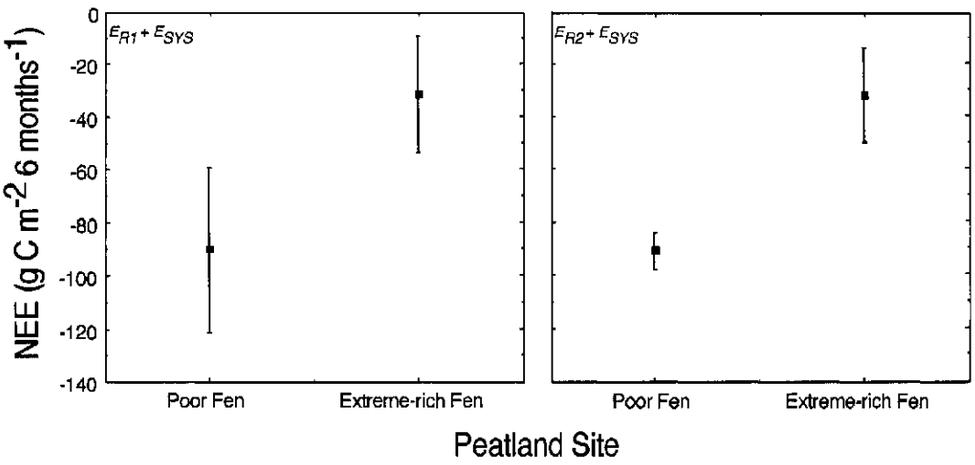

Figure 14. Total uncertainty of the 2004 growing season CO_2-C budgets for the two contrasting northern Alberta peatland sites. Symbols represent the cumulative 6 month CO_2-C balances for each site, as calculated using the Q_{10} - NEE model (Eq. 13) approach. Error bars represent the total relative uncertainty of the growing season C budgets, as estimated using two separate methods for determining the random error associated with the EC measurements of NEE: $E_{R1} + E_{SYS}$ (left-hand side) and $E_{R2} + E_{SYS}$ (right-hand side). E_{R1} is the random error associated with the EC measurements calculated with Eq. 16, E_{R2} is the random error associated with the EC measurements calculated with Eq. 17, and E_{SYS} is the systematic error of the EC measurements, estimated by performing a u_* threshold sensitivity analysis on the 6 month CO_2-C balances.

5. Conclusions

The two peatland ecosystems examined in the present study had significantly different growing season CO_2-C budgets during 2004. The poor fen was calculated to be a moderate sink for atmospheric CO_2, between 90 and 108 g C m^{-2} 6 $months^{-1}$, while the extreme-rich fen was a small CO_2 sink between 31 and 50 g C m^{-2} 6 $months^{-1}$, depending on the method employed to estimate cumulative NEE (Table 16).

Light intensity (PPFD) was found to be the major abiotic factor controlling GPP in the ecosystems, while temperature was the most significant variable regulating TER. The main biological factor influencing the net growing season CO_2 balances at the sites were the dominant plant species in each peatland and the resulting difference in the timing of biological activity for each respective ecosystem. The contrasting seasonality of net CO_2 fluxes between the sites is illustrated by the monthly CO_2-C budgets (Figure 13) and reflects the dominance of evergreen *Sphagnum* spp. at the poor fen site compared to the activity of the deciduous perennial, *C. lasiocarpa*, at the extreme-rich fen site. Although the poor fen site had a lower peak photosynthetic capacity than the extreme-rich fen (A_{max}, Table 10, Table 11; Figure 8), the evergreen plant species at the poor fen were metabolically active earlier and later in the growing season than the *C. lasiocarpa* at the extreme-rich fen, which had a dominating influence on the cumulative 6 month carbon budgets derived. As well, the rate of net CO_2 loss through TER was greater at the sedge-dominated extreme-rich fen compared to the *Sphagnum* spp.-dominated poor fen. This was reflected by larger R_{10} values determined from peak season EC measurements of NEE (Table 10; Table 11), chamber measurements of TER in July (Table 12; Figure 9), and the ratio of cumulative growing season TER:GPP (Table 16) at the two sites. The higher respiratory capacity of the extreme-rich fen site resulted in a similar mean diurnal pattern of NEE as the poor fen during the peak

of the 2004 growing season (Figure 7), despite the extreme-rich fen having a higher photosynthetic capacity at this time (Table 10; Table 11; Figure 8). The most significant reasons why the extreme-rich fen had a larger amount of net CO_2 loss through TER during the 2004 growing season compared to poor fen include the relationship between ecosystem productivity and both autotropic and heterotropic respiration, greater belowground biomass, and the greater lability of *Carex* spp. litter and peat compared to that derived from the more recalcitrant *Sphagnum* spp.

The results from this study indicate that peatland types which differ significantly in vegetative and chemical characteristics along the bog to rich fen gradient may also exhibit contrasting rates of net CO_2 exchange when integrated over the entire growing season. The characteristics (species composition, plant functional types, total N content of green tissue) and amount of live aboveground biomass at a particular peatland site appear to be good indicators for estimating the net CO_2 balance and how it may compare with contrasting peatland ecosystems within the same climatic region. The use of mobile EC systems, portable gas exchange instruments, meteorological measurements and empirical modelling can facilitate the testing of such hypotheses, as was the case in the present study. Future studies exploring inter-annual variability, wintertime effluxes of CO_2, and other components of peatland C cycling (CH_4 emissions and DOC exports), as well as, the further development and refinement of standardized NEE models by conducting campaigns at more sites would greatly enhance understanding the influence these important terrestrial wetland ecosystems exert on the global C cycle and potential feedbacks resulting from climate change.

References

Alberta Natural Heritage Information Center. 2005. Community Development, Government of Alberta. [http://www.cd.gov.ab.ca/preserving/parks/anhic/] Accessed on July 12, 2005.

Amthor J.S. 2000. The McCree-de Wit-Penning de Vries-Thornley respiration paradigms: 30 years later. *Annals of Botany* 86: 1-20.

Anderson L.E. 1990. A checklist of *Sphagnum* in North America north of Mexico. *The Bryologist* 93: 500-501.

Anderson L.E., Crum H.A., and Buck W.R. 1990. List of the mosses of North America north of Mexico. *The Bryologist* 93: 448-499.

Andrus R.E. 1986. Some aspects of *Sphagnum* ecology. *Canadian Journal of Botany* 64: 416-426.

Asner G.P., and Seastedt T.R. 1997. The decoupling of terrestrial carbon and nitrogen cycles. *Bioscience* 47: 227-235.

Aubinet M., Grelle A., Ibrom A., Rannik Ü., Moncrieff J., Foken T., Kowalski A.S., Martin P.H., Berbigier P., Bernhofer C., Clement R., Elbers J., Granier A., Grünwald T., Morgenstern K., Pilegaard K., Rebmann C., Snijders W., Valentini R., and Vesala T. 2000. Estimates of the annual net carbon and water exchange of forests: The EUROFLUX methodology. *Advances in Ecological Research* 30: 113-176.

Aurela M., Laurila T., and Tuovinen J.-P. 2002. Annual CO_2 balance of a subarctic fen in northern Europe: Importance of the wintertime efflux. *Journal of Geophysical Research* 107, No. D21, 4607 (doi: 10.1029/2002JD002055).

Baldocchi D.D., Hicks B.B., and Meyers T.D. 1988. Measuring biosphere-atmosphere exchanges of biologically related gases with micrometeorological methods. *Ecology* 69: 1,331-1,340.

Baldocchi D., Falge E., Gu L., Olson R., Hollinger D., Running S., Anthoni P., Bernhofer C., Davis K., Evans R., Fuentes J., Goldstein A., Katul G., Law B., Lee X., Malhi Y., Meyers T., Munger W., Oechel W., Paw U K.T., Pilegaard K., Schmid H.P., Valentini R., Verma S., Vesala T., Wilson K., and Wofsy S. 2001. FLUXNET: A new tool to study the temporal and spatial variability of ecosystem-scale carbon dioxide, water vapor, and energy flux densities. *Bulletin of the American Meteorological Society* 82: 2,415-2,434.

Baldocchi D.D. 2003. Assessing the eddy covariance technique for evaluating carbon dioxide exchange rates of ecosystems: past, present and future. *Global Change Biology* 9: 479-492.

Barford C.C., Wofsy S.C., Goulden M.L., Munger J.W., Pyle E.H., Urbanski S.E., Hutyra L., Saleska S.R., Fitzjarrald D., and Moore K. 2001. Factors controlling the long- and short-term sequestration of atmospheric CO_2 in a mid-latitude forest. *Science* 294: 1,688-1,691.

Barnola J.-M., Raynaud D., Lorius C., and Barkov N.I. 2003. Historical CO_2 record from the Vostok ice core. *In* Trends: A Compendium of Data on Global Change. Carbon Dioxide Information Analysis Center, Oak Ridge National Laboratory, U.S. Department of Energy, Oak Ridge, Tenn., U.S.A. [http://cdiac.esd.ornl.gov/trends/co2/vostok.htm] Accessed on July 12, 2005.

Bowes G. 1993. Facing the inevitable: plants and increasing atmospheric CO_2. *Annual Review of Plant Physiology and Plant Molecular Biology* 44: 309-332.

Bubier J.L., Bhatia G., Moore T.R., Roulet N.G., and Lafleur P.M. 2003. Spatial and temporal variability in growing-season net ecosystem carbon dioxide exchange at a large peatland in Ontario, Canada. *Ecosystems* 6: 353-367.

Bubier J.L., Crill P.M., Moore T.R., Savage K., and Varner R.K. 1998. Seasonal patterns and controls on net ecosystem CO_2 exchange in a boreal peatland complex. *Global Biogeochemical Cycles* 12: 703-714.

Bubier J.L., Moore T.R., Bellisario L., Comer N.T., and Crill P.M. 1995. Ecological controls on methane emissions from a northern peatland complex in the zone of discontinuous permafrost, Manitoba, Canada. *Global Biogeochemical Cycles* 9: 455-470.

Campbell M.K. 1999. Biochemistry (3rd edition). Harcourt Brace & Company, Orlando, Florida, USA. pp. 155-161.

Campbell D., and Smith J. 2001. Peatland Carbon and Water Budgets. The University of Waikato, Department of Earth Sciences, Waikato, New Zealand. [http://erth.waikato.ac.nz/research.campbell/carbon.flux/] Accessed on July 12, 2005.

Carroll P., and Crill P. 1997. Carbon balance of a temperate poor fen. *Global Biogeochemical Cycles* 11: 349-356.

Chapin III F.S., Matson P.A., and Mooney H.A. 2002. Principles of Terrestrial Ecosystem Ecology. Springer-Verlag, New York, New York. pp. 99-100.

Chen J.M., Rich P.M., Gower S.T., Norman J.M., and Plummer S. 1997. Leaf area index of boreal forests: Theory, techniques and measurements. *Journal of Geophysical Research* 102: 29,429-29,443.

Curtis P.S., and Wang X.Z. 1998. A meta-analysis of elevated CO_2 effects on woody plant mass, form, and physiology. *Oecologia* 113: 299-313.

Dang Q.L., Margolis H.A., Sy M., Coyea M.R., Collatz G.J., and Walthall C.L. 1997. Profiles of photosynthetically active radiation, nitrogen and photosynthetic capacity in the boreal forest: Implications for scaling from leaf to canopy. *Journal of Geophysical Research* 102: 28,845-28,859.

Drake B.G., Gonzalez-Meler M.A., and Long S.P. 1997. More efficient plants: A consequence of rising atmospheric CO_2? *Annual Review of Plant Physiology and Plant Molecular Biology* 48: 609-639.

Eamus D. 1991. The interaction of rising CO_2 and temperatures with water use efficiency. *Plant, Cell and Environment* 14: 843-852.

Environment Canada. 1995. The state of Canada's climate: monitoring variability and change. Environment Canada, Ottawa, Ontario. State of the Environment Report, #95-1.

Environment Canada. 1999. Climate trends and variations bulletin for Canada: Annual 1998 temperature and precipitation in historical perspective. Environment Canada, Atmospheric Environment Service, Climate Research Branch, Downsview, Ontario. [http://collection.nlc-bnc.ca/100/201/301/climate-e/1998/annual/index.html] Accessed on July 12, 2005.

Environment Canada. 2002a. Canada's Greenhouse Gas Inventory 1990-2000. Greenhouse Gas Division, Environment Canada. [http://www.ec.gc.ca/pdb/ghg/1990_00_report/foreword_e.cfm] Accessed on July 12, 2005.

Environment Canada. 2002b. Canadian Climate Normals or Averages: 1971 - 2000. [http://climate.weatheroffice.ec.gc.ca/climate_normals/] Accessed on July 12, 2005.

Eugster W., Mcfadden J.P., and Chapin III F.S. 1997. A comparative approach to regional variation in surface fluxes using mobile eddy correlation towers. *Boundary-Layer Meteorology* 85: 293-307.

Evans J.R. 1989. Photosynthesis and nitrogen relationships in leaves of C_3 plants. *Oecologia* 78: 9-19.

FACE Program. 2004. Office of Biological and Environmental Research, U.S. Department of Energy.
[http://www.face.bnl.gov/] Accessed on July 12, 2005.

Fang C., and Moncrieff J.B. 2001. The dependence of soil CO_2 efflux on temperature. *Soil Biology and Biochemistry* 33: 155-165.

Falge E., Baldocchi E., Olson R., Anthoni P., Aubinet M., Bernhofer C., Burba G., Ceulemans R., Clement R., Dolman H., Granier A., Gross P., Grünwald T., Hollinger D., Jensen N.-O., Katul G., Keronen P., Kowalski A., Lai C.T., Law B.E., Meyers T., Moncrieff J., Moors E., Suyker A., Tenhunen J., Tu K., Verma S., Vesala T., Wilson K., and Wofsy S. 2001. Gap filling strategies for defensible annual sums of net ecosystem exchange. *Agricultural and Forest Meteorology* 107: 43-69.

Farquhar G.D., von Caemmerer S., and Berry J.A. 1980. A biochemical model of photosynthetic CO_2 assimilation in leaves of C_3 species. *Planta* 149: 78-90.

Fearnside P.M. 2000. Global warming and tropical land use change: greenhouse gas emissions from biomass burning, decomposition and soils in forest conversion, shifting cultivation and secondary vegetation. *Climatic Change* 46: 115-158.

Flanagan L.B., Wever L.A., and Carlson P.J. 2002. Seasonal and interannual variation in carbon dioxide exchange and carbon balance in a northern temperate grassland. *Global Change Biology* 8: 599-615.

Flanagan L.B., and Johnson B.G. 2005. Interacting effects of temperature, soil moisture, and plant biomass production on ecosystem respiration in a northern temperate grassland. *Agricultural and Forest Meteorology* 130: 237-253.

FLUXNET Project. 2005. Distributed Active Archive Center for Biogeochemical Dynamics, Oak Ridge National Laboratory.
[http://www-eosdis.ornl.gov/FLUXNET/] Accessed on July 12, 2005.

FCRN. 2005. Fluxnet-Canada Research Network.
[http://www.fluxnet-canada.ca/] Accessed on July 12, 2005.

Frantz J.M., Cometti N.N., and Bugbee B. 2004. Night temperature has a minimal effect on respiration and growth in rapidly growing plants. *Annals of Botany* 94: 155-166.

Freeman C., Fenner N., Ostle N.J., Kang H., Dowrick D.J., Reynolds B., Lock M.A., Sleep D., Hughes S., and Hudson J. 2004. Export of dissolved organic carbon from peatlands under elevated carbon dioxide levels. *Nature* 430: 195-198.

Freeman C., Ostle N., and Kang H. 2001. An enzymatic 'latch' on a global carbon store. *Nature* 409: 149.

Friedli H., Lötscher H., Oeschger H., Siegenthaler U., and Stauffer B. 1986. Ice core record of 13C/12C ratio of atmospheric CO_2 in the past two centuries. *Nature* 324: 237-238.

Frolking S.E., Bubier J.L., Moore T.R., Ball T., Bellisario L.M., Bhardwaj A., Carrol P., Crill P.M., Lafleur P.M., McCaughey J.H., Roulet N.T., Suyker A.E., Verma S.B., Waddington J.M., and Whiting G.J. 1998. Relationship between ecosystem productivity and photosynthetically active radiation for northern peatlands. *Global Biogeochemical Cycles* 12: 115-126.

Gorham E. 1991. Northern peatlands: Role in the carbon cycle and probable responses to climatic warming. *Ecological Applications* 1: 182-195.

Goulden M.L., Munger J.M., Fan S.-M., Daube B.C., and Wofsy S.C. 1996. Measurements of carbon sequestration by long-term eddy covariance: Methods and a critical evaluation of accuracy. *Global Change Biology* 2: 169-182.

Goulden M.L., Wofsy S.C., Harden J.W., Trumbore S.E., Crill P.M., Gower S.T., Fries T., Daube B.C., Fan S.-M., Sutton D.J., Bazzaz A., and Munger J.W. 1998. Sensitivity of boreal forest carbon balance to soil thaw. *Science* 279: 214-216.

Gower S.T., Kucharik C.J., and Norman J.M. 1999. Direct and indirect estimation of leaf area index, f_{APAR}, and net primary production of terrestrial ecosystems. *Remote Sensing of Environment* 70: 29-51.

Grace J., and Malhi Y. 2002. Carbon dioxide goes with the flow. *Nature* 416: 594-595.

Griffis T.J., Black T.A., Morgenstern K., Barr A.G., Nesic Z., Drewitt G.B., Gaumont-Gauy D., and McCaughey J.H. 2003. Ecophysiological controls on the carbon balances of three southern boreal forests. *Agricultural and Forest Meteorology* 117: 53-71.

Gu L., Baldocchi D.D., Wofsy S.C., Munger J.W., Michalsky J.J., Urbanski S.P., and Boden T.A. 2003. Response of a deciduous forest to the Mount Pinatubo eruption: Enhanced photosynthesis. *Science* 299: 2,035-2,039.

Gullet D.W., and Skinner W.R. 1992.The state of Canada's climate: temperature change in Canada, 1895-1991. Environment Canada, Ottawa, Ontario. State of the Environment Report, #92-2.

Hilbert D.W., Roulet N., and Moore T. 2000. Modelling and analysis of peatlands as dynamical systems. *Journal of Ecology* 88: 230-242.

Hogg E.H., and Hurdle P.A. 1995. The aspen parkland in western Canada: A dry-climate analogue for the future boreal forest? *Water, Air and Soil Pollution* 82: 391-400.

Hogg E.H., Brandt J.P., and Kochtubajda B. 2002. Growth and dieback of aspen forests in northwestern, Alberta, Canada, in relation to climate and insects. *Canadian Journal of Forest Research* 32: 823-832.

Hollinger D.Y., Goltz S.M., Davidson E.A., Lee J.T., Tu K., and Valentine H.T. 1999. Seasonal patterns and environmental control of carbon dioxide exchange in an ecotonal boreal forest. *Global Change Biology* 5: 891-902.

Hollinger D.Y., and Richardson A.D. 2005. Uncertainty in eddy covariance measurements and its application to physiological models. *Tree Physiology* 25: 873-885.

Houghton R.A., Davidson E.A., and Woodwell G.M. 1998. Missing sinks, feedbacks, and understanding the role of terrestrial ecosystems in the global carbon balance. *Global Biogeochemical Cycles* 12: 25-34.

Intergovernmental Panel on Climate Change (IPCC). 2001. Working Group 1: Third Assessment Report. Climate Change 2001: The Scientific Basis. [http://www.grida.no/climate/ipcc_tar/wg1/index.htm] Accessed on July 12, 2005.

Jacobs A.F.G., Ronda R.J., and Holtslag A.A.M. 2003. Water vapour and carbon dioxide fluxes over bog vegetation. *Agricultural and Forest Meteorology* 116: 103-112.

Janssen P.H.M, and Heuberger P.S.C. 1995. Calibration of process-orientated models. *Ecological Modelling* 83: 55-66.

Johnson D., Kershaw L., MacKinnon A., and Pojar J. 1995. Plants of the Western Boreal Forest and Aspen Parkland. Lone Pine Publishing, Edmonton, Alberta. pp. 15-16.

Joiner D.W., Lafleur P.M., McCaughey J.H., and Bartlett P.A. 1999. Interannual variability in carbon dioxide exchanges at a boreal wetland in the BOREAS northern study area. *Journal of Geophysical Research* 104: 27,663-27,672.

Jones H.G. 1992. Plants and microclimate: A quantitative approach to environmental plant physiology (2nd Ed.). Cambridge University Press, Cambridge, UK. pp. 163-214.

Kavanau J.L. 1951. Enzyme kinetics and the rate of biological processes. *Journal of General Physiology* 34: 193-209.

Keeling C.D. and Whorf T.P. 2004. Atmospheric CO_2 records from sites in the SIO air sampling network. *In* Trends: A Compendium of Data on Global Change. Carbon Dioxide Information Analysis Center, Oak Ridge National Laboratory, U.S. Department of Energy, Oak Ridge, Tenn., U.S.A. [http://cdiac.esd.ornl.gov/trends/co2/sio-mlo.htm] Accessed on July 12, 2005.

Kim J., and Verma S.B. 1992. Soil surface CO_2 flux in a Minnesota peatland. *Biogeochemistry* 18: 37-51.

Kljun N., Calanca P., Rotach M.W., and Schmid H.P. 2004a. A simple parameterisation for flux footprint predictions. *Boundary-Layer Meteorology* 112: 503-523.

Kljun N., Calanca P., Rotach M.W., and Schmid H.P. 2004b. A simple parameterisation for flux footprint predictions. Online footprint. [http://footprint.kljun.net/] Accessed on July 12, 2005.

Körner C., Kowalski S., Sartore M., Burlett R., Berbigier P., and Loustau D. 2003. The annual carbon budget of a French pine forest (*Pinus pinaster*) following harvest. *Global Change Biology* 9: 1051-1065.

Lafleur P.M., McCaughey J.H., Joiner D.W., Bartlett P.A., and Jelinski D.E. 1997. Seasonal trends in energy, water, and carbon dioxide fluxes at a northern boreal wetland. *Journal of Geophysical Research* 102: 29,002-29,020.

Lafeur P.M., Moore T.R., Roulet N.T., and Frolking S. *in press*. Ecosystem respiration in a cool temperate bog: dependency on peat temperature and moisture content. *Ecosystems*.

Lafleur P.M., Roulet N.T., and Admiral S.W. 2001. Annual cycle of CO_2 exchange at a bog peatland. *Journal of Geophysical Research* 106: 3,071-3,081.

Lafleur P.M., Roulet N.T., Bubier J.L., Frolking S., and Moore T.M. 2003. Interannual variability in the peatland-atmosphere carbon dioxide exchange at an ombrotrophic bog. *Global Biogeochemical Cycles* 17, (doi: 10.1029/2002GB001983).

Landsberg J.J. 1977. Some useful equations for biological studies. *Experimental Agriculture* 13: 273-286.

Leuning R., and Judd M.J. 1996. The relative merits of open- and closed-path analyzers for measurement of eddy fluxes. *Global Change Biology* 2: 241-253.

Leuning R., and King K.M. 1992. Comparison of eddy-covariance measurements of CO_2 fluxes by open- and closed-path CO_2 analyzers. *Boundary-Layer Meteorology* 59: 297-311.

Leuning R., and Moncreiff J.B. 1990. Eddy-covariance CO_2 flux measurements using open- and closed-path CO_2 analyzers: corrections for analyzer water vapour sensitivity and damping of fluctuations in air sampling tubes. *Boundary-Layer Meteorology* 53: 63-76.

LI-COR Inc. 1998. Considerations for measuring ground CO_2 effluxes with chambers. LI-COR Application Note #124. LI-COR Inc., Lincoln, NE, U.S.A.

Limnology Service Unit. 2005. Limnology Laboratory, Department of Biological Sciences, Faculty of Science, University of Alberta, Edmonton, AB. [http://www.biology.ualberta.ca/facilities/limnology/] Accessed on July 12, 2005.

Lloyd J., and Taylor J.A. 1994. On the temperature dependence of soil respiration. *Functional Ecology* 8: 315-323.

Mahli Y., Baldocchi D.D., and Jarvis P.G. 1999. The carbon balance of tropical, temperate and boreal forests. *Plant, Cell and Environment* 22: 715-740.

Marland G., Boden T.A., and Andres R.J. 2003. Global, Regional, and National CO_2 Emissions. *In* Trends: A Compendium of Data on Global Change. Carbon Dioxide Information Analysis Center, Oak Ridge National Laboratory, U.S. Department of Energy, Oak Ridge, Tenn., U.S.A. [http://cdiac.esd.ornl.gov/trends/emis/tre_glob.htm] Accessed on July 12, 2005.

McGuire A.D., Melillo J.M., and Joyce L.A. 1995. The role of nitrogen in the response of forest net primary production to elevated atmospheric carbon dioxide. *Annual Review of Ecology and Systematics* 26: 473-503.

Mitchell E.A.D., Buttler A., Grosvernier P., Rydin H., Siegenthaler A., and Gobat J.-M. 2002. Contrasted effects of increased N and CO_2 supply on two keystone species in peatland restoration and implications for global change. *Journal of Ecology* 90: 529-533.

Moncrieff J.B., Massheder J.M., de Bruin H., Elbers J., Friborg T., Heusinkveld B., Kabat P., Scott S., Soegaard H., and Verhoef A. 1997. A system to measure surface fluxes of momentum, sensible heat, water vapour and carbon dioxide. *Journal of Hydrology* 188-189: 589-611.

Monteith J.L. 1965. Light distribution and photosynthesis in field crops. *Annals of Botany* 29: 17-37.

Moore G.W.K., Holdsworth G., and Alverson K. 2002. Climate change in the North Pacific region over the past three centuries. *Nature* 420: 401-403.

Moore T.R., Roulet N.T., and Waddington J.M. 1998. Uncertainty in predicting the effect of climatic change on the carbon cycling of Canadian peatlands. *Climatic Change* 40: 229-245.

Moss E.H. 1983. Flora of Alberta: A Manual of Flowering Plants, Conifers, Ferns and Fern Allies Found Growing Without Cultivation in the Province of Alberta, Canada. 2nd edition, revised by J. G. Packer. University of Toronto Press, Toronto, Ontario.

National Wetlands Working Group. 1988. Wetlands of Canada. Ecological Land Classification Series No. 24. Sustainable Development Branch, Environment Canada, Ottawa, Ontario, Canada. Polyscience Publications, Inc., Montreal, Quebec.

National Oceanic and Atmospheric Administration (NOAA). 1999. Climate of 1998 annual review. National Oceanic and Atmospheric Administration, National Climatic Data Center, Asheville, North Carolina, U.S.A. [http://www.ncdc.noaa.gov/oa/climate/research/1998/ann/ann98.html] Accessed on July 12, 2005.

Neftel A., Friedli H., Moor E., Lötscher H., Oeschger H., Siegenthaler U., and Stauffer B. 1994. Historical CO_2 record from the Siple Station ice core. *In* Trends: A Compendium of Data on Global Change. Carbon Dioxide Information Analysis Center, Oak Ridge National Laboratory, U.S. Department of Energy, Oak Ridge, Tenn., U.S.A. [http://cdiac.esd.ornl.gov/trends/co2/siple.htm] Accessed on July 12, 2005.

Neumann H.H., den Hartog G., King K.M., and Chipanshi A.C. 1994. Carbon dioxide fluxes over a raised open bog at Kinosheo Lake tower site during the Northern Wetlands Study (NOWES). *Journal of Geophysical Research* 99: 1,529-1,538.

Oechel W.C., Vourlitis G.L., Hastings S.J., Ault Jr. R.P., and Bryant P. 1998. The effects of water table manipulation and elevated temperature on the net CO_2 flux of wet sedge tundra ecosystems. *Global Change Biology* 4: 77-90.

Oke T.R. 1987. Boundary layer climates (2nd Ed.). Routledge, New York, New York, U.S.A. pp. 14-15.

O'Neill K.P. 2000. Role of bryophyte dominated ecosystems in the global carbon budget. *In:* Bryophyte Biology. Shaw A.J., and Goffinet B. (editors). Cambridge University Press, Cambridge, UK. pp. 344-368.

Peterson A.G., Ball J.T., Luo Y., Field C.B., Reich P.B., Curtis P.S., Griffin K.L., Gunderson C.A., Norby R.J., Tissue D.T., Forstreuter M., Rey A., Vogel C.S., and CMEAL pariticipants. 1999. The photosynthesis-leaf nitrogen relationship at ambient and elevated atmospheric carbon dioxide: A meta-analysis. *Global Change Biology* 5: 331-346.

Price D.T., and Apps M.J. 1996. Boreal forest responses to climate-change scenarios along an ecoclimatic transect in central Canada. *Climatic Change* 34: 179-190.

Reader R.J., and Stewart J.M. 1972. The relationship between net primary production and accumulation for a peatland in southeastern Manitoba. *Ecology* 53: 1,024-1,037.

Reichstein M., Tenhunen J.D., Roupsard O., Ourcival J.-M., Rambal S., Dore S., and Valentini R. 2002. Ecosystem respiration in two Mediterranean evergreen Holm Oak forests: drought effects and decomposition dynamics. *Functional Ecology* 16: 27-39.

Rogers H.H., Runion G.B., Prior S.A., and Torbert H.A. 1999. Response of plants to elevated CO_2: Root growth, mineral nutrition and soil carbon. *In:* Carbon Dioxide and Environmental Stress. Mooney H.A., and Luo Y. (editors). Academic Press, Toronto, Ontario. pp. 224-244.

Ruimy A., Jarvis P.G., Baldocchi D.D., and Saugier B. 1995. CO_2 fluxes over plant canopies and solar radiation: A review. *Advances in Ecological Research* 26: 1-68.

Ryan M.G. 1991. Effects of climate change on plant respiration. *Ecological Applications* 1: 157-167.

Schimel D.S. 1995. Terrestrial ecosystems and the carbon cycle. *Global Change Biology* 1: 77-91.

Schimel D.S., House J.I., Hibbard K.A., Bousquet P., Ciais P., Peylin P., Braswell B.H., Apps M.J., Baker D., Bondeau A., Canadell J., Churkina G., Cramer W., Denning A.S., Field C.B., Friedlingstein P., Goodale C., Heimann M., Houghton R.A., Melillo J.M., Moore III B., Murdiyarso D., Noble I., Pacala S.W., Prentice I.C., Raupach M.R., Rayner P.J., Scholes R.J., Steffen W.L., and Wirth C. 2001. Recent patterns and mechanisms of carbon exchange by terrestrial ecosystems. *Nature* 414: 169-172.

Schindler D.W. 1997. A dim future for boreal waters and landscapes. *Bioscience* 48: 157-164.

Schulze E.-D., Wirth C., and Heimann M. 2002. Managing forests after Kyoto. *Science* 289: 2,058-2,059.

Shurpali N.J., Verma S.B., Kim J., and Arkebauer T.J. 1995. Carbon dioxide exchange in a peatland ecosystem. *Journal of Geophysical Research* 100: 14,319-14,326.

Silvola J., Alm J., Ahlholm U., Nykanen H., and Martikainen P.J. 1996. CO_2 fluxes from peat in boreal mires under varying temperature and moisture conditions. *Journal of Ecology* 84: 219-228.

Sjörs H. 1952. On the relation between vegetation and electrolytes in north Swedish mire waters. *Oikos* 2: 241-258.

Sjörs H. 1991. Phyto- and necromass above and below ground in a fen. *Holarctic Ecology* 14: 208-218.

Smith E.L. 1938. Limiting factors in photosynthesis: Light and carbon dioxide. *Journal of General Physiology* 22: 21-35.

Smith J.C., Campbell D.I., and Schipper L.A. *submitted for publication.* CO_2 exchange at a Southern Hemisphere raised peat bog. *Agricultural and Forest Meteorology.*

Sokal R.R., and Rohlf F.J. 1995. Biometry (3rd edition). W.H. Freeman & Co., New York, New York, USA. pp. 541-546.

Sprugel D.G. 1983. Correcting for bias in log-transformed allometric equations. *Ecology* 64: 209-210.

Stoy P., and Zhang M. 2004. Understanding Respiration: A study of driving variables and models. [http://www.biology.duke.edu/bio265/zhangmin/] Accessed on July 12, 2005.

Suyker A.E., Verma S.B., and Arkebauer T.J. 1997. Season-long measurement of carbon dioxide exchange in a boreal fen. *Journal of Geophysical Research* 102: 29,021-29,028.

Swanson R.V., and Flanagan L.B. 2001. Environmental regulation of carbon dioxide exchange at the forest floor in a boreal black spruce ecosystem. *Agricultural and Forest Meteorology* 108: 165-181.

Szumigalski A.R., and Bayley S.E. 1996a. Net aboveground primary production along a bog-rich fen gradient in central Alberta, Canada. *Wetlands* 16: 467-476.

Szumigalski A.R., and Bayley S.E. 1996b. Decomposition along a bog to rich fen gradient in central Alberta, Canada. *Canadian Journal of Botany* 74: 573-581.

Thormann M.N., and Bayley S.E. 1997a. Aboveground plant production and nutrient content of the vegetation in six peatlands in Alberta, Canada. *Plant Ecology* 131: 1-16.

Thormann M.N., and Bayley S.E. 1997b. Aboveground net primary production along a bog-fen-marsh gradient in southern boreal Alberta, Canada. *Ecoscience* 4: 374-383.

Tjoelker M.G., Oleksyn J., and Reich P.B. 2001. Modelling respiration of vegetation: evidence for a general temperature-dependent Q_{10}. *Global Change Biology* 7: 223-230.

Turetsky M.R., Wieder R.K., Williams C.J., and Vitt D.H. 2000. Organic matter accumulation, peat chemistry, and permafrost melting in peatlands of boreal Alberta. *Ecoscience* 7: 379-392.

Updegraff K., Pastor J., Bridgham S.D., and Johnston C.A. 1995. Environmental and substrate controls over carbon and nitrogen mineralization in northern wetlands. *Ecological Applications* 5: 151-163.

Valentini R., Matteucci G., Dolman A.J., Schulze E.-D., Rebmann C., Moors E.J., Granier A., Gross P., Jensen N.O., Pilegaard K., Lindroth A., Grelle A., Bernhofer C., Grünwald T., Aubinet M., Ceulemans R., Kowalski A.S., Vesala T., Rannik Ü, Berbigier P., Loustau D., Guomundsson J., Thorgeirsson H., Ibrom A., Morgenstern K., Clement R., Moncrieff J., Montagnani L., Minerbi S., and Jarvis P.G. 2000. Respiration as the main determinant of carbon balance in European forests. *Nature* 404: 861-865.

Van der Heijden E., Verbeek S.K., and Kuiper P.J.C. 2000. Elevated atmospheric CO_2 and increased N deposition: effects on C and N metabolism and growth of the peat moss *Sphagnum recurvum* P. Beauv. var. *mucronatum* (Russ.) Warnst. *Global Change Biology* 6: 201-212.

Verhoeven J.T.A., and Toth E. 1995. Decomposition of *Carex* and *Sphagnum* litter in fens: Effect of litter quality and inhibition by living tissue homogenates. *Soil Biology and Biochemistry* 27: 271-275.

Verma S.B., Kim J., and Clement R.J. 1989. Carbon-dioxide, water vapor, and sensible heat exchanges of a tallgrass prairie. *Boundary-Layer Meteorology* 46: 53-67.

Vitt D.H., Achuff P., and Andrus R.E. 1975. The vegetation and chemical properties of patterned fens in the Swan Hills, north central Alberta. *Canadian Journal of Botany* 53: 2,776-2,795.

Vitt D.H., and Slack N.G. 1984. Niche diversification of *Sphagnum* relative to environmental factors in northern Minnesota peatlands. *Canadian Journal of Botany* 62: 1,409-1,430.

Vitt D.H. 1994. An overview of the factors that influence the development of Canadian peatlands. *Memoirs of the Entomological Society of Canada* 169: 7-20.

Vitt D.H., Bayley S.E., and Jin T-L. 1995. Seasonal variation in water chemistry over a bog-rich fen gradient in continental Western Canada. *Canadian Journal of Fisheries and Aquatic Sciences* 52: 587-606.

Vitt D.H., Halsey L.A., Thormann M.N., and Martin T. 1998. Peatland Inventory of Alberta, Phase 1: Overview of peatland resources in the natural regions and subregions of the province. Sustainable Forest Management Network, University of Alberta, Edmonton, Alberta.

Vourlitis G.L., and Oechel W.C. 1999. Eddy covariance measurements of net CO_2 and energy fluxes of an Alaskan tussock tundra. *Ecology* 80: 686-701.

Wieder R.K., and Yavitt J.B. 1994. Peatlands and global climate change: Insights from comparative studies of sites situated along a latitudinal gradient. *Wetlands* 14: 229-238.

Williams T.G., and Flanagan, L.B. 1998. Measuring and modelling environmental influences on photosynthetic gas exchange in *Sphagnum* and *Pleurozium*. *Plant, Cell and Environment* 21: 555-564.

Wofsy S.C., Goulden M.L., Munger J.W., Fan S.-M., Bakwin P.S., Daube B.C., Bassow S.L., and Bazzaz F.A. 1993. Net exchange of CO_2 in a mid-latitude forest. *Science* 260: 1,314-1,317.

Wohlfahrt G., Anfang C., Bahn M., Haslwanter A., Newesly C., Schmitt M., Drosler M., Pfadenhauer J., and Cernusca A. 2005. Quantifying nighttime ecosystem respiration of a meadow using eddy covariance, chambers and modeling. *Agricultural and Forest Meteorology* 128: 141-162.

Woodward F.I., and Smith T.M. 1994. Global photosynthesis and stomatal conductance: Modelling the controls by soil and climate. *Advances in Botanical Research* 20: 1-41.

World Meteorological Organization. 2004. WMO statement on the status of global climate (annual). World Meteorological Organization, Geneva, Switzerland. WMO-#966. [http://www.wmo.ch/web/wcp/wcdmp/statement/html/statement.html] Accessed on July 12, 2005.

World Meteorological Organization. 2005. WMO press release #718 (December 15, 2004). World Meteorological Organization, Geneva, Switzerland. [http://www.wmo.ch/index-en.html] Accessed on July 12, 2005.

Wyngaard J.C. 1990. Scalar fluxes in the planetary boundary layer - Theory, modeling, and measurement. *Boundary-Layer Meteorology* 50: 49-75.

Appendix A

Comparison between open-path and closed-path eddy covariance systems

Introduction

There are two kinds of commonly utilized infra-red gas analyzers (IRGAs) in eddy covariance (EC) field studies for measuring fluctuating CO_2 and water vapour concentrations, the open-path IRGA and the closed-path IRGA. The major difference between the two types of gas analyzers is that an open-path IRGA directly measures scalar concentrations in eddies within an open optical path, from a mounted position on an instrument tower, whereas in a closed-path EC system, air is drawn down from near the sonic anemometer-thermometer (SAT) location on the tower via a sampling tube to the IRGA, prior to the assessment of scalar concentrations within a closed optical cell (Leuning and Moncrieff, 1990; Leuning and King, 1992; Leuning and Judd, 1996). Because an open-path IRGA measures scalar concentrations in the open optical path of the instrument, they are sensitive to environmental conditions that interfere with the sensors, such as dust, frost, snow, rain, dew or condensation (Leuning and Judd, 1996). Under such unfavourable environmental conditions, data from open-path systems must be discarded, which can decrease the amount of data coverage significantly for a field campaign. Closed-path IRGAs are more appropriate for long-term eddy covariance studies, as detectors are located in protective housing. Open-path IRGAs are adequate for shorter campaigns, especially in drier environments, and are desired when making measurements over aerodynamically smooth terrain, where high-frequency response is required. Additionally, open-path EC systems consume less power because they do not require a pump, so they are more suitable for remote sites with limited electricity available.

The purpose of the following exercise was to compare data simultaneously collected by two contrasting EC systems at the main Fluxnet-Canada Research Network (FCRN) Western Peatland flux station in order to evaluate how the methodology of measurements and post-processing techniques applied with each system affects the outcome of final flux calculations. The two EC systems employed contained different IRGAs (open- and closed-path), sonic anemometers, and data acquisition systems. Both EC packages were mounted on the same instrumentation tower so agreement in the measured ecosystem fluxes of CO_2, latent (LE) and sensible (H) heat would provide confidence in the measurements and data processing procedures employed with each of the systems.

Materials and Methods

The main FCRN Western Peatland flux station (54.95°N, 113.32°W; 550 m a.s.l.) was located approximately 100 km northeast of Athabasca, AB in the Dry Mixedwood Subregion of the Boreal Natural Region of Alberta. The climate at the site was similar to that described for the poor fen and extreme-rich fen site in section 2.1.1. The site was a treed, moderate-rich fen and fell in between the poor and extreme-rich fen sites on the poor to rich fen gradient, in terms of surface water chemistry (surface water pH = 6.2 in late July) and vegetation characteristics. The aboveground plant biomass of the treed, moderate-rich fen was dominated by the coniferous tree species, *Picea mariana* and *Larix laricina*. There was

a well developed understory at the site consisting of numerous shrub (*Betula pumila var. glandulifera*, *Salix* spp., and *Ledum groenlandicum*), dwarf shrub (*Andromeda polifolia*, *Oxycoccus microcarpus* and *Vaccinium vitis-idaea*) and herbaceous (including *Carex* spp., *Menyanthes trifoliata*, *Smilacina trifolia* and other) vascular plant species, as well as, non-vascular *Sphagnum* spp. and the feather moss, *Pleurozium schreberi*.

A comparison between the mobile open-path eddy covariance system (OPECS) employed in the present study and the closed-path eddy covariance system (CPECS) that operates year-round at the main FCRN Western Peatland flux station was conducted between September 1 and September 7, 2004. Details of the OPECS, general EC theory and the analysis of high-frequency data are given in section 2.4.1. The CPECS consisted of a 3-D sonic anemometer-thermometer (SAT; model R3, Gill Instruments Ltd., Lymington, England) used to measure temperature, wind velocity and direction, and a fast response closed-path IRGA (model LI7000, LI-COR Inc., Lincoln, NE) to measure concurrent fluctuations of scalar (CO_2 and H_2O) concentrations. The CPECS SAT, OPECS SAT and open-path IRGA were mounted on separate horizontal booms at a height of 10 m on a triangular instrumentation tower and orientated into the direction of prevailing winds (west). The CPECS IRGA was mounted within temperature-controlled housing (kept at 37°C) on a scaffold tower next to the triangular instrumentation tower. Air for analysis of CO_2 and H_2O concentrations was drawn from an inlet located near the head of the CPECS SAT transducer array through a heated (9°C above ambient temperature) sampling tube by a diaphragm pump located downstream from the closed-path IRGA. A flow rate of 17 l min^{-1} was applied to ensure turbulent flow through the sampling tube. With this system configuration and flow rate, the pressure in the CPECS IRGA optical cell was approximately 12 kPa below ambient. The output from the CPECS SAT and IRGA was logged at a frequency of 20 Hz by a computer located within a temperature-controlled hut near the towers, using the University of Edinburgh EdiSol software (Moncrieff et al. 1997). Post-processing of high frequency data and the calculation of net ecosystem fluxes of CO_2, H_2O and sensible heat measured by the CPECS was done with a MATLAB program in a manner similar to that described for the OPECS (Section 2.4.1). The OPECS and CPECS were compared based on H, LE ($u_* \geq 0.15$ m s^{-1}), and NEE ($u_* \geq 0.15$ m s^{-1}) measurements with Model II (geometric mean) regressions (Sokal and Rohlf, 1995).

Results and Discussion

There was excellent agreement for the measured fluxes of H between the OPECS SAT and the CPECS SAT (Figure 15) but lower correspondence in LE measurements between the two EC systems (Figure 16). Although, the slope of the regression for LE between the two EC systems was close to 1 and the coefficient of determination (r^2) was relatively high, there was scatter evident in the data set (Figure 16). Exact reasons for the slight discrepancy in measured LE fluxes between the two systems are unclear, but it could be due to cool temperatures, high relative humidities (Figure 18) and precipitation (Figure 19) during the system comparison, and subsequent limitations of the open-path IRGA under such climatic conditions. However, the comparison of measured NEE between the OPECS and CPECS exhibited good agreement (Figure 17), despite the observed variability in the measured water vapour fluxes.

Overall, there was close correspondence between the two different EC systems in the measured net ecosystem fluxes of CO_2, H_2O, and H at the treed, moderate-rich fen site from September 1 and September 7, 2004. The comparisons of measured turbulent energy and scalar fluxes (Figure 15, Figure 16, Figure 17) provided further confidence in previous and ongoing measurements at the main FCRN Western Peatland site obtained from the CPECS, and those obtained with the mobile OPECS during the 2004 growing season at the poor and extreme-rich fen sites.

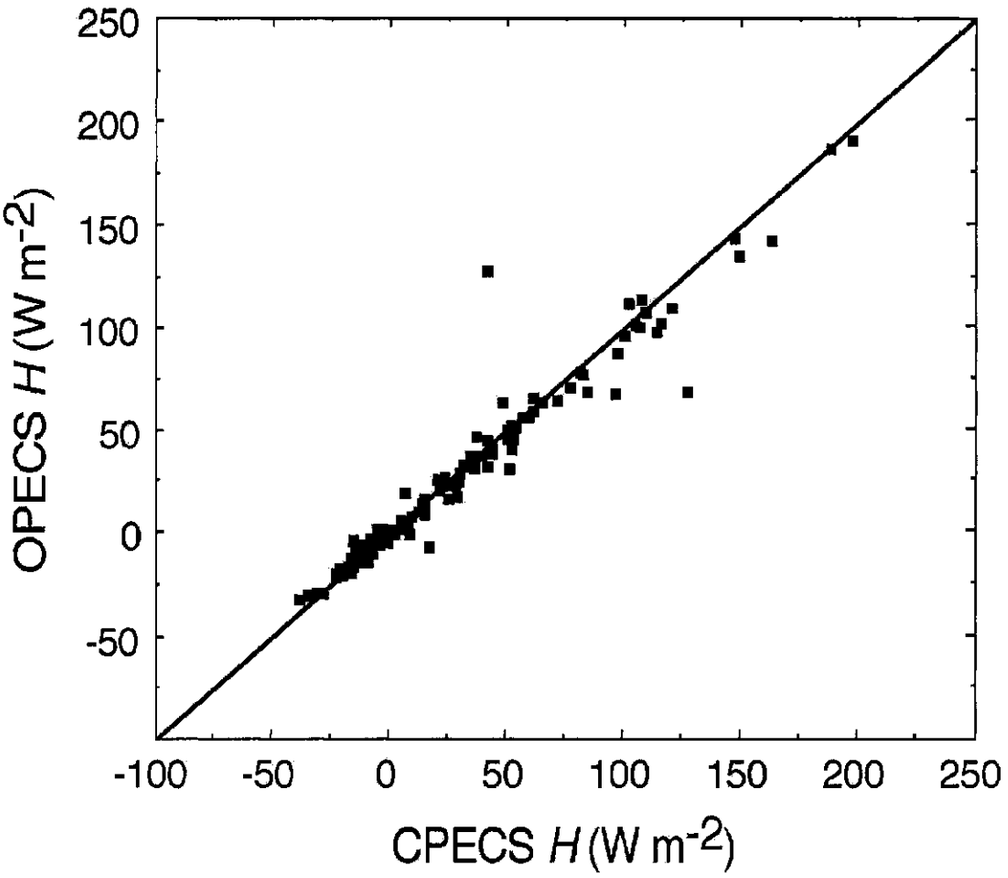

Figure 15. Comparison of measured sensible heat (*H*) fluxes between the open-path eddy covariance system (OPECS) and closed-path eddy covariance system (CPECS) at a treed, moderate-rich fen in northern Alberta from September 1 to September 7, 2004. The 1:1 line is shown on the figure. Regression: slope (± 95 % C.I.) = 0.95 ± 0.03, y-intercept = - 0.17, r^2 = 0.95, n = 158.

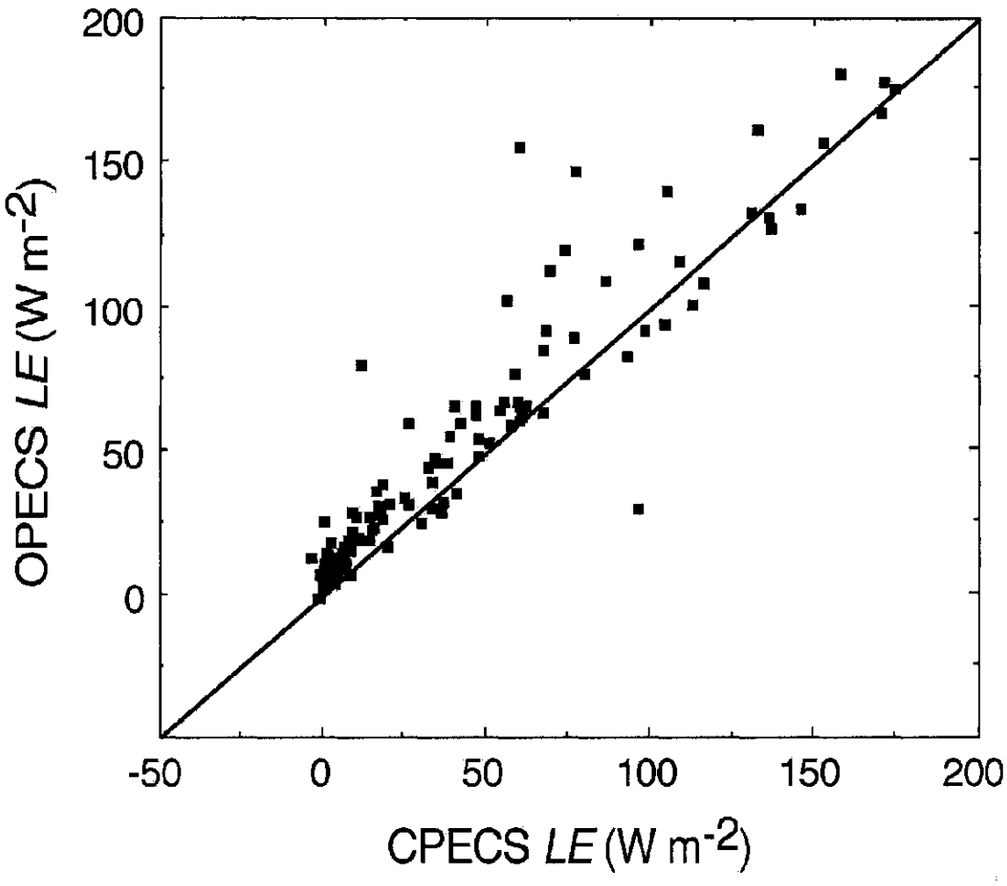

Figure 16. Comparison of measured latent heat (*LE*; $u_* \geq 0.15$ m s^{-1}) fluxes between the open-path eddy covariance system (OPECS) and closed-path eddy covariance system (CPECS) at a treed, moderate-rich fen in northern Alberta from September 1 to September 7, 2004. The 1:1 line is shown on the figure. Regression: slope (± 95 % C.I.) = 1.04 ± 0.06, y-intercept = 7.59, $r^2 = 0.88$, n = 122.

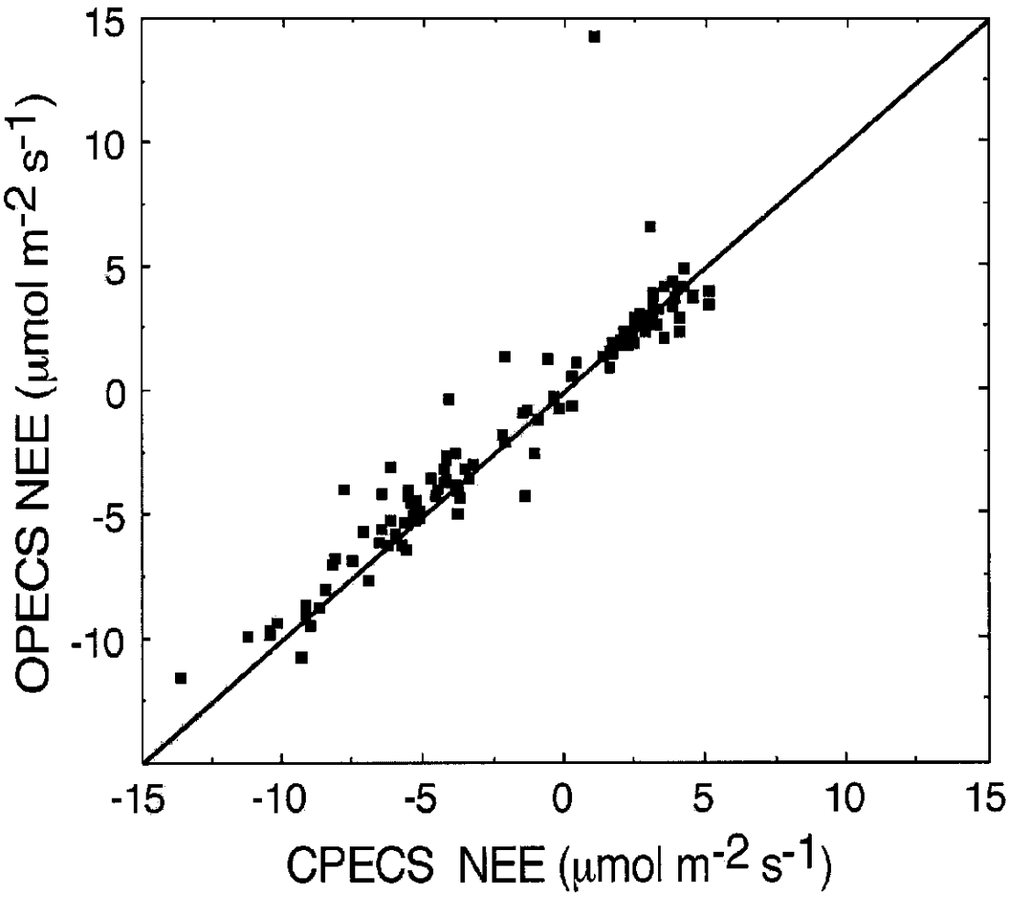

Figure 17. Comparison of measured net ecosystem exchange (NEE; $u_* \geq 0.15$ m s^{-1}) between the open-path eddy covariance system (OPECS) and closed-path eddy covariance system (CPECS) at a treed, moderate-rich fen in northern Alberta from September 1 to September 7, 2004. The 1:1 line is shown on the figure. Regression: slope (± 95 % C.I.) = 0.99 ± 0.06, y-intercept = 0.40, r^2 = 0.89, n = 113.

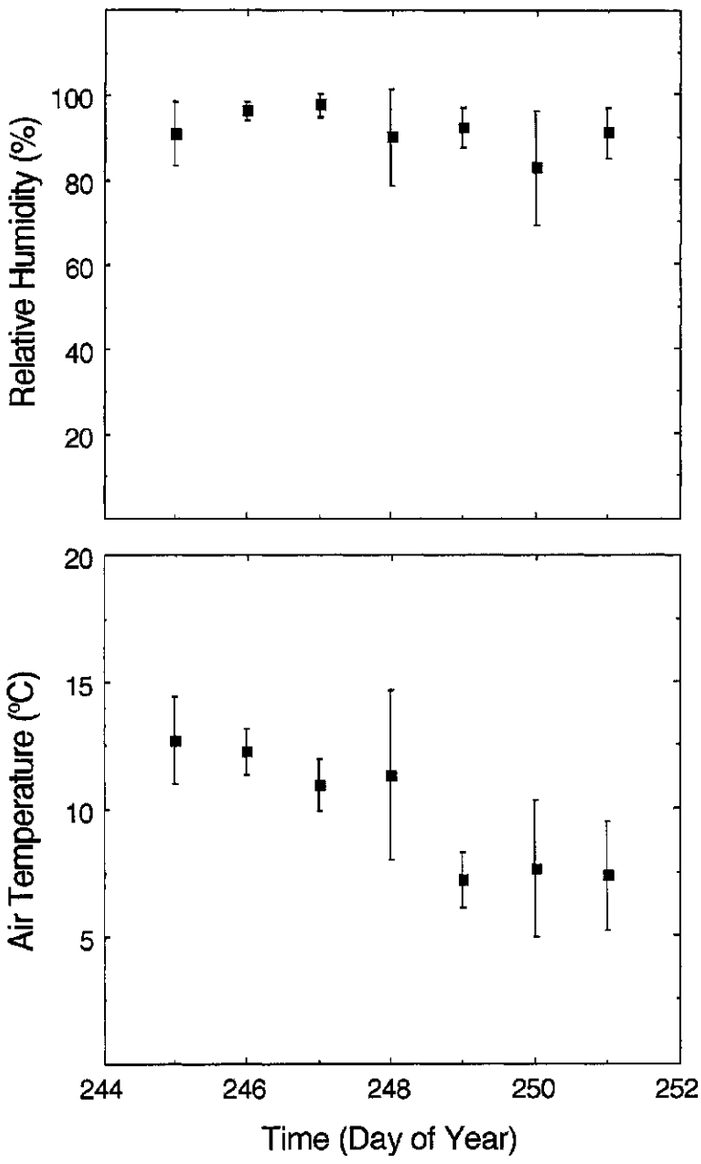

Figure 18. Average daily relative humidities and air temperatures at the treed, moderate-rich fen during the 7 day comparison between the open-path and closed-path eddy covariance systems. Symbols represent daily mean ± SD.

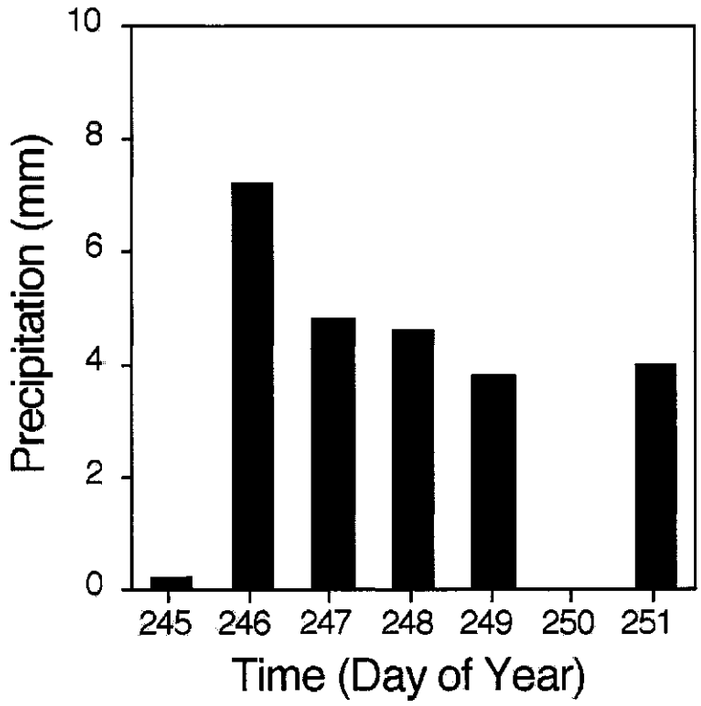

Figure 19. Daily precipitation totals at the treed, moderate-rich fen during the 7 day comparison between the open-path and closed-path eddy covariance systems.

Appendix B

Digital photographs of peatland sites and instrumentation used during the 2004 growing season campaign

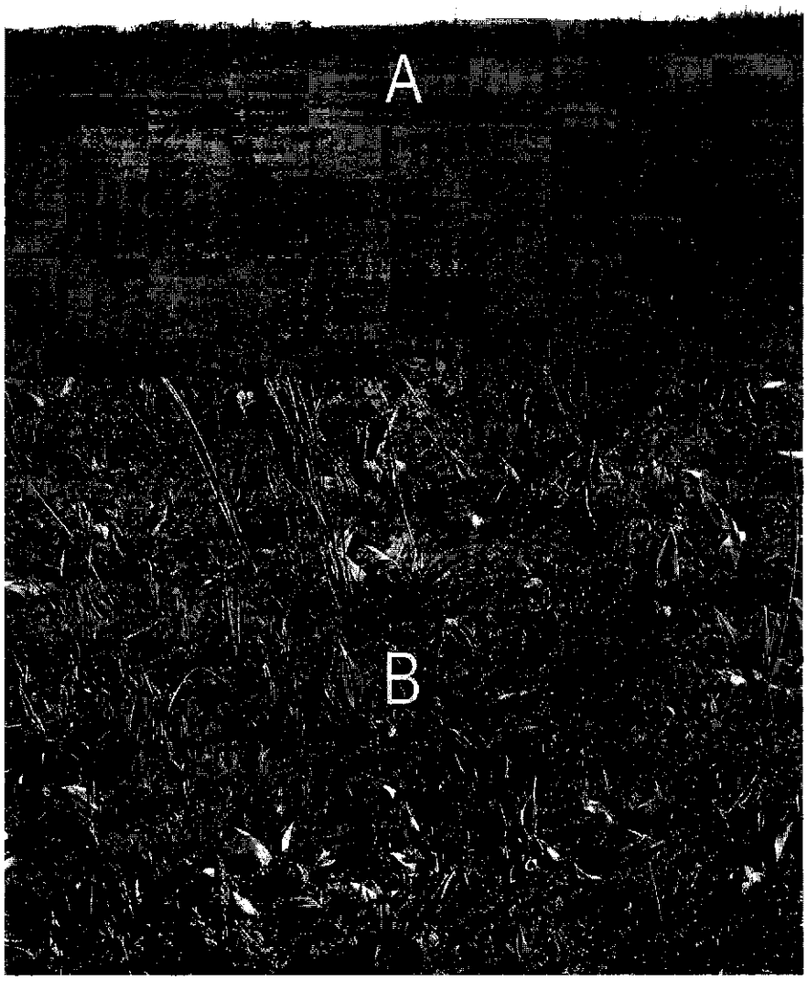

Figure 20. West fetch from eddy covariance tower (photo A) and ground cover (photo B) at the poor fen site during the summer of 2004.

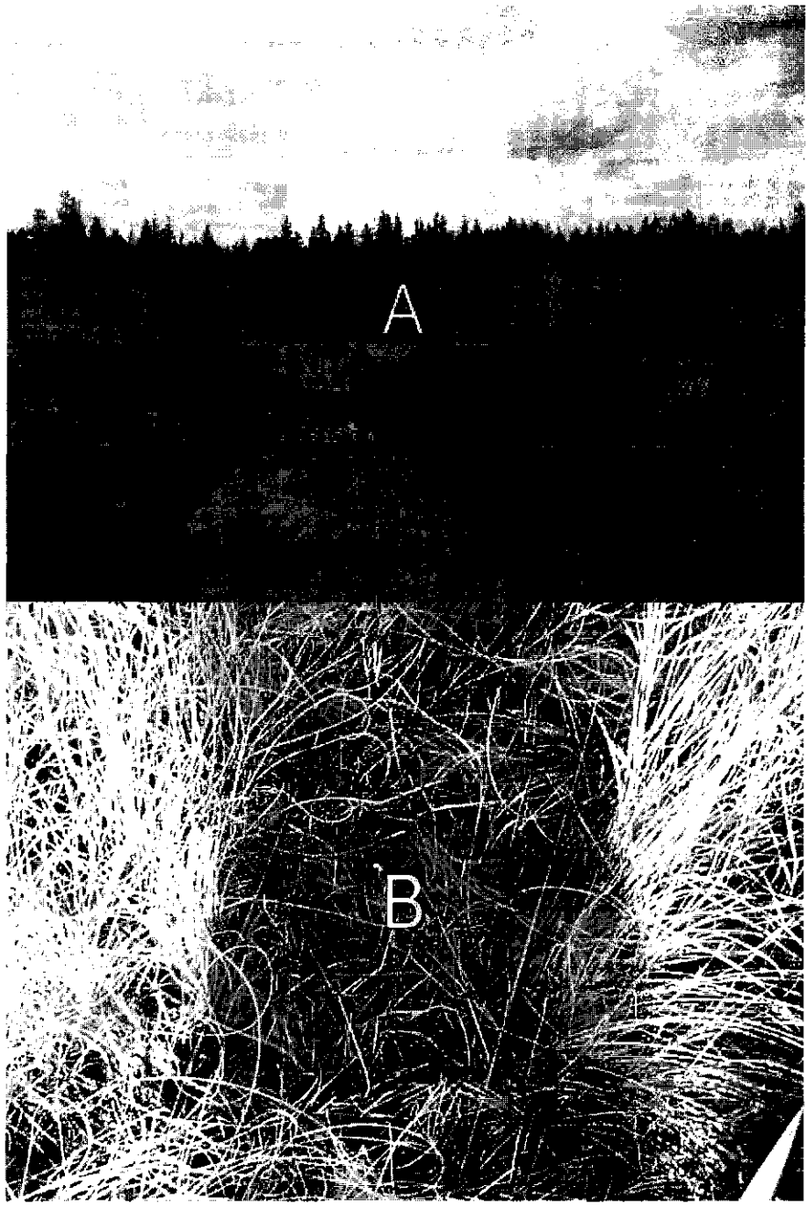

Figure 21. West fetch from eddy covariance tower (photo A) and ground cover (photo B; showing the brown moss understory in a clip-plot where the *Carex* has been harvested) at the extreme-rich fen site during the summer of 2004.

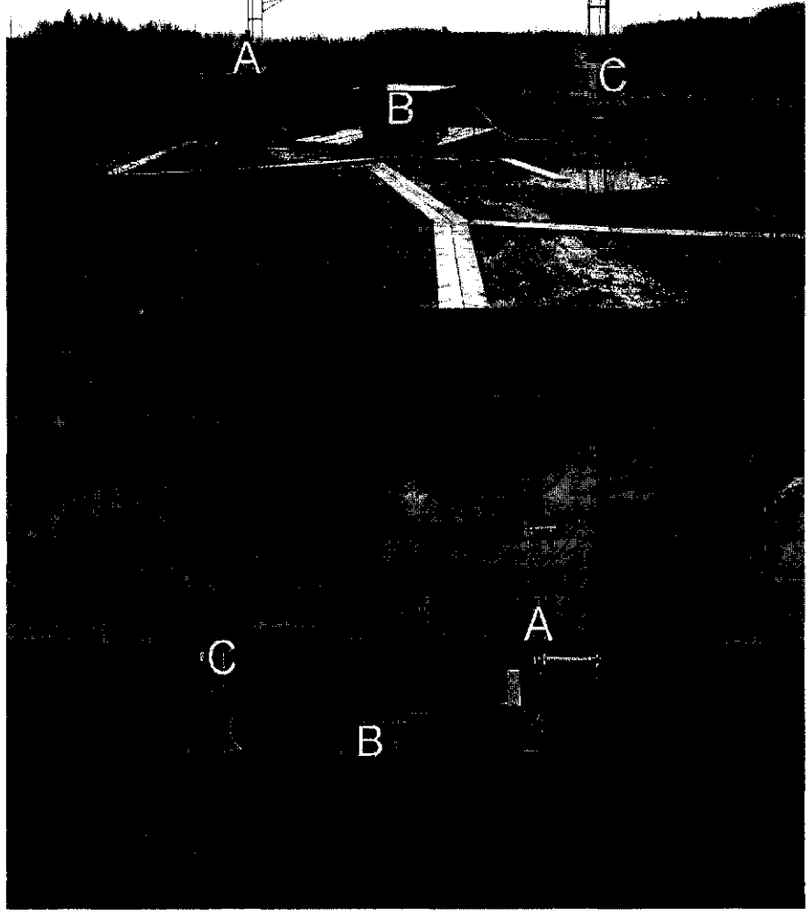

Figure 22. Peatland site micrometeorological instrumentation during the 2004 growing season campaign. The meteorological tower (label A), power supply enclosure (label B) and eddy-covariance tower (label C) at each site are shown. The top photograph shows the set-up at the poor fen, the bottom photograph shows the set-up at the extreme-rich fen.

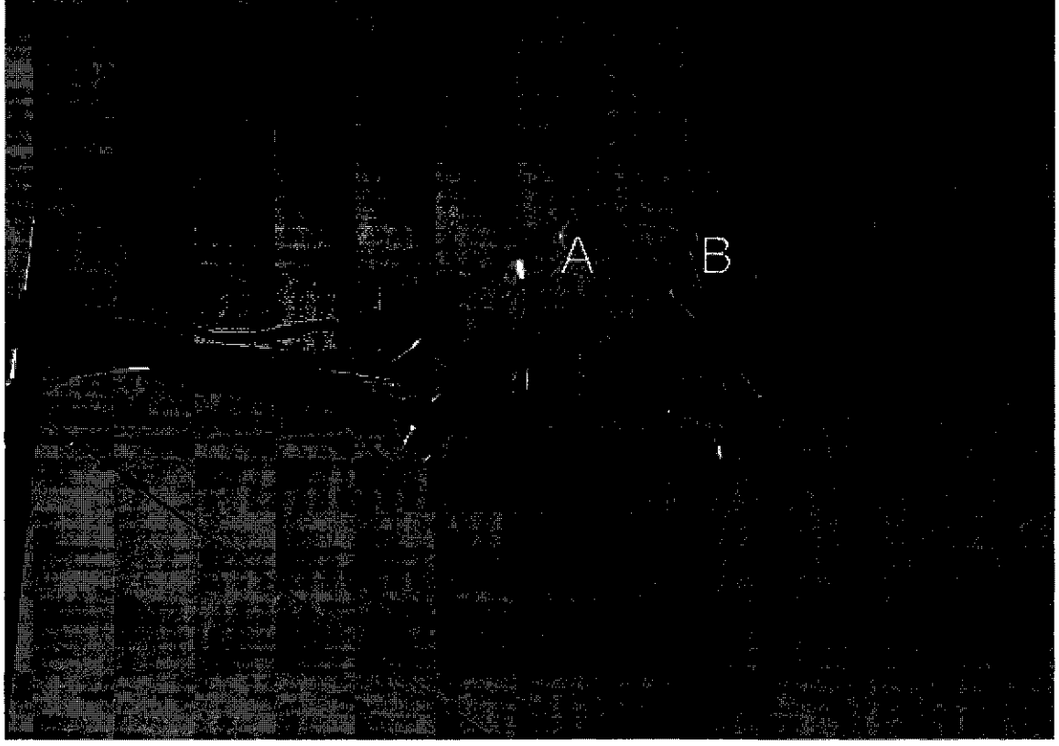

Figure 23. Mobile eddy covariance system used at the two peatland sites in northern Alberta during the 2004 growing season. The open-path infra-red gas analyser (model 7500, LI-COR, Inc.) is labelled A and the sonic anemometer-thermometer (model CSAT3, Campbell Scientific, Inc.) is labelled B in the photograph shown.

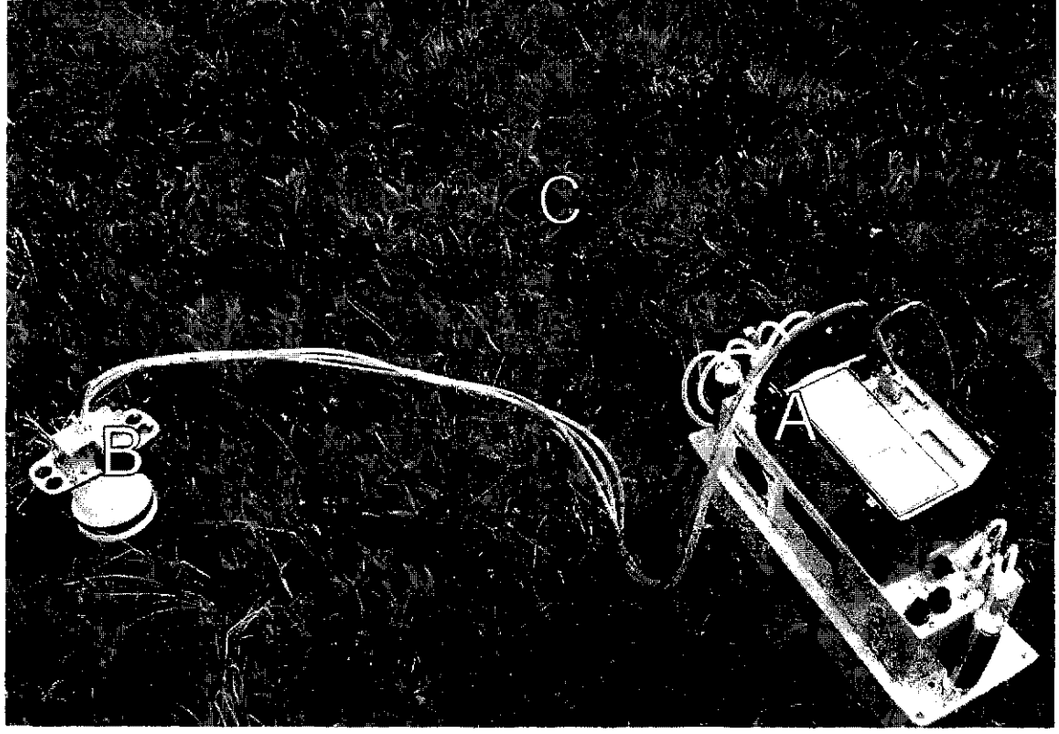

Figure 24. Portable gas exchange system (model LI-6200, LI-COR Inc.; label A), dynamic, closed chamber (model LI-6000-09, LI-COR Inc.; label B) and collars (label C) used to measure total ecosystem respiration at the two peatland sites in July, 2004. The photograph shown was taken at the poor fen site.